GENERAL

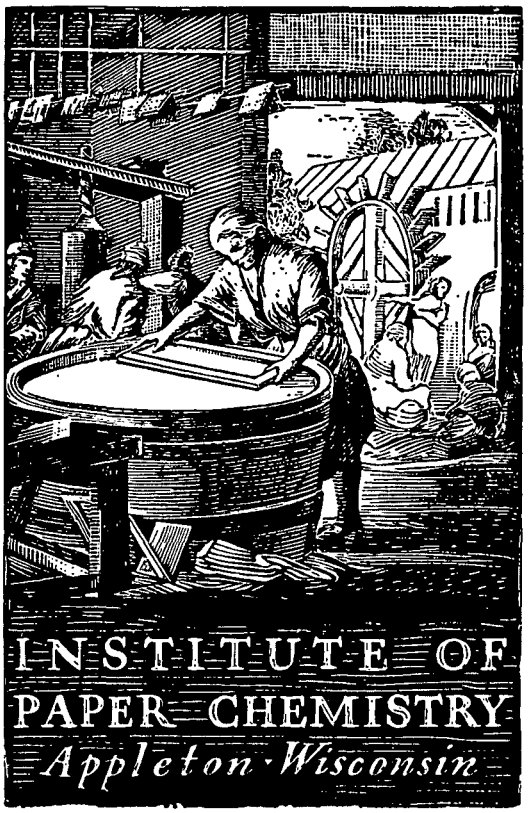

INVESTIGATION OF THE NATURE AND MAGNITUDES OF THE CYCLIC FLUCTUATIONS IN WEB TENSION AND TOP CORRUGATING ROLL MOLDING FORCE COMPONENTS AND THEIR RELATIONSHIP TO HIGH-LOWS

Project 2696-8

Report Two

A Summary Report

to

FOURDRINIER KRAFT BOARD INSTITUTE, INC.

October 18, 1972

FORM LETTER

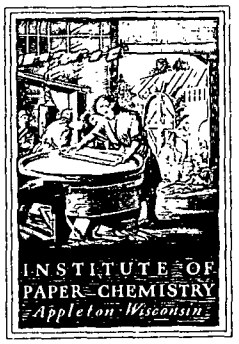

THE INSTITUTE OF PAPER CHEMISTRY
Appleton, Wisconsin 54911
Phone 414/734-9251

December 4, 1972

Project 2695-9
Project 2696-8

Mr. T. J. Gross
Technical Director
Fourdrinier Kraft Board Institute, Inc.
Suite 810
1605 Main Street
Sarasota, Florida 33577

Dear Mr. Gross:

We are enclosing copies of the following reports:

1. Effect of Relative Humidity and Temperature on Stacking Performance. Project 2695-9, Report One, to the Technical Division, Fourdrinier Kraft Board Institute, Inc. dated November 10, 1972.

2. Investigation of the Nature and Magnitudes of the Cyclic Fluctuations in Web Tension and Top Corrugating Roll Molding Force Components and Their Relationship to High-Lows. Project 2696-8, Report Two, a summary report to Fourdrinier Kraft Board Institute, Inc., dated October 18, 1972.

The first report is concerned with the stacking performance of corrugated boxes and combined board at the following conditions: 50% R.H., 73°F. 85% R.H. It was found that at a given applied load ratio, stacking failure times significantly increased as the test atmosphere changed from 90% R.H. at 90°F. to 85% R.H. at 73°F. and from 85% R.H. at 73°F. to 50% R.H. at 73°F. Furthermore, the allowable box stacking loads decrease with increasing moisture content at a significantly greater rate than is the case for top load compression strength. As a consequence, greater stacking safety factors are required when high R.H. levels are encountered in storage than has been believed necessary in the past.

For a given storage period, the applied loads (expressed as a percentage of the box strength at standard conditions) for a given storage time varied exponentially with moisture content. For example, for a 180-day storage period, the applied load percentages (essentially the maximum load the box would sustain for 180 days) declined from 55% at 7.5% moisture to 11% at 20% moisture when individual boxes were tested.

Somewhat higher allowable load percentages were obtained for stacked palletized boxes. Thus the allowable stacking load decreases very rapidly with increased moisture content. For this reason it can be costly to overdesign a package to meet extreme environmental conditions if they are rarely encountered.

Two further items deserve mention. First, the boxes were fabricated from combined boards made with regular starch adhesion. It is possible that high moisture contents might have a lesser effect on stacking behavior if weather-resistant adhesives were used. Second, the stacked boxes exhibited higher stacking load efficiencies than the individual boxes. Further work in these areas should be of interest.

The second report is concerned with a study of (1) the "Cyclic" variations in web tension and top corrugating roll molding stress on the medium from flute-to-flute during corrugating, and (2) the relationship between fluctuations in these variables and high-low flute formation. For this purpose, the Institute's corrugator was instrumented so as to continuously record the fluctuations in web tension, top corrugating roll pressure and the "up-and-down" acceleration of the top corrugating roll. The latter induces an inertial force on the medium which contributes to the molding of the flute. The records were then analyzed to determine the amplitudes and frequencies of the principal stresses applied to the medium. Among the conclusions reached in the study were the following:

1. Web tension, top roll pressure and acceleration exhibit significant cyclic components occurring at the flute forming frequency and its higher harmonics. Thus, the medium is stressed in a very complex way as each flute is formed.

2. High-lows were correlated with (a) the average tension semiamplitudes of the flute frequency component, and (b) the average acceleration semiamplitudes at the flute frequency of the top corrugating roll. Thus high-lows are responsive to vibration components associated with the "up-and-down" motion of the top corrugating roll and web tension. More work is needed to determine how corrugator condition and medium properties affect these stress components.

3. A detailed analysis for one run showed that these highly significant differences in the amplitudes and phases of the stress components from flute-to-flute. Such variations could affect the molding of the medium from flute-to-flute and promote high-low flute formation.

4. High-lows exhibit behavior characteristic of autoregressive processes -- i.e., the height of one flute is dependent in the height of the preceding flute(s) and a random component. It is speculated that

variations in the web tension and molding force in the corrugating labyrinth affect the degree of molding of the flute and subsequent meshing in the pressure roll nip. Further study of the behavior of the medium in the pressure roll nip would be of value.

Based on these results, it is believed that reductions in machine vibrations should reduce high-lows and promote higher machine speeds.

After you have had a chance to review these reports, we would appreciate any comments you may have.

Yours very truly,

R. C. McKee

R. C. McKee
Chairman
Container Section

RCM/mjm
Enclosures

Copy to: A. R. Boren

Mailing List attached

ERRATA

Project 2696-8 Report Two October 18, 1972

Page 52, Fig. 11. In the Figure Caption, please change (Run 3, Operator Side) to (Run 3, Drive Side).

Page 54, Fig. 12. Figure Caption should read as follows: Autocovariance Function vs. Time Lag for Operator Side Flute Height Differences

Page 114, Line 17. Please change 67.5 to 67.6.
" 20. " " 90.6 to 90.3.

Page 119, Line 17. Please change 'above' to 'about'.

THE INSTITUTE OF PAPER CHEMISTRY

Appleton, Wisconsin

INVESTIGATION OF THE NATURE AND MAGNITUDES OF THE CYCLIC FLUCTUATIONS IN WEB TENSION AND TOP CORRUGATING ROLL MOLDING FORCE COMPONENTS AND THEIR RELATIONSHIP TO HIGH-LOWS

Project 2696-8

Report Two

A Summary Report

to

FOURDRINIER KRAFT BOARD INSTITUTE, INC.

October 18, 1972

TABLE OF CONTENTS

THE INSTITUTE OF PAPER CHEMISTRY

Appleton, Wisconsin

INVESTIGATION OF THE NATURE AND MAGNITUDES OF THE CYCLIC FLUCTUATIONS IN WEB TENSION AND TOP CORRUGATING ROLL MOLDING FORCE COMPONENTS AND THEIR RELATIONSHIP TO HIGH-LOWS

SUMMARY

When corrugating medium is molded to the flute contour, it is subjected to the following stresses:

(1) Tension stresses due to transport tension and frictional effects as it is drawn into the corrugating labyrinth.

(2) Transverse stresses due to (a) top corrugating roll pressure and (b) inertial forces generated by the "up-and-down" acceleration of the top corrugating roll.

These stresses oscillate in magnitude during the formation of each flute. Inasmuch as variations in the amplitudes of these oscillating stresses may be related to high-low flute formation, a study was initiated with the following objectives:

1. To determine by means of spectral and Fourier analyses the amplitudes and frequencies of the principal vibration components present in the following variables: web tension, top corrugating roll pressure and top corrugating roll transverse ("up-and-down") acceleration.
2. To investigate relationships between the fluctuations in these variables and high-low flute formation.

For these purposes the Institute's corrugator was instrumented so as to continuously record the fluctuations in top corrugating roll pressure, top

corrugating roll transverse acceleration, and web tension. Pressure and acceleration measurements were made on both operator and drive side of the machine. Fabrication trials were carried out in which the following machine factors were varied: speed, web tension, top roll pressure, and shower pressure. Semichemical mediums (26 and 33 lb.) from two suppliers were employed in the study. During each fabrication run oscillograph records were obtained for each of the measured variables over 120 consecutive flutes. The oscillograph records were converted to digital form for computer time series analysis.

Fourier, power spectral density, and autocorrelation analysis techniques were employed. Fourier analysis is a method for analyzing periodic time series. It essentially reduces the series to a static component plus a series of sinusoidal components or harmonics having frequencies which are integral multiples of a fundamental frequency. Power spectral density analysis determines the frequency components present in a time series. Autocorrelation analysis evaluates how the values of the series at one time are related to the values at another time and is a means for detecting periodic components in a series.

As an illustration, when the corrugator is in operation, fluctuations in medium web tension or top corrugating roll pressure can occur even though the average tension or pressure level is held constant. For example, when a recording of the fluctuations in tension vs. time is made, the resulting curve is not the result of just brake tension but may reflect the presence of many vibration force factors or components. Fourier or spectral analysis are ways of breaking down the composite tension vs. time curve into the various tension force components. For example, the recorded tension vs. time curve might be composed of ten different tension vibration components. The analysis techniques mentioned are directed toward identifying the individual components in order to provide information

relative to their source. For example, vibration components may originate due to rough gearing, worn bearing, vibrations of parts of the machine structure, etc. When the cause of the vibration is known, remedial steps can be taken to reduce or eliminate the vibration.

During each run, the single-faced board was "flagged" so as to be able to reference it to the oscillograph records. Flute height measurements were made on both operator and drive sides over the 120-flute segment corresponding to the oscillograph record. Power spectral and autocorrelation techniques were used to analyze the flute height differences and, in a limited way, the measured (undifferenced) flute height values. The following results were obtained:

1. Flute height differences

   (a) The power spectrums for all runs generally peaked at frequencies near half the flute-forming frequency. They then declined rapidly and rather smoothly toward zero at lesser frequencies. Thus, most of the variations in flute height differences were associated with the high-low pattern. Because two flute height differences are required to form a high-low pattern, the characteristic frequency will be half the flute-forming frequency.

   (b) The autocorrelation coefficients for all runs alternated from positive-to-negative as they decayed toward zero. This type of pattern is characteristic of certain types of autoregressive processes — i.e., a process where the value at time t is dependent on (1) the preceding value or values and (2) a random component. An autoregressive

process may have a spectrum similar to those mentioned in (a) above. It is speculated that the autoregressive behavior is characteristic of the flute meshing process at the pressure roll. In past work, high-speed motion pictures have shown that successive flutes often tend to drop off the finger in an alternate pattern of large and small amounts. This may be caused by variations in molding force and/or web tension in the corrugating labyrinth. Because of this behavior, the medium contacts the liner on the pressure roll at slightly different times before the nip and this may affect the way in which the flutes mesh in the pressure roll nip and consequently affect flute heights. Further investigation of phenomena occurring at the pressure roll nip is warranted.

(c) In most cases the power spectrums indicated the flute height differences did not exhibit statistically significant components of variation at the lower frequencies. This occurs, in part, because the differencing operation attenuates lower frequency components — particularly near zero. Also, because only 120 consecutive flute heights were measured, the power spectra tended to lack statistical sensitivity and very low frequencies such as might be related to corrugating roll rotation could not be studied. The spectra of the undifferenced flute heights generally indicated the presence of low frequency variations; however, they were not studied in detail because of the limitations due to the number of observations. Further work in this area should be carried out.

2. Power spectrums of measured variables

(a) The power spectrums for all variables under all corrugating conditions indicated that the dominant vibration components were those occurring at the flute-forming frequency (F) and its second, third, and fourth harmonics (2F, 3F, 4F). Higher harmonics may be present but were not analyzed in this study.

(b) The relative importance of the vibration components at F, 2F, 3F, and 4F, varied substantially as speed and corrugator operational conditions were changed — i.e., at one speed the flute-forming frequency component had the greatest amplitude; at other speeds one or more of the harmonic components had the greatest amplitude. This probably occurs because certain parts of the corrugator are excited to vibrate at their resonant frequency and, hence, influence the magnitudes of the harmonic components. For the Institute's corrugator it appeared that high vibration amplitudes generally occurred if a harmonic frequency was in the range of about 540 or 720 Hz (cycles per second). Each corrugator would probably exhibit different critical frequencies and analysis of such behavior for a given machine should be helpful in improving board quality.

(c) Small but sometimes significant vibration components in the measured signal were, at times, detected which had frequencies near the high-low frequency — i.e., half the flute-forming frequency (F). In some cases these components appeared to be traceable to gear vibrations. However, their low magnitudes

relative to the other components at F, 2F, etc., made positive identification difficult. It suggests that rough or worn gears could cause vibrations which would affect flute formation in some cases.

(d) Using multiple regression techniques it appeared there was a relationship between average flute height differences and the mean square values of the pressure and acceleration. The mean square values are measures of the general intensity of the variations in the signals. Thus, high-lows appeared to be related to the two variables — pressure and acceleration — which affect the fluctuations in molding force on the medium.

3. Fourier analyses. A Fourier analysis was carried out to determine the amplitudes and phases of the vibration components at frequencies of F, 2F, and 3F in each measured variable.

(a) The overall average magnitudes of the components at the flute-forming frequency were as follows:

	Semiamplitude	
	Operator Side	Drive Side
Top roll acceleration, g.	± 1.02	± 0.91
Top roll pressure, p.s.i.	± 3.69	± 2.98
Web tension, lb./in.	± 0.25	

Relative to the average top roll operating pressure of 260 p.s.i., the above pressure semiamplitudes are relatively small. The acceleration semiamplitudes correspond to forces of 86 and 78 lb./in. for the operator and drive

sides, respectively. The line load due to a top corrugating roll pressure of 260 p.s.i. is estimated to be about 350 lb./in. for the Institute's corrugator. Thus, on the average, the acceleration semiamplitudes correspond to a force variation during the formation of each flute of about ± 25%. Relative to an operating level of 0.5 lb./in. web tension, the tension semiamplitude results in about a 50% variation during the formation of each flute. It appears possible that variations in the magnitudes of the web tension and top roll acceleration from flute-to-flute could be related to the occurrence of high-lows.

(b) The average semiamplitudes of the second and third harmonics of the flute-forming frequency component are shown below:

	Semiamplitude, %[a]	
	Second Harmonic	Third Harmonic
Top roll acceleration		
Operator side	55.4	21.5
Drive side	97.2	24.7
Top roll pressure		
Operator side	44.1	19.3
Drive side	43.7	12.2
Web tension	67.5	87.7

[a]Percent of semiamplitude at flute frequency.

Thus, there were important harmonic components in all measured variables. These harmonic components affect the stresses in the medium; hence, variations in their magnitude or phase affect the molding of the flute and subsequent behavior at the pressure roll nip.

(c) Using multiple regression techniques it appeared that average flute height differences were best correlated with (1) the tension semiamplitudes of the flute frequency component and (2) the acceleration semiamplitudes on the drive side of the flute frequency component. The greater the semiamplitudes of the tension and acceleration variables, the greater the high-lows. Thus, these results indicate that high-lows are responsive to vibration components associated with the top corrugating roll acceleration and the tension of the web. Future work would be warranted to determine how corrugator condition and medium properties affect these variables. Also, the influence of fluctuations in pressure and acceleration of the pressure roll deserves study.

4. Fourier Analyses — Run 6. A more detailed analysis was carried out for this run with the following results.

(a) In most cases the vibration components at the flute-forming frequency or its harmonics exhibited statistical significance at the 0.01 level. Components at frequency ratios of 0.5, 1.5, 2.5, and 3.5 relative to the flute-forming frequency were not statistically significant at

the 0.05 level except in one instance. Thus, the principal vibration components are those associated with the flute frequency or its harmonics.

(b) The analyses of variance indicated that in many cases there were highly significant differences in the Fourier coefficients between replicate flutes. Generally, differences in both amplitude and phase were involved. Such variations could affect the stresses imposed on the medium from flute-to-flute and, hence, promote high-low flute formation. Differences in amplitude and phase could result from the presence of vibration components not accounted for in the analysis and also local variations in medium quality — e.g., formation, density, or moisture content. Possible sources of other vibration components include gear, bearings, roll unbalance, etc.

(c) When Fourier coefficients were calculated for each flute, the semiamplitudes of the flute frequency component and its harmonics exhibited the following coefficients of variation.

	Coefficient of Variation, %
Top roll acceleration	
Operator side	13.6 to 37.6
Drive side	16.3 to 33.7
Top roll pressure	
Operator side	15.1 to 57.2
Drive side	25.5 to 56.5
Web tension	16.0 to 52.5

Thus, appreciable variations in magnitude occurred from flute-to-flute.

(d) It was observed that the flute frequency components of all variables exhibited an irregular cyclic variation in phase, having a frequency of about 15 Hz (about a 12-flute period at 300 f.p.m. corrugating speed). The peaks in phase often appeared to coincide with regions of greater high-low differences. Phase refers to the location or time during the formation of a flute when the particular variable component exhibits its maximum amplitude. Thus, this observation suggests that the occurrence of greater than normal high-lows may be partly dependent on the points in time when stresses are applied during formation of a given flute. The cause for the phase variations is not known, but they could possibly originate due to a low frequency component or possibly to small cyclic changes in machine speed superimposed on all the other vibration components present.

5. General. While the above results are not conclusive, they suggest that high-lows are caused, in part, by machine vibrations associated with stationary and rotating elements of the machine. The vibration components are varied and complex. Inasmuch as the medium functions as a combination nonlinear spring/damper as it is molded, it appears that the properties of the medium will affect vibration levels. Hence, different mediums will exhibit varying degrees of high-lows.

It is believed that reductions in machine vibrations should reduce high-lows and promote higher machine speeds. Further work is needed to better define the more important types of problem vibrations on both commercial and pilot plant machines. When the sources of the vibrations are known, it should be possible to reduce their magnitudes by design changes, etc.

INTRODUCTION

High-low corrugations are a manifestation of the fact that the heights of consecutive flutes vary in a definite pattern, i.e., the heights tend to be alternately high and low. The height periodicity appears to be present in all single-faced corrugated board regardless of type of medium, but the magnitude may differ from medium-to-medium (1). The fact that the phenomenon is invariably encountered indicates that the basic cause is inherent in the process although the magnitude is influenced by the medium and operating variables.

Among the operating variables which are known to influence the occurrence of high-lows are (1) web tension, (2) top corrugating roll pressure, (3) shower steam, and (4) speed (2, 3). While top corrugating roll pressure is usually controlled at some nominal level, it is known that the pressure oscillates about the nominal level in a periodic manner at the flute-forming frequency and higher frequencies (4). Thus, even though the nominal top corrugating roll pressure is held constant, the medium is exposed to a fluctuating pressure which varies in magnitude from instant-to-instant in the corrugating process. Web tension behaves in a similar manner.

The top corrugating roll can also move along a line joining the centers of the top and bottom corrugating rolls (4-6). The significance of this "up-and-down" motion to molding stresses is that the force which drives the top roll upwards is provided by the bottom corrugating roll acting through the medium, i.e., the driving force is the molding force. The force will depend on the mass of the top corrugating roll and its acceleration at any instant. This inertial force also varies in a periodic manner.

Thus, during the formation of each flute the medium is exposed to a fluctuating stress environment. The stresses are (1) tension stresses due to transport tension and friction in the labyrinth, and (2) transverse (molding) stresses due to top corrugating roll pressure and the inertial force of the top roll. Corrugating, in its simplest concepts, consists of inducing a permanent set in the medium so it will retain a fluted shape. Hence, it seems possible that variations in the intensities of the molding forces and web tension may result in varying degrees of "springback" in the molded flute after the medium leaves the corrugating labyrinth. Such variations may contribute to high-low flute formation because only small changes in absolute length of medium per flute will cause a considerably larger change in flute height.

In Report Eight, Project 1108-22, high-speed motion pictures were taken of the pressure roll nip area. It was observed that as the fluted medium drops off the end of the finger, the distance which it dropped followed, in many cases, a regular pattern. Thus, successive flutes often tended "to drop in an alternate pattern of large and small amounts." This may be caused by variations in molding force and/or web tension in the labyrinth. In turn, the uneven dropping off the finger may affect meshing in the pressure roll nip and consequently affect flute heights.

With the above in mind, a study was carried out with the following objectives:

1. To determine by means of spectral analysis and other time series methods the amplitudes and frequencies of vibration components in the tension and molding forces as affected by type of medium, speed, and other operating conditions.

2. To investigate relationships between the variations in tension, molding force and high-lows.

Thus, this study focuses attention on variations in web tension and top roll molding force. Extension of the study to phenomena at the pressure roll nip also appears desirable in view of the observation cited above.

BACKGROUND CONSIDERATIONS

As background information, Fig. 1 illustrates the manner in which the top corrugating roll pressure, displacement, and acceleration and corrugating medium web tension vary during the formation of one flute [see also Ref. (4)]. When the corrugating medium arch which is subsequently bonded to the single-face liner is at the center line of the corrugating rolls the hydraulic force and displacement are at maxima — Points R_1 and R_3 in Fig. 1. This corresponds to a root of the top corrugating roll at the center line. A lesser maxima is obtained when the corrugating medium arch which is subsequently bonded to the double-face liner is at the center line — Point R_2 in Fig. 1. The difference in the maxima may be related to the effect of the pressure roll acting against the bottom corrugating roll.

It may be noted that the maxima and minima of the displacement and top corrugating roll pressure curves coincide timewise. As the top roll moves upward away from the bottom roll, the top roll pressure increases. Conversely, as the roll displacement diminishes, the top roll pressure decreases. At a maximum point on the curves the increased top roll pressure provides the negative acceleration required to bring the top roll "upward" velocity to zero and reverses its direction. At a minimum point the top roll pressure reaches its least value, which in conjunction with the driving force supplied by the bottom corrugating roll acting through the medium accounts for the positive acceleration necessary to reverse the roll motion.

It also may be noted that the web tension is near its minimum value when the top corrugating roll pressure and displacement are at the maximum (R_1 and R_3). The maximum value of web tension in Fig. 1 occurred about when the unbonded area of the single-faced board was at the center line (Point R_2).

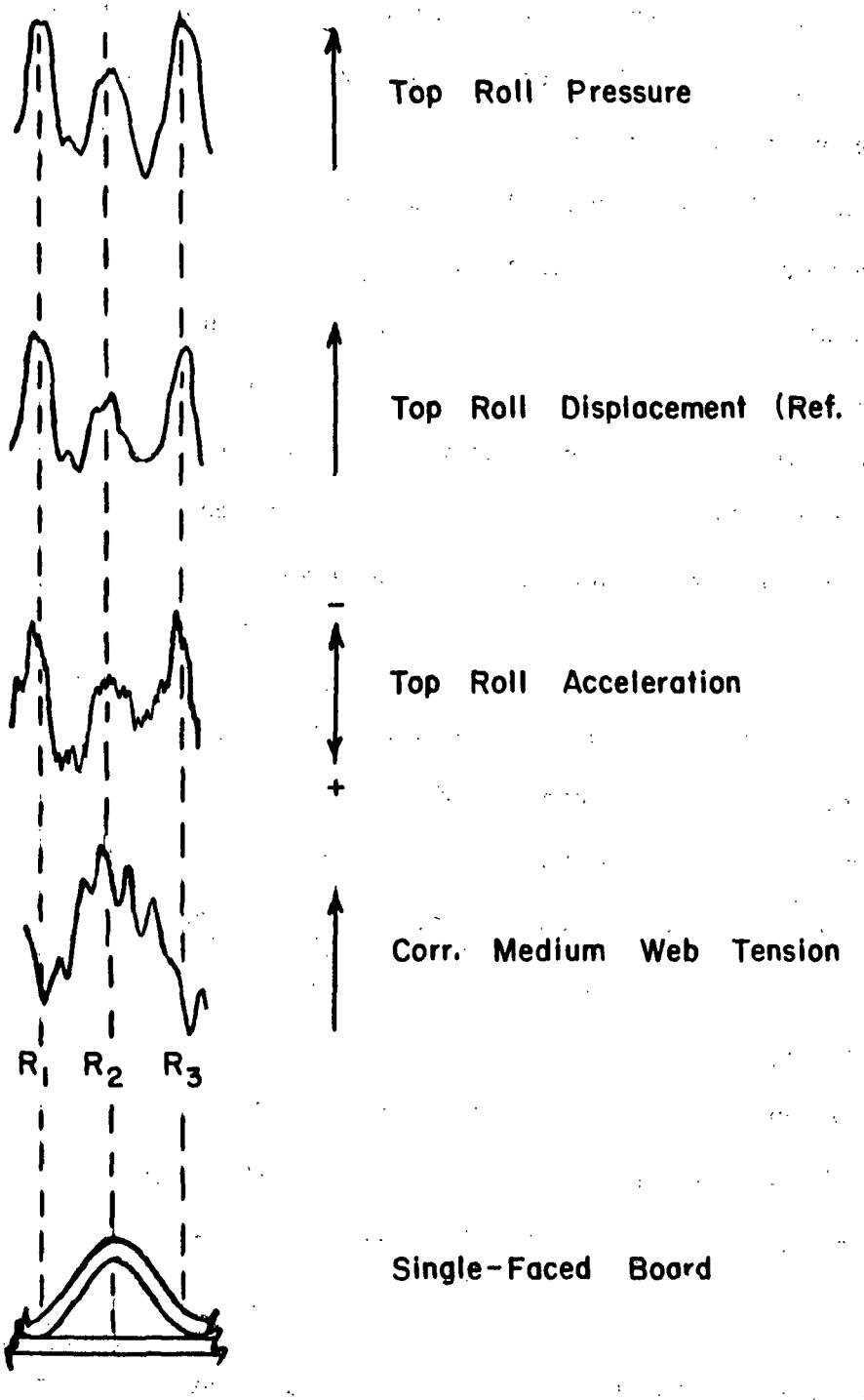

Figure 1. Relationships Between Top Corrugating Roll Pressure, Acceleration, Displacement, Web Tension, and Flute Configuration (150 f.p.m.)

Figure 1 illustrates the general manner in which such variables as pressure, tension, and acceleration vary during the formation of one flute. However, it was observed in the recordings obtained in this study that the appearance of the signals exhibited considerable variation depending on corrugating speed, operational variables, operator vs. drive side, etc. In gross terms, however, the signals always exhibit a periodic oscillation at the flute-forming frequency, i.e., a cyclic oscillation with a period corresponding to the time to go from R_1 to R_3. The flute-forming frequency may be termed the fundamental frequency of the corrugating process. A noticeably large cyclic component with a frequency equal to twice the flute-forming frequency is also evident in some of the signals in Fig. 1, i.e., for example, the pressure signal displays three marked maxima during the formation of one flute. Relative to the flute-forming frequency this component may be termed the second harmonic. Higher frequency components are also evident in the signals.

A simple example may be helpful in visualizing the above remarks. If an A-flute single-facer (36 flutes/foot) is operated at a speed of 167 f.p.m. the flute-forming frequency would be 100 Hz, i.e., 100 cycles per second. Assume that the top corrugating roll pressure oscillations are comprised of two cyclic components at 200 Hz and 100 Hz, as shown in Fig. 2A and 2B. When these components are added together the curve shown in Fig. 2C is obtained. Broadly speaking, the resultant curve is similar in form to the pressure signal in Fig. 1 and illustrates how a complex waveform can result when many cyclic frequencies are present.

The periodic curves in Fig. 2 exactly repeat themselves from cycle-to-cycle, i.e., in this case, from flute-to-flute. If they represented a variable which affected flute height, e.g., web tension, the medium would be exposed to exactly the same tension stress variations during the formation of each flute.

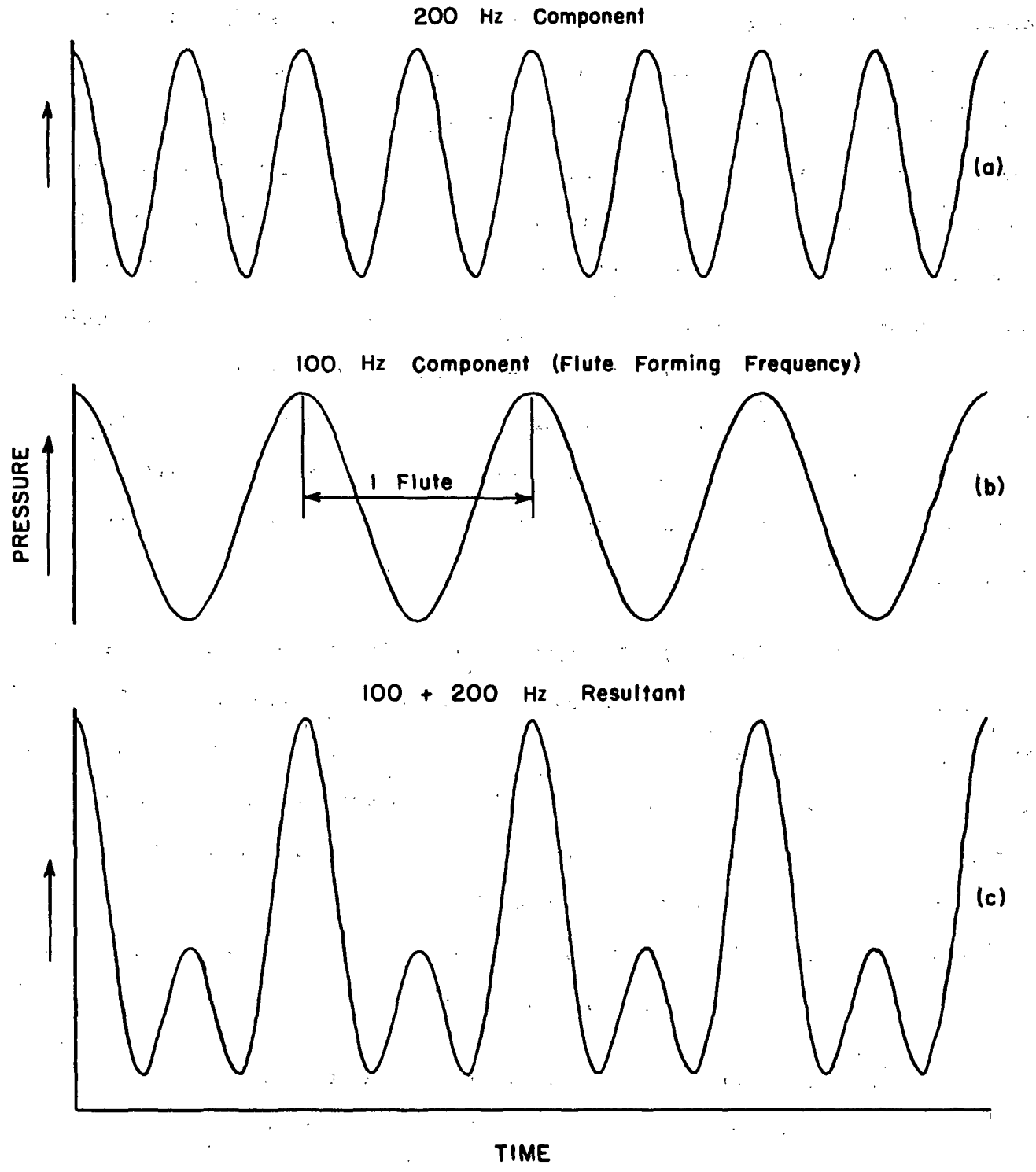

Figure 2. Addition of 100 Hz (Flute-Forming Frequency) and 200 Hz Cyclic Components

Hence, no flute height variations would occur due to this variable. Variations in amplitude (or phase) from flute-to-flute would be required to cause differences in flute height under these circumstances. Such variations could be either periodic or random, or both in nature.

One way in which a high-low pattern could be induced in the periodic curves shown in Fig. 2 would be to introduce components having frequencies such as 1/2 or 3/2 the flute-forming frequency. For example, Fig. 3 illustrates the effect of adding a 50 Hz component to the 100 and 200 Hz components previously shown in Fig. 2. The 50 Hz component corresponds to one-half the flute-forming frequency in this example and induces a pronounced high-low pattern in the resultant curve. If the molding force on the medium or web tension varied in this manner, alternate flutes would be formed under different stress conditions. As a consequence, this would produce a tendency for the heights of alternate flutes to be either high or low relative to their neighbors due to differing degrees of stress and strain relaxation in the flute walls before the bond between liner and medium is set.

Cyclic components having frequencies near but not exactly at 1/2 or 3/2 the flute-forming frequency would result in composite patterns somewhat similar to Fig. 3; however, the high-low pattern would change with time. This would be one way to explain the reversals in high-low pattern which occur.

At the outset of the study, it was speculated that the basic high-low flute height mechanism might be explained in the way outlined above. This hypothesis appears questionable based on the data from this study. This is discussed further in the text.

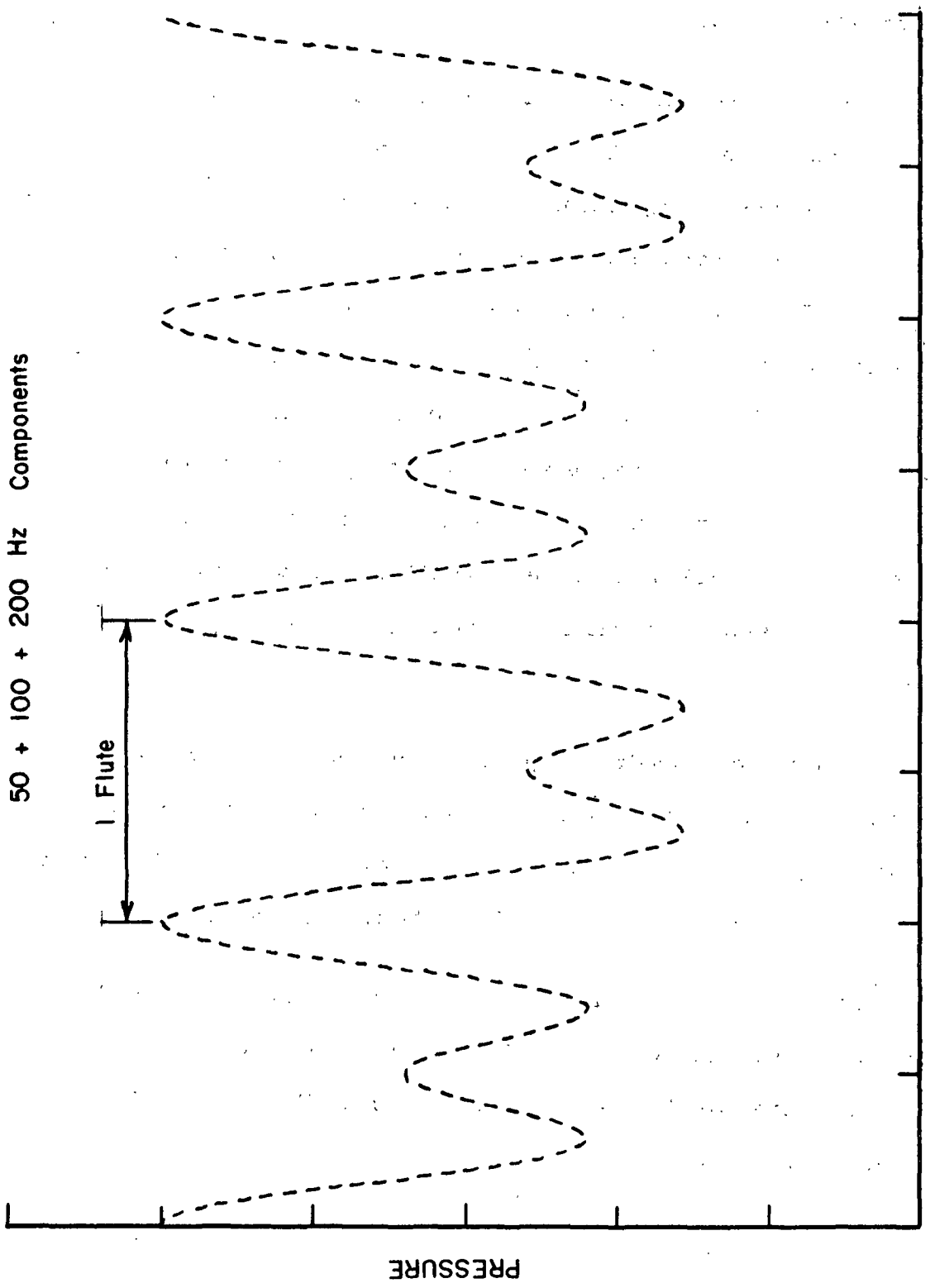

Figure 3. Illustration of a High-Low Pattern Induced by Consideration of a 50 Hz Cyclic Component at Half the Flute-Forming Frequency

The high-low flute height pattern is in some respects similar to certain types of autoregressive processes wherein the current value of a process at time t is dependent on (a) preceding process values and (b) a random component at time t. Box and Jenkins (7) indicate that this behavior is often characteristic of processes where "carry-over effects" occur, e.g., when residues from one batch affect the output of the next batch. In the case of corrugating, this would imply that the way in which one flute is "set" at the pressure roll nip affects the next succeeding flute.

With regard to the amplitude of motion of the top corrugating roll, Peters (6) reported values ranging from about 0.0004 to 0.0008 inch. More recently, Nordman and Toroi (8) reported that the largest amplitudes measured were about 0.002 inch though in most cases they were less. While these amplitudes are small in comparison with many flute height differences, this does not mean that the amplitudes of motion are necessarily unrelated to high-low flute formation. Even a small amplitude of motion could result in relatively large differences in the effective molding force on the medium and, hence, in the degree of molding of a given flute.

The previous discussion focussed attention on random or periodic variations in molding force or web tension as a possible explanation for the high-low mechanism. The term periodic means that the oscillation exactly repeats itself after one full cycle or period. The curves shown in Fig. 2 and 3 are periodic. However, high-lows vary in magnitude from one pair of flutes to the next and sporadically large differences in height occur. Some of the latter could be caused by transient or low frequency vibration disturbances due to out-of-round medium rolls, unbalanced idler rolls, corrugating roll concentricity, tooth imperfections, etc. A portion of the variability in flute height from flute-to-flute

probably must be attributed to the medium itself. Local variations in medium density, thickness, compressibility, etc., should affect the way the medium responds to the molding and tension stresses in the labyrinth and its subsequent relaxation.

Thus, it may be speculated that high-lows are the net result of the following:

(a) Random or possibly periodic oscillations in the molding force and web tension which would induce high-low variations in the molding force or web tension.

(b) Transient or low frequency disturbances in molding force or web tension associated with sporadic occurrences of large flute height differences.

(c) Local variations in medium properties causing more or less random variations in flute height.

The above concepts are highly oversimplified. For example, even if true in part, it is not clear how to explain the propagation or lack of propagation of high-lows across the machine. This is troublesome in the case of the Institute's narrow single-facer and perhaps more so in the case of wide commercial machines where roll flexure and crown may be important. As another example, both web tension and top corrugating roll pressure (and presumably top roll inertial forces) are known to affect high-low flute formation. How to allow for the interaction of the various cyclic components in these factors on high-lows is a critical question.

It may be noted that machine vibrations are cited as a cause of high-lows by the Langston Company (9). Among the sources of vibration mentioned are damaged

bearings, empty accumulators, dirty gears, misaligned corrugating rolls, broken siphon pipes, worn corrugating rolls, and erratic tension due to out-of-round medium rolls.

One of the major objectives of the present study was to analyze signals of the type shown in Fig. 1 in terms of frequency content in order to determine whether vibration frequencies were present which might be related or corelated to high-low flute formation. For this purpose, two time series analysis techniques were employed as follows:

1. Periodic Regression (Fourier analysis)
2. Spectral and autocorrelation analysis

A brief discussion of these techniques follows this section.

TIME SERIES ANALYSES PROCEDURES

A time series is a set of data which vary in magnitude with time. The data may vary in a periodic manner (Fig. 4A) or in a random manner (Fig. 4B). Both periodic and random fluctuations may be present as illustrated in Fig. 4C where random noise is superimposed on a sinusoidal signal.

Two ways of analyzing time series are as follows:

1. Fourier or harmonic analysis (also termed periodic regression by Bliss (10).
2. Spectral and autocovariance analysis.

Fourier analysis is a method for analyzing periodic time series. A periodic series is one which exactly repeats itself after one full cycle or period (T). The number of cycles per unit time is called the frequency (f). A simple sinusoidal series is illustrated in Fig. 4A and a series composed of two sinusoidal harmonically related components was illustrated previously (Fig. 2).

In general, a periodic time series may be described by a Fourier series, one form of which is shown below (9):

$$x(t) = a_o/2 + X_1 \cos [2\pi f_1 t - \Theta_1] + X_2 \cos [4\pi f_2 t - \Theta_2] \quad (1)$$

where

t = time

f_1 = fundamental frequency, Hz

$X_1, X_2, \ldots$ = semiamplitudes of components 1, 2, ...

$\Theta_1, \Theta_2, \ldots$ = phase angles of components 1, 2, ...

$a_o/2$ = mean

$x(t)$ = magnitude of x at time, t

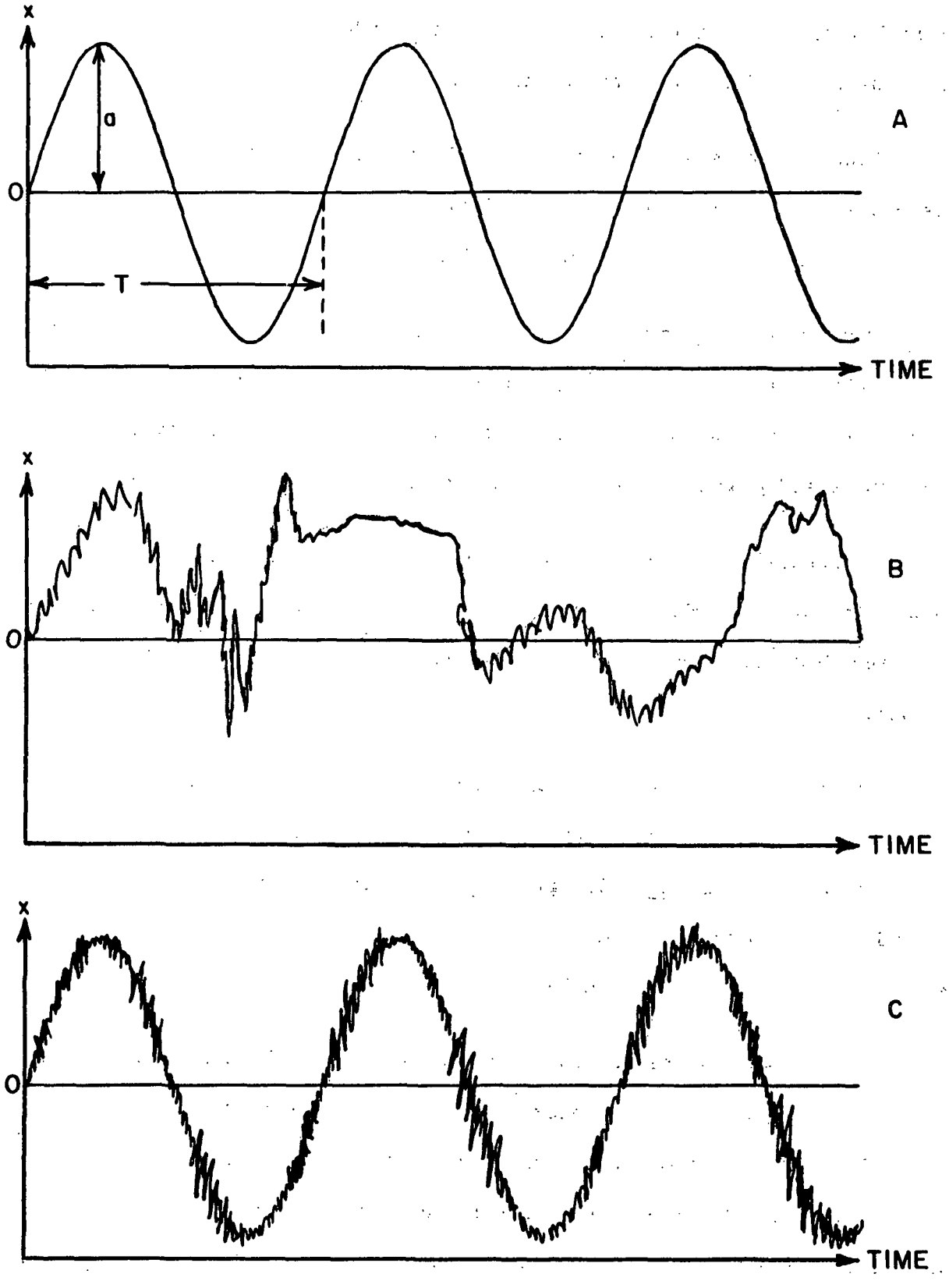

Figure 4. Illustrative Time Series (A = Sinusoidal, B = Random, C = Sinusoidal Plus Random)

Thus, a periodic time series may be reduced to a static component ($a_o/2$) plus a number of sinusoidal components or harmonics having frequencies which are integral multiples of the fundamental frequency.

Fourier analysis procedures are well known and statistical methods have been developed to evaluate the statistical significance of the harmonic terms. A description of such tests may be found in Bliss (10).

Fourier analysis procedures were used in this study to describe the periodic variations in the pressure, tension, and translational acceleration signals measured on the corrugator. In this way a given signal is described in terms of the amplitudes and phases of the flute-forming frequency (F) and its harmonics.

In general, the pressure, tension and acceleration signals obtained in this study appeared to exhibit periodic characteristics with a fundamental frequency equal to the flute frequency. Fourier methods appear appropriate for studying these variations.

The second general method of analysis used in this study involved power spectral density and autocorrelation techniques as described by Blackman and Tukey (11), Bendat and Piersol (12), Granger (13), and many others. These techniques were developed for analyzing random time series (see Fig. 4) so as to be able to characterize such series and to detect periodic components hidden in such series.

The power spectral density is a measurement of the variance in magnitude of a series within a narrow frequency band. A plot of power spectral density vs. frequency is termed the power spectrum. Peaks in the power spectrum at certain frequencies indicate the presence of significant oscillatory components at such frequencies. For example, in the case of machinery vibrations the appearance of

significant peaks in power spectral density at certain frequencies can indicate which elements of the machine cause the vibrations and, in turn, lead to corrective measures. This was one of the objectives in mind in applying this technique to the corrugator.

For a sine curve such as that shown in Fig. 4A, Bendat and Piersol (12) indicate that the power spectrum would appear as in Fig. 5A. The power spectral density [$G_x(f)$] is zero at all frequencies except the frequency of the sine curve. At this frequency the spectral density is theoretically infinitely great; however, over a finite frequency range which includes the sinusoidal frequency the spectral density will have a finite value equal to the mean square value of the sine curve.

For "white" noise the power spectrum is constant over all frequencies. Thus, the random series illustrated in Fig. 4B would have a relatively smooth broad spectrum as illustrated in Fig. 5D. For the case of a random noise superimposed on a sinusoidal curve the power spectrum is "the sum of the power spectra for the sine wave and random noise separately ..." (12). This is illustrated in Fig. 5B while Fig. 5C shows the power spectrum for narrow band random noise.

Thus, the power spectrum is a powerful tool for detecting periodic components in a time series. As a practical example, Foster (14) analyzed the speed variations of a multiwall sack tuber in order to determine the causes of tube length variations. A number of significant peaks were obtained in the power spectrum. Two of the peaks were associated with variations in line shaft and knife drive speed which, in turn, were responsible for the tube length variations.

Another example cited by Mitchell and Lynch (15) may be of interest. They investigated the noise levels of a set of involute gears operating at a tooth frequency of 1038 Hz; the pinion and wheel rotated at 38.44 and 27.33 Hz,

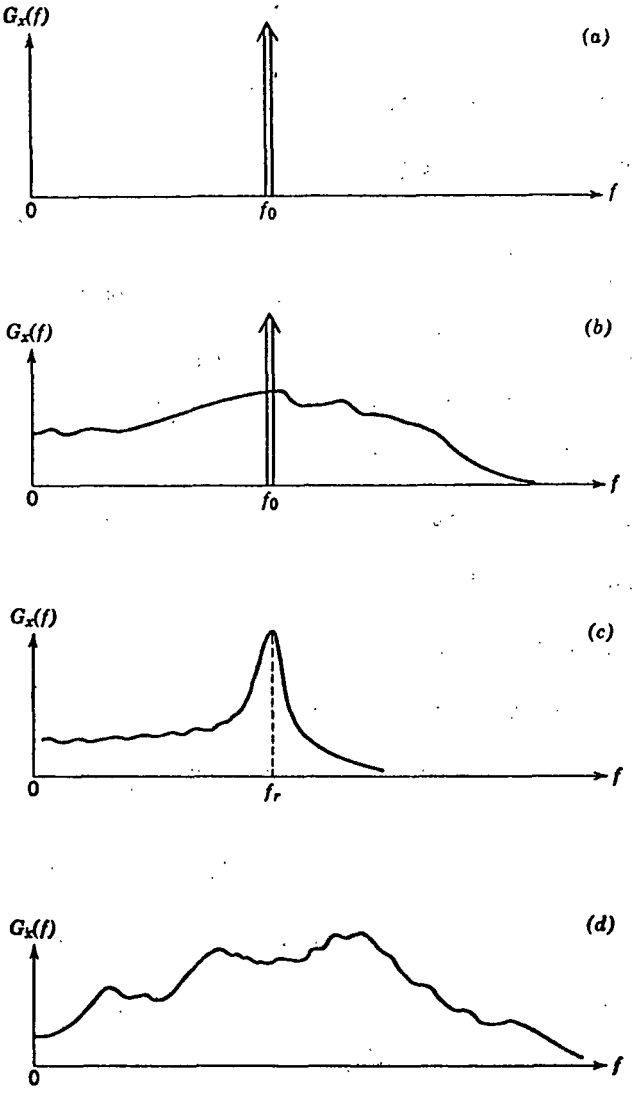

Figure 5. Power Spectral Density Function Plots (Power Spectra). (a) Sine Wave; (b) Sine Wave Plus Random Noise; (c) Narrow-Band Random Noise; (d) Wide-Band Random Noise [Ref. (12)]

respectively. Figure 6 shows the power spectrum of the sound pressure level vs. frequency. The authors concluded that there were three major regions of noise level — namely, around 885, 2035, and 2649 Hz. Amplitude modulation due to pinion eccentricity was responsible for the 885 Hz region. This corresponded to the fourth lower sideband [1038 − 4(38.44)]. The components having frequencies near 2035 Hz corresponded to sidebands of the second harmonic of the tooth contact frequency. The authors also stated that the last major frequency region near 2649 Hz was associated with "inaccuracies manufactured into the pinion." Thus, power spectral density analysis can be a powerful tool for identifying the sources of vibration in practical problems. This particular example is included because of its possible relevance to corrugating, i.e., corrugating rolls are a type of gear and the machines are usually gear driven.

Power spectra can be measured using analog devices and also by digital computer analysis. In the latter case, analog recordings must be digitized by reading magnitudes at equally spaced time intervals over the length of the record. This procedure was followed in this study. The computer program (BMD02T) was taken from the BMD Biomedical Computer programs prepared by the University of California. Some modifications in the program were necessary to adapt it to the Institute's IBM 360 computer.

The autocorrelation function of a time history describes the "dependence of the data at one time on the values at another time" (12). Thus, while power spectral density is concerned with the properties of the data in terms of frequency, the autocorrelation function performs a similar function in terms of time. They are mathematically related to each other.

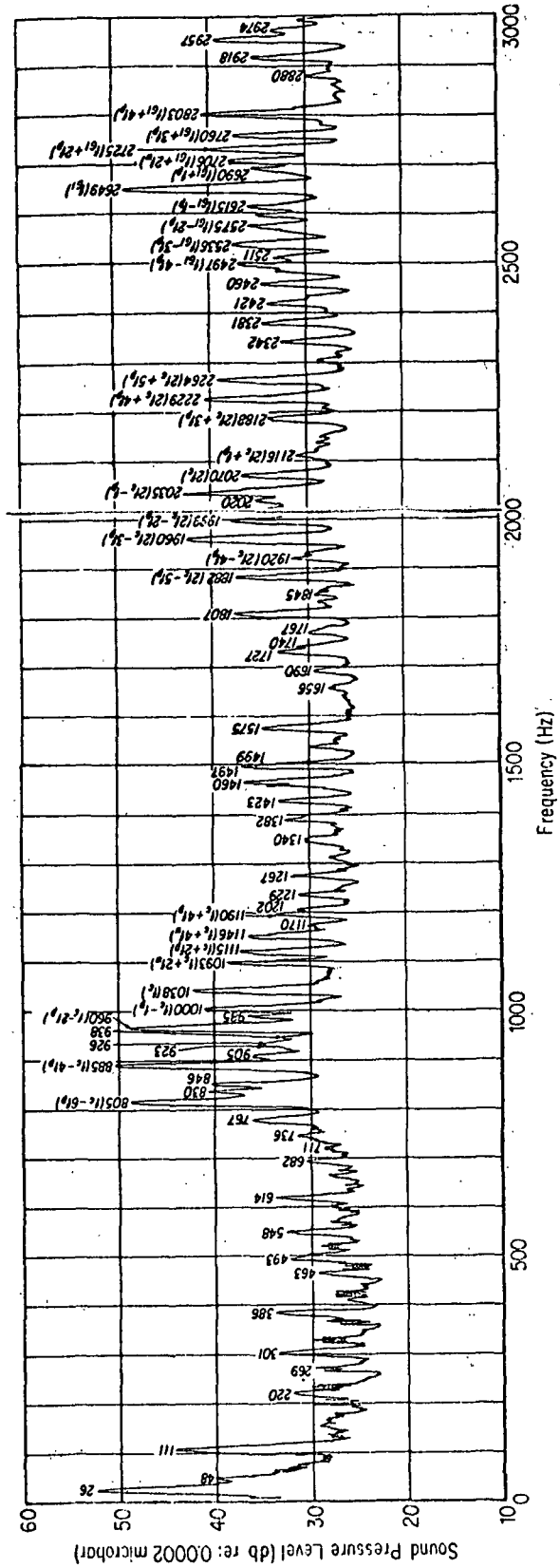

Figure 6. Gear Noise Analysis by Constant-Bandwidth, 10-Hz Filter [Ref. (15)]

For a given time history "an estimate of the autocorrelation between the values of $x(t)$ at times t and $t + \tau$ may be obtained by taking the product of the two values and averaging over the observation time (T)." Thus, the time history is compared with a time shifted version of itself and a graph of the resulting autocorrelation function is plotted as a function of the delay time.

For a sinusoidal curve the autocorrelation function [$R_x(\tau)$] is periodic over all time displacements (τ) with the same period as the original curve as shown in Fig. 7a. This occurs because the sine curve is identical to itself whenever the time shift is an integral number of periods.

For random noise the autocorrelation is sharply peaked at zero time lag and diminishes rapidly as the delay time is increased (Fig. 7d). This occurs because even small time shifts are sufficient to disturb the similarity between the wave shape and its time shifted version.

For a sine wave with superimposed random noise the autocorrelation function is "the sum of the autocorrelatograms for the sine wave and random noise separately" (12). This is illustrated in Fig. 7b. There is a sharp peak at zero delay time and thereafter the function displays a sinusoidal form which persists over all time displacements.

Thus, the autocorrelation function is a means for detecting deterministic data which may be hidden or masked by random fluctuations.

Both autocorrelation and power spectral analysis techniques can also be used to determine the similarities between two time histories. They are then termed cross-correlation and cross-spectral density. Finally, the correlation between two time histories as a function of frequency can be calculated from the

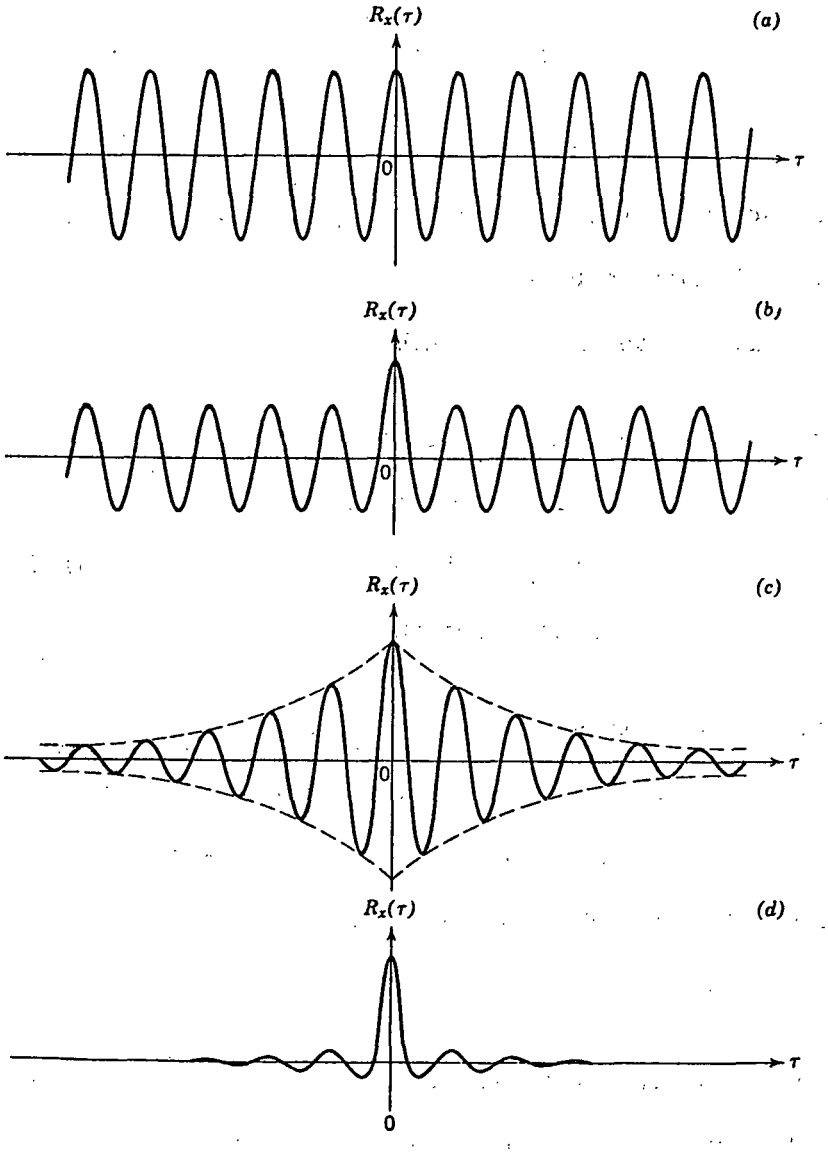

Figure 7. Autocorrelation Function Plots (Autocorrelograms). (a) Sine Wave; (b) Sine Wave Plus Random Noise; (c) Narrow-Band Random Noise; (d) Wide-Band Random Noise [Ref. (12)]

cross-spectral density and the spectral densities of the two parent series. This correlation function is termed the coherence function and it behaves in a similar manner to the conventional correlation coefficient employed in simple or multiple regression. Thus, if the two series are not related at all at a particular frequency, the coherence function is zero. If the two series were perfectly related at a given frequency, the coherence would equal unity.

The Computer Program used for power spectral density analysis also was used to obtain autocovariance, cross covariance, cross spectra, and coherences.

MATERIALS

Four semichemical medium samples were used in this study as follows:

Nominal Weight, lb./M ft.^{2}	Mill	Roll Numbers
26	A	14614, 14644
26	B	14646
33	A	5334
33	B	5333

INSTRUMENTATION

For each corrugating run, the instantaneous variations in the following variables were measured:

1. Top corrugating roll pressure: operator and drive side
2. Web tension
3. Top corrugating roll transverse acceleration: operator and drive side

TOP CORRUGATING ROLL PRESSURE

Two pressure transducers with characteristics as follows were used:

Type:	CEC4-329
Range:	0 to 500 p.s.i.
Natural frequency:	in excess of 25,000 Hz

The pressure transducers were installed in the hydraulic pressure lines between the hydraulic piston and accumulator on each side of the machine. Provisions were made to allow for bleeding any air in the hydraulic system at the point where the transducers were installed. Figure 8 illustrates the location of the transducer on the operator side.

The output from the transducer was fed into high and low gain amplifiers connected in series allowing gain factors ranging up to 25,000. From the amplifiers, the output was fed into a 14-channel Midwest Model 800 recording oscillograph.

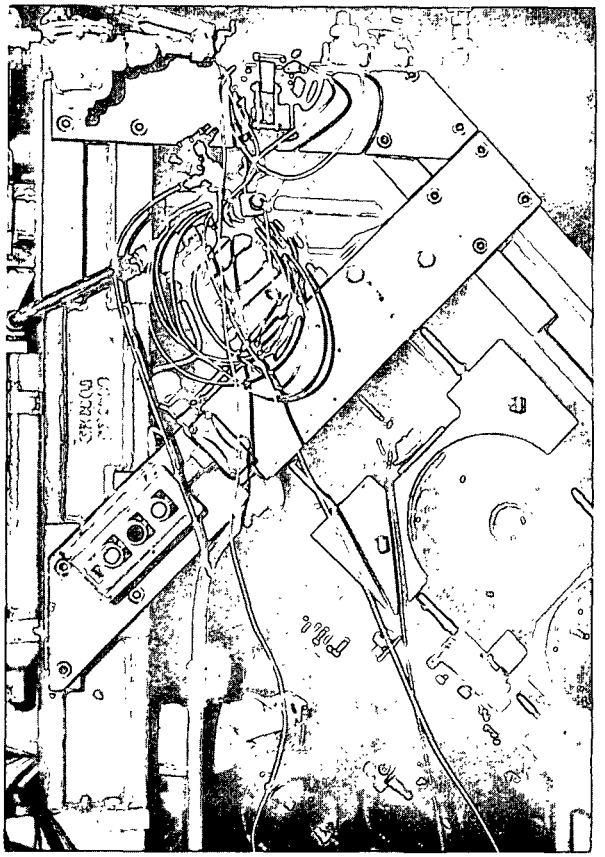

Pressure and Acceleration Transducers, Operator Side

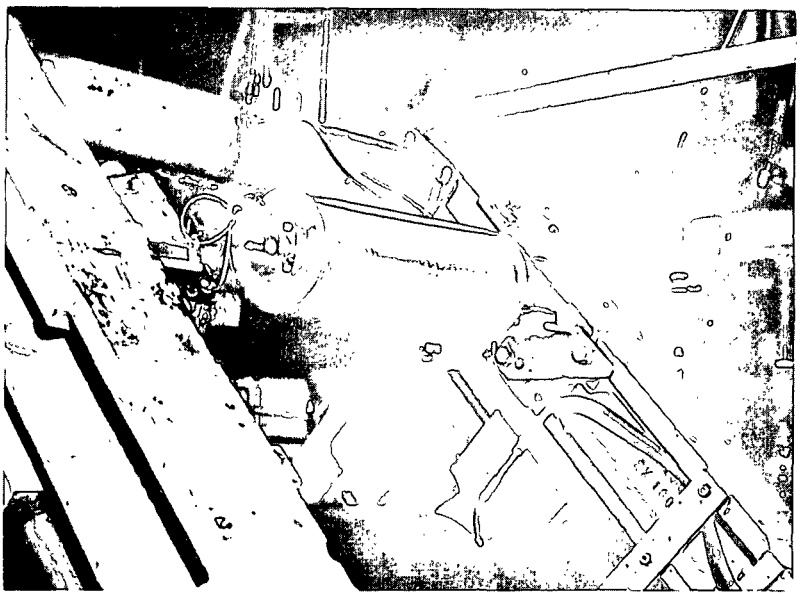

Web Tension

Figure 8. Location of Transducers

TOP CORRUGATING ROLL TRANSLATIONAL ACCELERATION MEASUREMENT

Two accelerometers with characteristics as follows were used:

Type:	Endevco 2217
Range:	to 1000 g., sinusoidal
Frequency response:	± 5%, 2 to 7000 Hz

The accelerometers were mounted on the top of the bearing blocks on each side of the machine. They were thermally and electrically isolated from the bearing block by means of one-inch thick (one-inch diameter) blocks of Micarta.

The accelerometers were connected to a Columbia Model 4101 charge follower. The output from the charge follower was fed into a low gain amplifier (gain factor 10 to 50) and then into the oscillograph galvanometers. Special shielding cable was installed over the cable leading from the accelerometers to the charge follower to eliminate stray electrical currents.

WEB TENSION MEASUREMENT

For the purpose of measuring web tension a special tension apparatus was installed on the corrugator after the main showers as shown in Fig. 8. The apparatus consisted of a 6-inch diameter roll weighing 7.3 lb. which was fixed to two sturdy cantilevered arms. The bases of the cantilevered arms were bolted to rigid support brackets which were in turn bolted to the main shower supports. The main shower supports rested on Unisorb shock pads to dampen out machine vibrations transmitted through the frame.

Two semiconductor strain gages (BLH, Type N) were installed on each arm so that one gage acted in tension and the other in compression when force

was applied to the end of the arm. The four gages were connected in a full wheatstone bridge configuration. An excitation power of 10 volts was supplied to the bridge. The output from the bridge was fed into a high and low gain amplifier connected in series allowing gain factors up to 25,000. From the amplifiers the signal was fed into the oscillograph galvanometers.

It may be remarked that the web tension measuring system was one which was used in a past study on the Institute's corrugator. For this study it was modified to increase its natural frequency so that more accurate tension measurements could be obtained. After modification, it appeared that the natural frequency of the strain gaged arms was near 1100 Hz. However, there was also an indication that the entire system exhibited a lower natural frequency. Therefore, caution must be exercised in interpreting the tension signals — particularly for frequencies above 500 Hz.

TIME SYNCHRONIZATION

In addition to the above, a Hewlett Packard frequency generator was set at 200 Hz, and the 200 Hz signal was recorded along one edge of each oscillographic trace. This provided a precise time measurement for checking the chart speed.

CALIBRATION

Calibration factors for the pressure measuring system were obtained by varying the hydraulic pressure control and observing the corresponding deflection of the pressure signal on the oscillograph record. The calibration was carried out for each gain setting used in the runs.

The calibration factors for the accelerometers were calculated from the manufacturers' literature.

The tension arm was calibrated by hanging weights from the fixed roll and observing the deflection of the tension signal on the oscillograph record. A correction factor was calculated to allow for the fact that the web entered the nip at an angle of about 6°20' from the vertical.

FABRICATION PROCEDURES

The operating conditions employed in the fabrication runs are outlined in Table I. In addition, the following operating conditions were employed for all runs:

1. Bottom roll pressure, p.s.i.
   - Operator side: 180
   - Drive side: 220
2. Accumulator pressure, p.s.i.
   - Operator side: 200
   - Drive side: 200
3. Finger clearance (relief style), in.: 0.016
4. Transfer to lower corrugating roll clearance, in.: 0.015

For each run the corrugator was brought up to the selected speed and the web tension was adjusted to the desired operating level (0.5 lb./in. for all but one run). The gain settings and balance for each transducer were then adjusted so as to obtain a reasonable amplitude (about one-inch deflection on the chart) and to space the five transducer signals across the chart paper. The recorder was then started and a small 3-mil aluminum shim faced with splicing tape was fed into the corrugator nip on the operator side of the web. As the shim passed between the rolls it forced the top corrugating roll up and caused a change in the transducer signals. This was done to relate the oscillographic

TABLE I

FABRICATION CONDITIONS

Run No.	Medium	Roll No.	Nominal Speed, f.p.m.	Top Corrugating Roll Pressure, p.s.i.		Web Tension, lb./in.	Shower Pressure, p.s.i.
				Operator Side	Drive Side		
1	26-lb., S.C., Mill A	14614	150	260	240	0.5	12-14
2	26-lb., S.C., Mill A	14614	225	260	240	0.5	12-14
3	26-lb., S.C., Mill A	14614	300	260	240	0.5	12-14
4	26-lb., S.C., Mill A	14614	375	260	240	0.5	12-14
5	26-lb., S.C., Mill A	14614	450	260	240	0.5	12-14
6	26-lb., S.C., Mill A	14644	300	260	240	0.5	12-14
7	26-lb., S.C., Mill A	14644	300	260	240	1.25	12-14
8	26-lb., S.C., Mill A	14644	300	120	100	0.5	12-14
9	26-lb., S.C., Mill A	14644	300	260	240	0.5	0
10	26-lb., S.C., Mill B	14646	150	260	240	0.5	12-14
11	26-lb., S.C., Mill B	14646	225	260	240	0.5	12-14
12	26-lb., S.C., Mill B	14646	300	260	240	0.5	12-14
13	26-lb., S.C., Mill B	14646	375	260	240	0.5	12-14
14	26-lb., S.C., Mill B	14646	450	260	240	0.5	12-14
15	33-lb., S.C., Mill A	5334	150	260	240	0.5	12-14
16	33-lb., S.C., Mill A	5334	300	260	240	0.5	12-14
17	33-lb., S.C., Mill B	5333	150	260	240	0.5	12-14
18	33-lb., S.C., Mill B	5333	300	260	240	0.5	12-14

recording to the single-faced board. For each run the length of the oscillograph record encompassed at least 120 flutes in most cases.

Moisture content measurements were obtained for each roll at the end of the runs. The moisture contents were as follows:

Roll No.	Moisture Content, %
14614	7.3
14644	6.1
14646	6.0
5334	6.6
5333	6.2

DATA REDUCTION

The oscillograph record for each run contained two top corrugating roll pressures, two top roll accelerations, one tension, and one timing signal encompassing at least 120 consecutive flutes. As mentioned previously, during the corrugating operation a small thin aluminum shim was placed on the medium just before the medium entered the corrugating labyrinth. As the shim passed through the labyrinth it raised the top roll slightly and produced a momentary shift in the signal levels. When the records were examined after each run, the location on the record corresponding to the shim location was noted. The starting point on the record was then determined by counting forward ten flutes from the point where the disturbance on the record indicated that the shim had emerged from the labyrinth. The ten-flute allowance appeared to be sufficient to avoid inclusion of any aftereffects of the disturbance caused by passage of the shim in analysis of the record or in the high-low measurements on the single-faced board. Using the above procedure, it is believed that the oscillograph records and high-low measurements were synchronized to within about one flute.

The time signal trace on each record was then analyzed to obtain an indication of the actual speed of the recorder. Those speeds were used to convert distance measurements on the chart to time.

The analog signals on each chart were then digitized, i.e., beginning at the starting point as defined above, readings were obtained of the magnitude of each signal at equally spaced time intervals over the length of chart corresponding to 120 flutes. The digitizing was performed by Computrex Computer Centres, Ltd., Calgary, Alberta, Canada. They used a Calma 485 digitizer and recorded the data on 800 bpi. nine-track tape.

The choice of digitizing interval involved consideration of several factors — namely, maximum frequency of interest (Nyquist cut-off frequency), resolution, statistical reliability, and cost. When continuous data are converted into discrete data, the maximum frequency which can be detected is determined as follows (12):

$$f_c = 1/2h \qquad (2)$$

where

f_c = Nyquist cut-off frequency, Hz

h = time interval between samplings, sec.

Thus, the smaller h is, the higher will be the cut-off frequency. Reference (12) suggests that f_c should be 1.5 to 2.0 times greater than the maximum frequency of interest. For this study, it appeared that the maximum frequency of interest would be twice the flute-forming frequency. Accordingly, the time increment h was selected so that f_c would be approximately four times greater than the flute-forming frequency for all runs with the exception of Run 6. In the case of Run 6, h was halved so that frequencies up to eight times the flute-forming frequency could be analyzed if needed. For 120 flutes the above procedure resulted in 960 readings per signal (eight data points per flute per signal) when h was chosen to make f_c approximately four times greater than the flute-forming frequency and 1920 readings per signal for Run 6.

Frequencies greater than f_c are aliased. This means that any higher frequencies in the data are confounded with frequencies below f_c. For example, a significant frequency component at five times the flute-forming frequency would appear as a component at three times the flute-forming frequency; a component at six times the flute-forming frequency would appear as a component at twice the flute-forming frequency, etc. One method which can be used to avoid this aliasing

is to filter the data prior to digitizing so that information contained in the signal above f_c is no longer present in the data. However, the instrumentation required to pursue this approach was not available for this study.

Further considerations involved in the selection of the digitizing interval (and hence, cut-off frequency) and number of observations involve statistical reliability. For spectral calculations, Reference (12) indicates that the normalized standard error (ε) and the degrees of freedom n are given by the following expressions

$$\varepsilon = 1/(B_e\ h\ N) \qquad (3)$$

$$n = 2N\ B_e\ h \qquad (4)$$

where

N = number of observations

n = degrees of freedom

h = time increment between data values

B_e = equivalent resolution band width

Band width is related to the minimum frequency interval to be resolved. Equations (3) and (4) show that if high resolution (small B_e) is desired then either h or N or both must be made large to maintain a low standard error or high number of degrees of freedom. Similarly, if h is made small to achieve a high cut-off frequency, then a large band width or N would be required to maintain a low standard error. Thus, in practice a compromise between resolution, cut-off frequency, and N is usually necessary.

For the spectral analyses of the digitized signals, N was constant at 960. In the spectral analyses, the product of $B_e hN$ was selected so as to give a standard error of about 0.3 or about 20 degrees of freedom.

The power spectrums for the flute height differences were based on 119 values. In most analyses, the band width was selected so as to provide spectral density estimates over 18 frequency intervals between zero and the upper frequency limit (half the flute-forming frequency). The number of degrees of freedom was only about seven. For improved sensitivity and reliability, a considerably greater number of flute height observations would have been desirable.

When the data were digitized the recorded readings in terms of chart divisions were multiplied by appropriate calibration factors. These factors are shown in Table II for the runs which were digitally processed. Because of cost considerations it was not possible to digitize the records for all runs.

After converting the oscillograph records to digital form the data for each signal were averaged. The observed value at each time was then subtracted from the average to give a residual deviation corresponding to the instantaneous fluctuations of the signal about the average level. This was necessary in the case of the pressure and tension signals because the true zero was off the chart scale and, hence, was not known.

TABLE II

DIGITAL SAMPLING INCREMENTS AND CALIBRATION FACTORS

Run	Nominal Corr. speed, f.p.m.	Nominal Flute Frequency, Hz	Chart Speed, in./sec.	Sampling Increment, usec.	Calibration Factors: Pressure, p.s.i./div. Op. Side	Pressure, p.s.i./div. Dr. Side	Tension, lb./in./div.	Acceleration, g./div. Op. Side	Acceleration, g./div. Dr. Side
1[a]	150	90	29.64	1447	1.29	1.00	0.083	0.320	0.320
2[a]	225	135	74.12	900	0.70	0.46	0.083	0.320	0.320
3[a]	300	180	73.81	680	1.29	0.46	0.083	0.320	0.320
4	375	225	73.82	530	1.29	0.46	0.083	0.727	0.727
5	450	270	73.76	446	2.65	1.00	0.370	0.727	0.727
6	300	180	73.89	385.5[b]	1.29	0.46	0.083	0.320	0.320
7	300	180	73.88	700	1.29	0.46	0.083	0.320	0.320
8	300	180	73.94	667	1.29	0.46	0.215	0.320	0.320
9	300	180	73.75	673	1.29	0.46	0.083	0.320	0.320
12	300	180	73.63	680	1.29	1.00	0.215	0.320	0.320
14	450	270	73.89	447	2.65	2.50	0.370	0.727	0.727
16	300	180	74.02	677	1.29	1.00	0.215	0.320	0.320
18	300	180	73.62	664	1.00	2.50	0.215	0.320	0.320

[a] Only tension, operator side pressure and acceleration signals digitized.

[b] Corresponds to a cut-off frequency equal to eight times the flute-forming frequency.

TEST PROCEDURES

For each run the samples of single-faced board were evaluated to determine their flute heights. The measurements were started on the tenth flute from the end of the aluminum flagging shim and continued to give a total of 120 flute height readings (88 flutes in the case of Run 2). Measurements were made on both operator and drive sides.

DISCUSSION OF RESULTS

FLUTE HEIGHT DIFFERENCES

During each fabrication run the single-faced board was flagged for later synchronization with the recorded fluctuations in top corrugating roll pressure, acceleration, and web tension. The samples of single-faced board were evaluated for flute height by measuring the heights of 120 consecutive flutes on the operator and drive side of each sample. For Run 2, only 88 flutes were measured because the oscillographic record did not extend over the full 120 flutes. Average flute height differences were calculated by taking the absolute difference between each pair of consecutive flutes and averaging the 119 (or 87, Run 2) differences so obtained. Thus, the average difference is a measure of high-low flute formation.

A summary of the flute height results is shown in Table III for the runs which were analyzed in detail. It should be kept in mind that the flute height differences (termed Av. Diff. in Table III) tend to have wide confidence limits despite the large number of measurements included in each average. For 120 measurements the data in Reference (2) indicate the 95% confidence limits would be about ± 25% or slightly greater. Thus, small differences in the Av. Diff. between runs are probably not statistically significant.

In general, it may be noted that the drive side exhibited greater flute height differences (high-lows) than the operator side in 12 of the 13 comparisons. It is not surprising that a difference exists between operator and drive sides because the motion of the top corrugating roll on the drive side must be affected to some extent by the steam piping. This is not to say that high-lows must necessarily always be higher on the drive side as it probably depends on the condition of the corrugator and other factors.

TABLE III

FLUTE HEIGHT RESULTS

Run	Nominal Speed, f.p.m.	Corrugating Conditions	Actual Flutes per Sec.	No. of Flutes	Operating Side: Av. Diff., pt.	Operating Side: Av. Flute Height, pt.	Operating Side: Percent of Diff. Less than 3 pt.	Drive Side: Av. Diff., pt.	Drive Side: Av. Flute Height, pt.	Drive Side: Percent of Diff. Less than 3 pt.
				26-lb. Semichemical Medium, Mill A						
1	150	Std.	88.9	120	1.01	193.3	98.3	1.15	194.2	96.6
2	225	Std.	139.0	88	1.12	194.6	96.6	1.79	194.5	85.7
3	300	Std.	184.0	120	1.47	194.2	86.6	1.70	194.3	85.7
4	375	Std.	226.0	120	1.43	194.6	89.1	1.72	194.4	84.9
5	450	Std.	280.0	120	1.41	194.6	90.8	1.41	194.7	91.6
6	300	Std.	186.0	120	1.53	195.1	88.2	1.91	195.1	79.0
7	300	Hi Tens.	178.8	120	1.13	193.2	98.3	2.11	193.4	76.5
8	300	Hi Pres.	187.2	120	1.66	194.4	86.6	2.15	193.5	71.4
9	300	No Show.	185.8	120	1.44	195.7	85.7	2.63	195.8	62.2
				26-lb. Semichemical Medium, Mill B						
12	300	Std.	183.8	120	1.06	194.2	100.0	1.59	194.2	86.6
14	450	Std.	279.7	120	1.57	193.9	86.6	1.84	193.8	79.8
				33-lb. Semichemical Medium, Mill A						
16	300	Std.	184.6	120	1.58	195.6	85.7	2.24	195.1	70.6
				33-lb. Semichemical Medium, Mill B						
18	300	Std.	188.1	120	1.81	196.7	84.9	2.37	196.5	68.9
Av.					1.40	194.6		1.89	194.6	

A typical high-low pattern is illustrated in Fig. 9 for Run 3 (300 f.p.m.). In Fig. 9, the algebraic differences in height ($\underline{H}$) between consecutive flutes ($\underline{H}_{\underline{n}} - \underline{H}_{\underline{n}+1}$) are graphed from $\underline{n} = 1$ to $\underline{n} = 119$, i.e., over 120 consecutive flutes. The differences display the well-known high-low pattern, i.e., they tend to be alternatively positive and negative. At sporadic intervals the pattern reverses. The magnitudes of the differences fluctuate in an apparently irregular or random manner.

At 300 f.p.m. the nominal flute-forming frequency is 180 flutes per second for A-flute corrugations (36 flutes/foot). In Run 3 the actual flute-forming frequency was about 184 flutes per second corresponding to a speed slightly in excess of 300 f.p.m. Thus, the flutes were being formed at a rate of about one every 0.0054 sec. in Run 3. Viewed in this way, the flute height readings form a time series in which each height reading is separated by a constant time interval (0.0054 sec. in this instance).

To obtain information relative to the frequency behavior of the flute height differences, power spectrums were obtained for Run 1 through 9. The power spectrums for the flute height differences for Run 3 are shown in Fig. 10 and 11 for the operator and drive sides, respectively. (Note: The natural logarithms of the spectral densities are plotted because this results in a constant confidence interval.) It may be noted that the spectral density is highest in both graphs at a frequency of about 92 Hz, i.e., at half the flute-forming frequency (184 Hz) for this run. This is caused by the high-low pattern in the flute height readings. The power spectral densities decrease rapidly as the frequency decreases from 92 Hz and no peaks, which would indicate significant variations at intermediate frequencies, are present. The differencing operation removes the power at zero

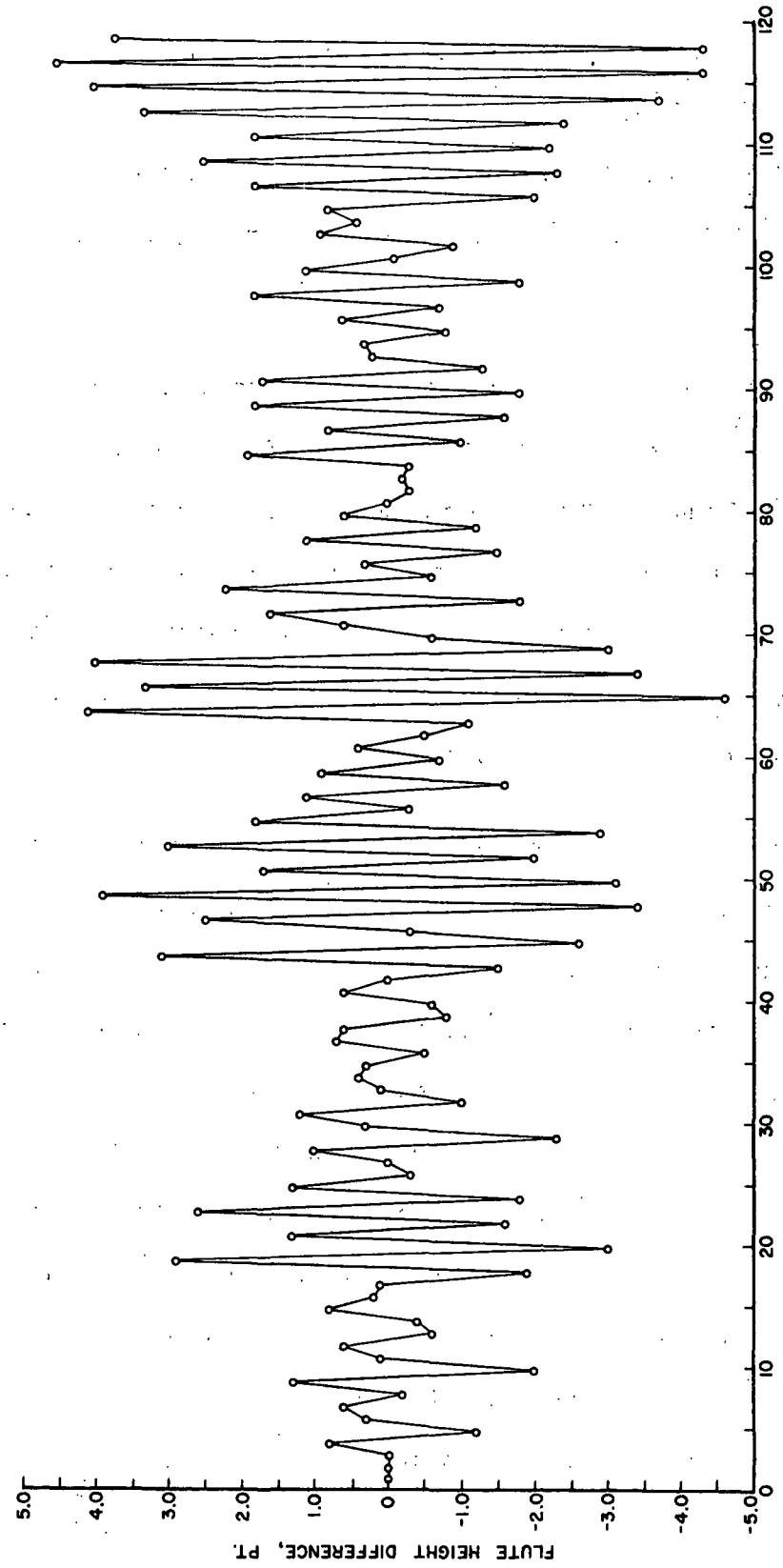

Figure 9. Flute Height Differences vs. Difference Number (Run 3, Operator Side)

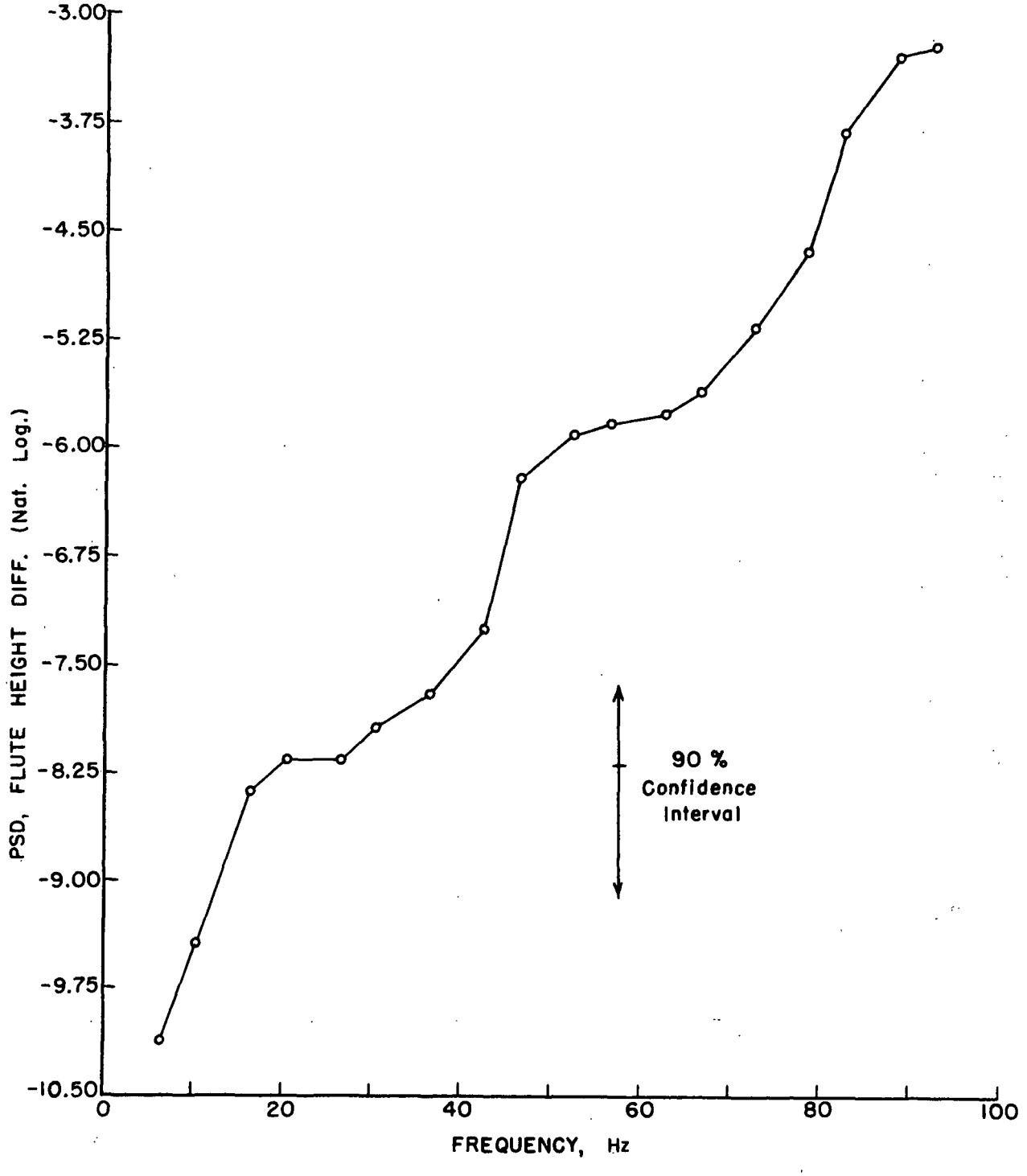

Figure 10. Power Spectral Density (PSD) of Flute Height Differences vs. Frequency (Run 3, Operator Side)

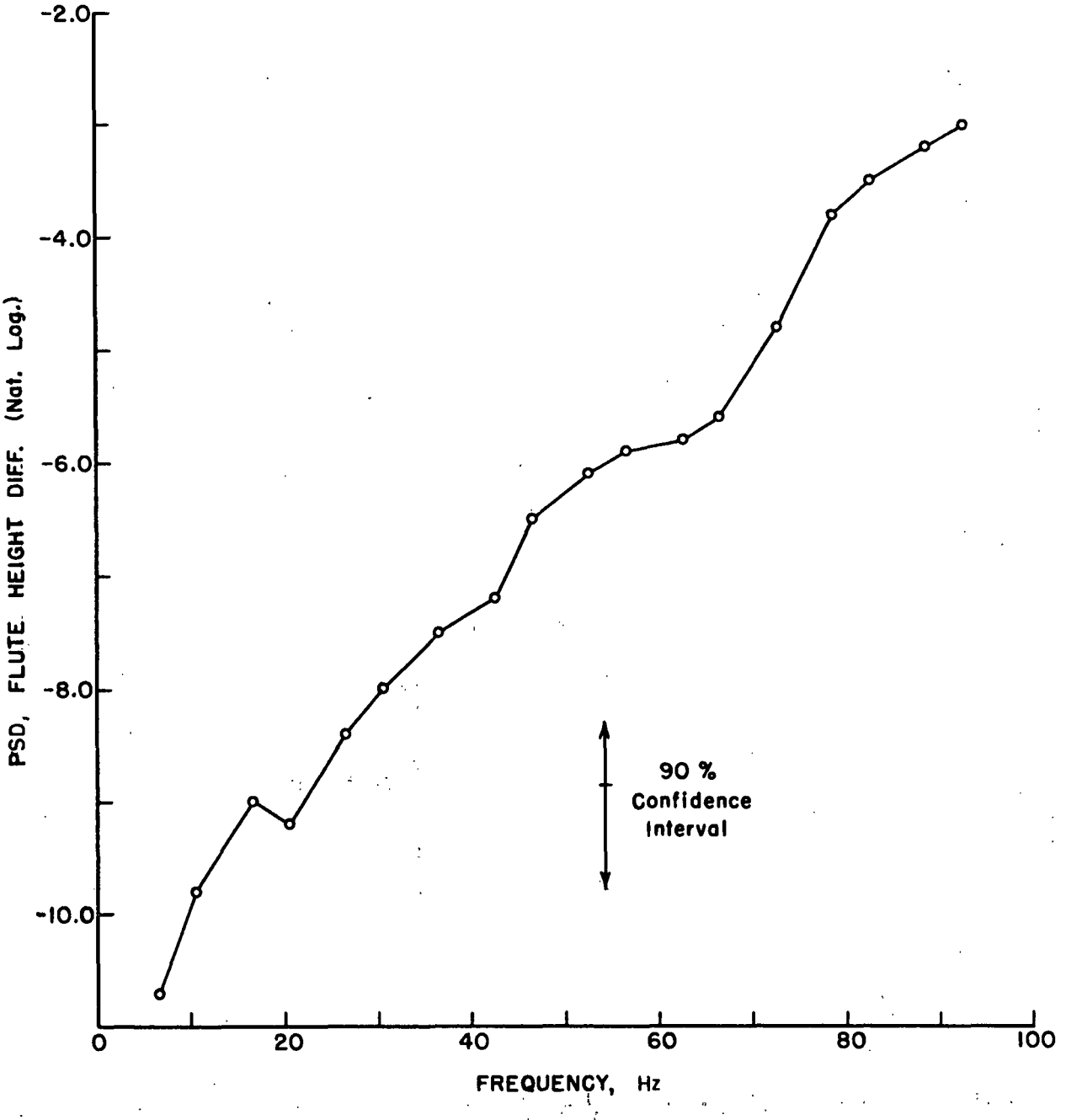

Figure 11. Power Spectral Density (PSD) of Flute Height Differences vs. Frequency (Run 3, Operator Side)

frequency and diminishes power at frequencies near zero (see Appendix I), and this accounts for the low spectral densities as zero frequency is approached.

To investigate the nature of the power spectrum at low frequencies such as might be associated with corrugating roll rotation or out-of-roundness of the corrugating medium roll would require a much longer record of flute heights than were obtained for this study.

The power spectrums in Fig. 10 and 11 were obtained using 18 lags, i.e., the spectral densities were determined at 18 frequency levels in addition to zero. Inasmuch as there were only 119 differences the number of degrees of freedom is about seven, hence the confidence limits about any point are relatively broad. The 90% confidence interval shown was estimated using the procedure given by Granger (13). Taking the confidence interval into consideration and the logarithmic PSD scale, it appears that much of the high-low variation has the appearance of being concentrated at frequencies at about half the flute-forming frequency.

Very similar power spectral graphs were obtained for all of the runs which were analyzed in this way. Further information on the nature of high-low variation is obtained from the autocorrelation function. Autocorrelograms are shown in Fig. 12 and 13 for the operator and drive side flute heights, respectively, for Run 3. As mentioned previously, the shape of the autocorrelogram is quite different for periodic and random variations. Used in this way it is possible to determine whether the variations in a given series are periodic or random.

Referring to the figures there are several features of the diagrams that are of importance as follows: First, the autocorrelation function in both plots decay rapidly to near zero for modest increases in time lag. The time interval between successive positive points is 0.0108 sec. which corresponds to half the

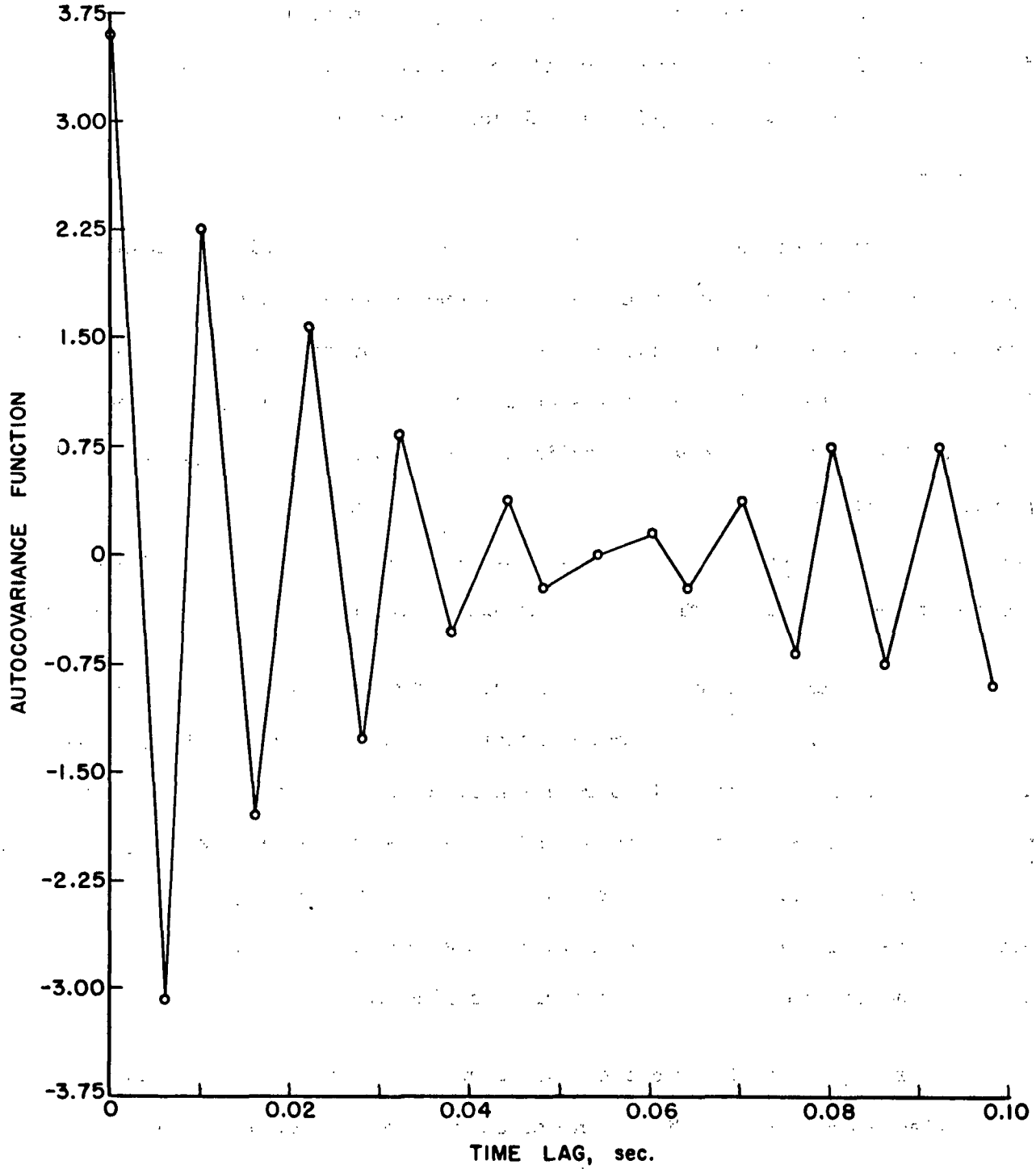

Figure 12. Autocovariance Function vs. Time Lag for Drive Side Flute Height Differences (Run 3)

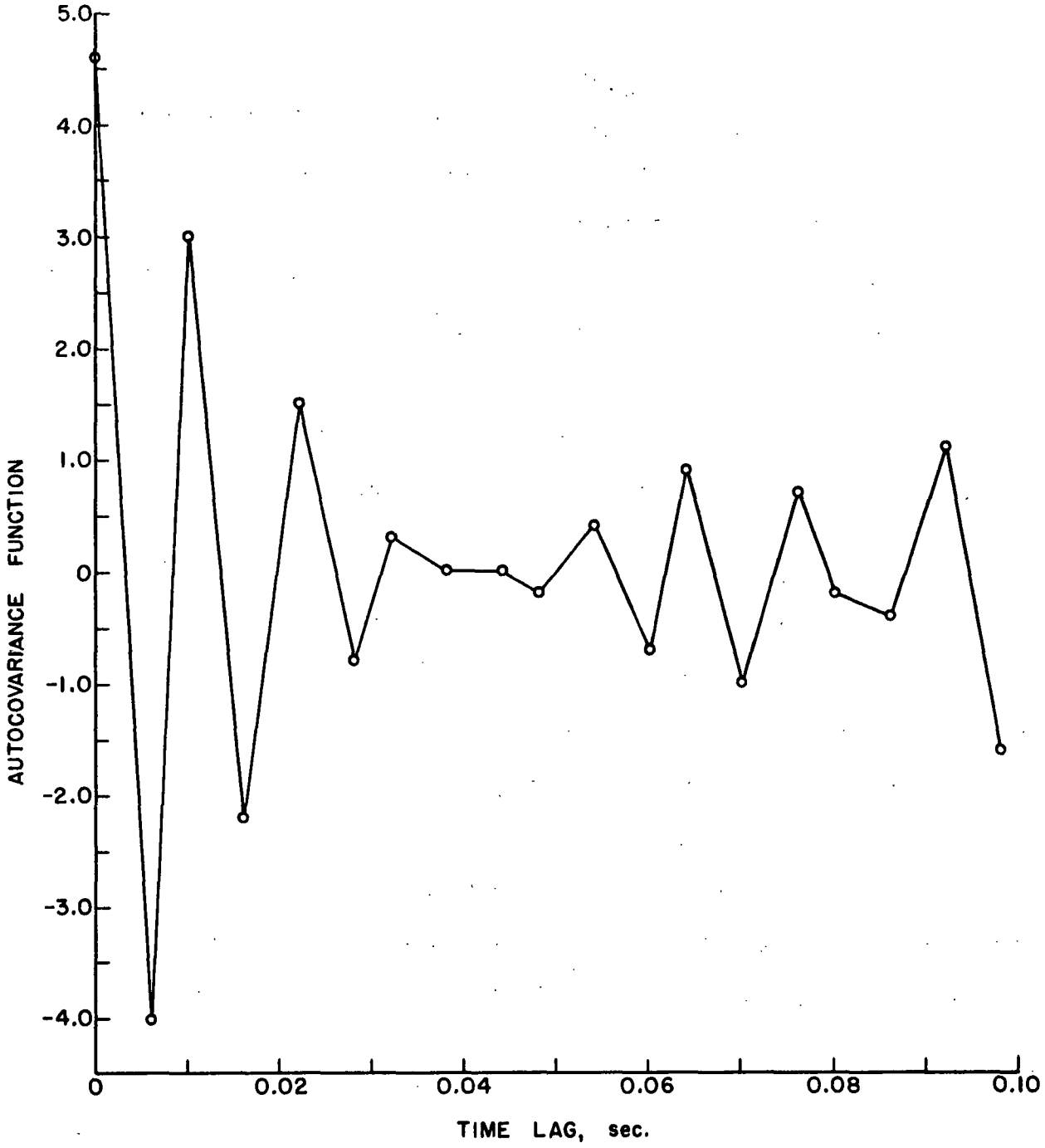

Figure 13. Autocovariance Function vs. Time Lag for Drive Side Flute Height Differences (Run 3)

flute frequency. The rapid decay indicates that the flute height differences which contribute so significantly to the power spectrum near half the flute-forming frequency are random in nature. They probably correspond to narrow band random vibration.

Second, in both diagrams there is a tendency for the points to diverge or oscillate about zero at the longer time lags. In a purely random series the autocorrelation function approaches zero as the time lag becomes large. It is not clear whether the deviations from zero at the longer time lags are statistically significant. However, they suggest there may be low-frequency variations in flute height differences of a periodic nature. While beyond the scope of this study, it would be of interest to determine the causes of such periodic variations. They might arise from such factors as medium roll out-of-roundness, corrugating roll or idler roll unbalance, etc.

Third, it may be noted, that starting at zero time lag, the autocorrelation function oscillates in a sawtooth fashion — positive to negative to positive, etc. This pattern was evident in the autocorrelograms for all the runs which were analyzed (nine in all). Box and Jenkins (7) indicate that this type of pattern is characteristic of certain types of autoregressive processes. An autoregressive process is one in which the current value of the process is dependent upon a combination of previous values of the process plus a random shock or component. For example, autoregressive processes of the first and second order would be defined as follows:

First order. $$d_t = \phi_1 d_{t-1} + a_t \quad (5)$$

Second order. $$d_t = \phi_1 d_{t-1} + \phi_2 d_{t-2} + a_t \quad (6)$$

where

d_t, d_{t-1}, d_{t-2} = values of process at times t, $t-1$, and $t-2$

ϕ_1, ϕ_2 = adjustable parameters

a_t = random shock component at time, t

Thus, in the first order process the value at time, t, is dependent on the previous value and the random component at time, t. The second order process involves the two previous process values. In general, the parameters ϕ_1, ϕ_2, etc., must satisfy certain conditions. For example, for the first order process, ϕ_1 must be less than unity for a stationary process. The parameters ϕ_1, ϕ_2, etc., can be estimated from the autocorrelation coefficients which are dependent on the autocovariance values at each lag. Thus, the autocorrelation coefficient at lag_n is obtained by dividing the autocovariance value at lag_n by the autocovariance value at zero lag.

Autocorrelation coefficients for the flute height differences are tabulated in Table IV for Runs 1 through 5. In these runs the speed was increased from 150 f.p.m. for Run 1 to 450 f.p.m. for Run 5. Table V summarizes results obtained for Runs 6 through 9 where various operating conditions were changed. For every run the autocorrelation coefficients alternate from positive to negative as they decay toward zero. This type of pattern is obtained with first order autoregressive processes when ϕ_1 has a large negative value. Also, in this case, the power spectrum would be similar to those obtained in this study, i.e., the spectral densities would peak at half the flute-forming frequency. Thus, as a first approximation it appears that high-lows behave as a first order autoregressive process. However, it is possible that more detailed analysis would reveal that higher order autoregressive models or other models incorporating autoregressive and moving average features better describe the high-low process.

TABLE IV

AUTOCORRELATION COEFFICIENTS OBTAINED AT VARIOUS CORRUGATING SPEEDS

Lag[a] No.	Autocorrelation Coefficient							
	Run 1 — 150 f.p.m.		Run 2 — 225 f.p.m.	Run 3 — 300 f.p.m.		Run 4 — 385 f.p.m.	Run 5 — 450 f.p.m.	
	Op. Side	Dr. Side	Op. Side	Op. Side	Dr. Side	Op. Side	Op. Side	Dr. Side
0	1.0	1.0	1.0	1.0	1.0	1.0	1.0	1.0
1	-0.796	-0.781	-0.828	-0.854	-0.877	-0.907	-0.836	-0.856
2	0.504	0.458	0.646	0.629	0.652	0.792	0.546	0.623
3	-0.336	-0.263	-0.548	-0.499	-0.470	-0.752	-0.333	-0.466
4	0.200	0.150	0.415	0.426	0.321	0.716	0.192	0.340
5	-0.084	-0.088	-0.315	-0.345	-0.183	-0.656	-0.093	-0.268
6	0.001	0.027	0.269	0.228	0.064	+0.574	0.020	0.242
7	0.020	0.000	-0.191	-0.147	0.000	-0.486	0.030	-0.192
8	-0.030	-0.015	+0.107	0.108	-0.001	0.409	-0.070	0.128
9	0.047	0.051	-0.065	-0.067	-0.043	-0.328	0.080	-0.115
10	-0.074	-0.097	+0.024	0.008	0.095	0.223	-0.041	0.127
11	0.105	0.159	+0.001	0.041	-0.151	-0.143	-0.041	-0.096
12	-0.083	-0.195	-0.032	-0.062	0.200	0.090	0.124	0.004
13	0.015	0.160	+0.057	0.111	-0.209	-0.021	-0.168	0.066
14	0.044	-0.117	-0.034	-0.188	0.158	-0.072	0.129	-0.080
15	-0.080	0.107	+0.005	0.213	-0.049	0.161	-0.028	0.078
16	0.121	-0.116		-0.202	-0.094	-0.222	-0.048	-0.035
17	-0.154	0.135		0.212	0.242	0.272	0.075	-0.035
18	0.164	-0.124		-0.253	-0.342	-0.320	-0.085	0.092

[a] Lag time constants were 0.0112, 0.0072, 0.0054, 0.0044, and 0.0036 sec. for Runs 1 through 5, respectively.

TABLE V

AUTOCORRELATION COEFFICIENTS OBTAINED
UNDER VARIOUS OPERATING CONDITIONS

Lag[a] No.	Autocorrelation Coefficient							
	Run 6 Standard Conditions		Run 7 High Tension		Run 8 Low Pressure		Run 9 No Shower Steam	
	Op. Side	Dr. Side	Op. Side	Dr. Side	Op. Side	Dr. Side	Op. Side	Dr. Side
0	1.000	1.000	1.000	1.000	1.000	1.000	1.000	1.000
1	-0.867	-0.874	-0.716	-0.851	-0.818	-0.776	-0.783	-0.888
2	0.618	0.664	0.283	0.589	0.516	0.411	0.439	0.679
3	-0.397	-0.497	-0.060	-0.392	-0.279	-0.171	-0.173	-0.526
4	0.223	0.383	-0.019	0.268	0.079	0.057	-0.017	0.433
5	-0.112	-0.319	0.007	-0.203	0.056	0.028	0.105	-0.345
6	0.036	0.251	0.044	0.185	-0.152	-0.114	-0.173	0.232
7	0.030	-0.171	-0.138	-0.185	0.003	0.141	0.184	-0.118
8	-0.051	0.087	0.146	0.162	-0.321	-0.151	-0.150	0.054
9	0.014	-0.004	0.016	-0.163	0.298	0.158	0.106	-0.058
10	0.045	-0.090	-0.170	0.213	-0.208	-0.139	-0.024	0.074
11	-0.073	0.170	0.197	-0.279	0.087	0.097	-0.073	-0.041
12	0.056	-0.233	-0.218	0.324	0.006	-0.051	0.121	-0.005
13	-0.023	0.279	0.299	-0.311	-0.049	0.033	-0.110	-0.004
14	-0.020	-0.309	-0.349	0.257	0.074	-0.028	0.074	0.053
15	0.060	0.345	0.291	-0.231	-0.105	-0.017	-0.049	-0.097
16	-0.106	-0.373	-0.177	0.261	0.125	0.028	0.055	0.113
17	0.167	0.381	0.157	-0.310	-0.107	0.071	-0.053	-0.109
18	-0.188	-0.358	-0.169	0.337	0.056	-0.204	0.065	0.107

[a] Lag time constant was 0.0054 sec. Corrugating speed was 300 f.p.m. for all runs.

Assuming a first order autoregressive model, an estimate of the magnitude of ϕ_1 is provided by the autocorrelation coefficient at lag 1. For example, for Run 1, operator side, the model would be

$$d_t = -0.796\, d_{t-1} + a_t \qquad (7)$$

where

$\underline{d}_t$, $\underline{d}_{t-1}$ = flute height differences at $\underline{t}$ and $\underline{t}$-1, pt.

$\underline{a}_t$ = random component

Thus, on the average, Equation (7) indicates that the difference in height at time, $\underline{t}$, is equal to -0.796 times the previous difference plus an additive component $\underline{a}_t$.

Before discussing the possible nature of $\underline{a}_t$ it may be noted that the coefficients at lag 1 in Tables IV and V vary from -0.716 to -0.907 and average -0.832. The changes in coefficient are relatively small considering the flute height differences between runs, the range of operating speeds, and the changes in operating conditions. There also appears to be no obvious relationship between the coefficient and the average level of flute height differences.

Thus, it appears that flute height differences on the Institute's corrugator exhibit behavior characteristic of an autoregressive process in which the coefficient ϕ_1 is highly negative and nearly a constant. The cause for such behavior is not known. However, it might arise if different lengths of medium are drawn into the labyrinth as alternate flutes are formed or if alternate flutes do not properly come into mesh at the pressure roll. There are objections to either explanation but both would tend to account for the dependence of a given flute height on the height of the previous flute.

As mentioned previously, the high-speed motion pictures discussed in Report Eight, Project 1108-22, appeared to indicate that the flutes fall off the fingers in a nonuniform high-low manner as the corrugated medium enters the pressure roll nip. Hence, they contact the liner on the pressure roll at slightly different times or distances from the nip, and this may possibly affect the way in which they mesh in the pressure roll nip.

Pursuing this viewpoint, the irregular variations in flute height from flute-to-flute would be associated with the random factor $\underline{a}_{\underline{t}}$. This could reflect local variations in the properties of the medium and the forces imposed on the medium in the labyrinth during the formation of each flute.

In the preceding analyses, the flute heights were differenced before analyses. As mentioned previously, the differencing operation removes any low-frequency trend in the data. Hence, it facilitated analysis of the high-low pattern. However, the attenuation of low frequencies makes it difficult to detect low-frequency variations in the data. Analysis of the undifferenced flute height observations avoids this difficulty. In this study, only 120 flutes were measured. This corresponds to slightly more than one revolution of the top corrugating roll. Thus, frequencies related to roll revolution, or lower frequencies could not be studied. Longer flute height records would be required to evaluate whether such frequency components are present.

With the foregoing in mind, Fig. 14 shows the power spectra obtained for the undifferenced flute height readings for Run 3. The power spectra suggest there may be low-frequency variations present in the flute height readings, e.g., on the operator side a component having a frequency near 20 Hz may be present. On the drive side the spectral densities increase steadily from about 20 to 0 Hz. However,

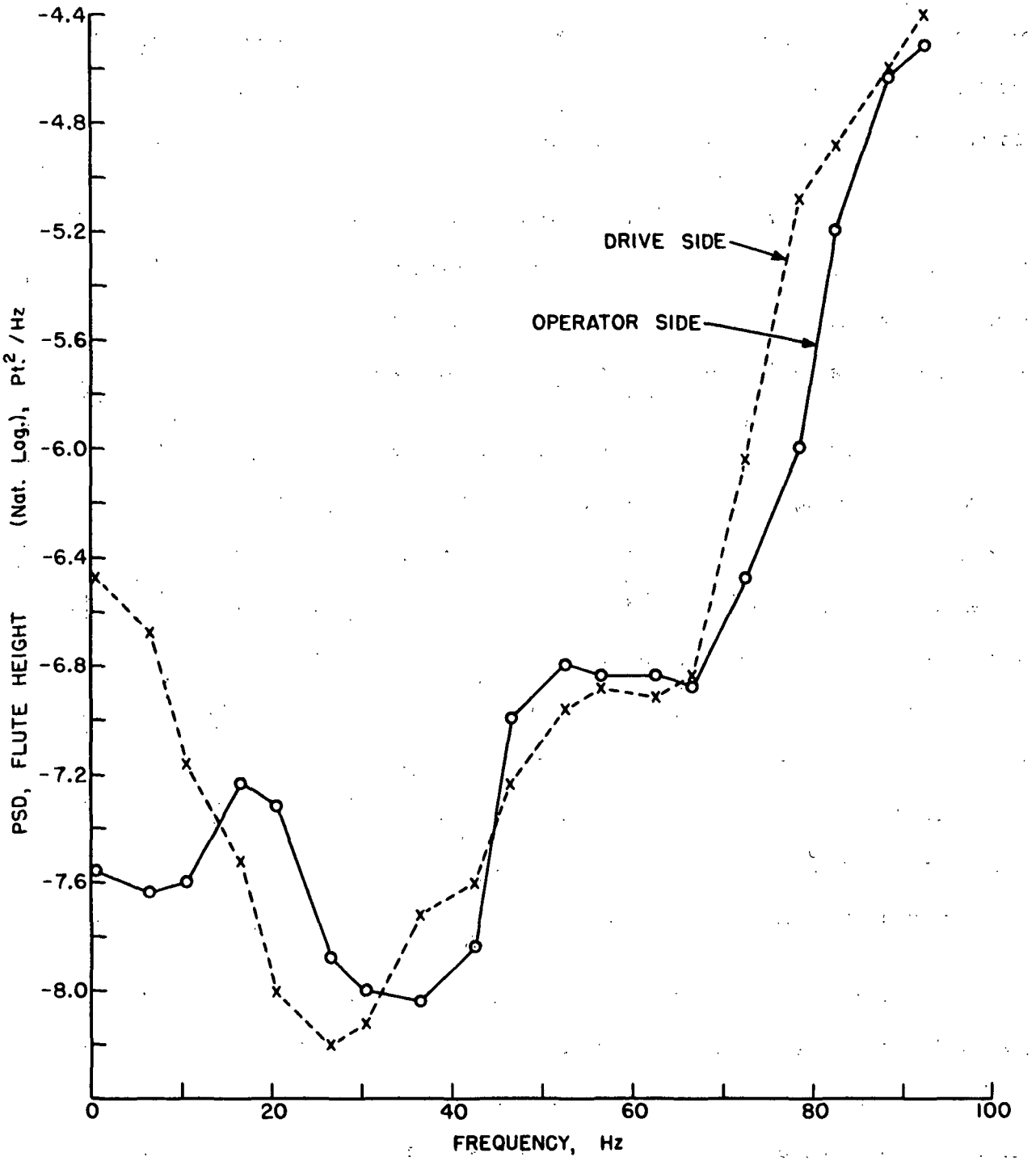

Figure 14. Power Spectral Density (PSD) of Flute Heights vs. Frequency for Run 3

because the spectra are based on only 120 readings, it is difficult to identify statistically significant components. For this reason, a detailed analysis of this type was not pursued for all runs.

GENERAL APPEARANCE OF MEASURED VARIABLES

For each fabrication run, an oscillograph record was obtained showing the fluctuations in the following variables:

1. Top corrugating roll pressure
2. Top corrugating roll acceleration along the plane passing through the roll centers
3. Corrugating medium web tension.

To illustrate the general appearance of the oscillograph records, a tracing of a short section of the record for Run 3 is shown in Fig. 15. The corrugating speed for Run 3 was approximately 300 f.p.m. corresponding to a flute-forming frequency of 180 Hz.

In general, the signals exhibit a major frequency component corresponding to the flute-forming frequency. This occurs because of the gear action of the corrugating rolls.

Oscillations at a frequency corresponding to twice the flute-forming frequency are particularly noticeable in the drive side pressure and acceleration signals. This may be termed the second harmonic of the flute-forming frequency. High frequency oscillations are also present in many cases. For example, the operator side pressure signal displays a noticeable fourth harmonic frequency component which appears to vary somewhat in amplitude and/or phase from flute-to-flute. The fourth harmonic corresponds to a frequency of about 720 Hz (4 x 180 Hz) at this speed.

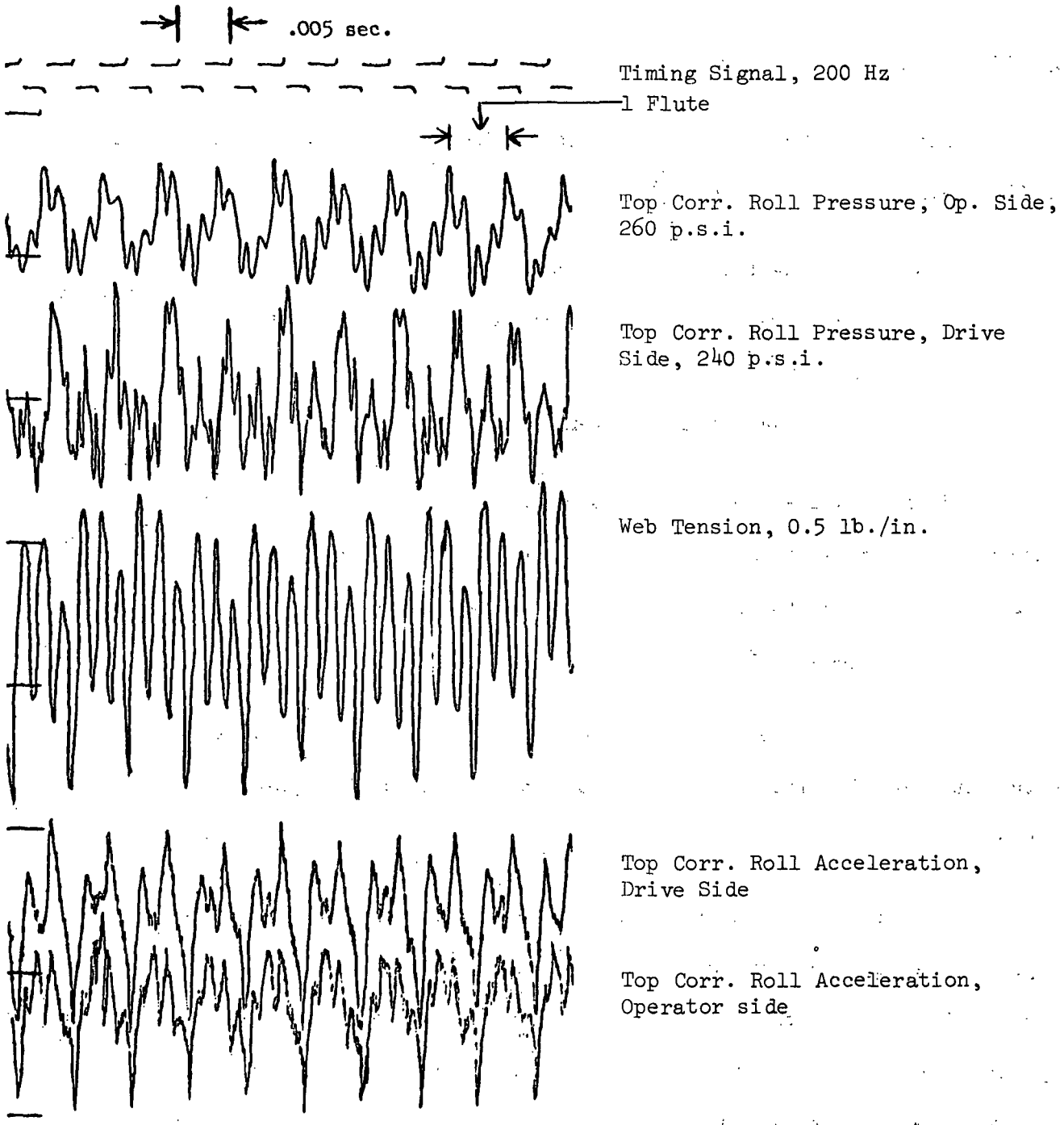

Figure 15. Oscillograph Record of Run 3. Nominal Corrugating Speed 300 f.p.m.

As mentioned previously, each oscillograph record of the type shown in Fig. 15 was digitized by reading values from each variable (signal) at constant time increments over a period corresponding to 120 flutes. The resulting data were then analyzed using (a) power spectral density techniques to determine the frequency content of the signals and (b) Fourier analyses techniques to determine the amplitudes and phases of the significant components.

POWER SPECTRAL DENSITY ANALYSES

Each signal from each run was analyzed to identify the important frequency components in the range from zero to four times the flute-forming frequency (F). Preliminary analyses indicated that the amplitudes of the components at F and its harmonics were so great as to introduce numerical instability in the spectral density calculations. To reduce this problem, the digitized data for each signal were "prewhitened" using the special digital filter described in Appendix I. This filter moderately reduced the power at F and its harmonics. The power spectrum of the "prewhitened" signal was then calculated and "recolored" to allow for the effect of the "prewhitening" filter. Discussions of "prewhitening" and "recoloring" techniques may be formed in References (11) and (13).

Top Roll Acceleration Power Spectrums

The up-and-down acceleration of the top corrugating roll is one of the factors affecting the molding force on the medium. Its units in this study are expressed in terms of multiples of the gravitational acceleration, g, where g equals 386 in./sec.^{2} For example, an acceleration of 193 in./sec.^{2} equals 0.5 g. The force at any instant due to the up-and-down acceleration of the top roll will equal the mass of the upper roll (including bearing blocks and bearings) times the acceleration. Mass equals weight divided by g; hence, the force may be

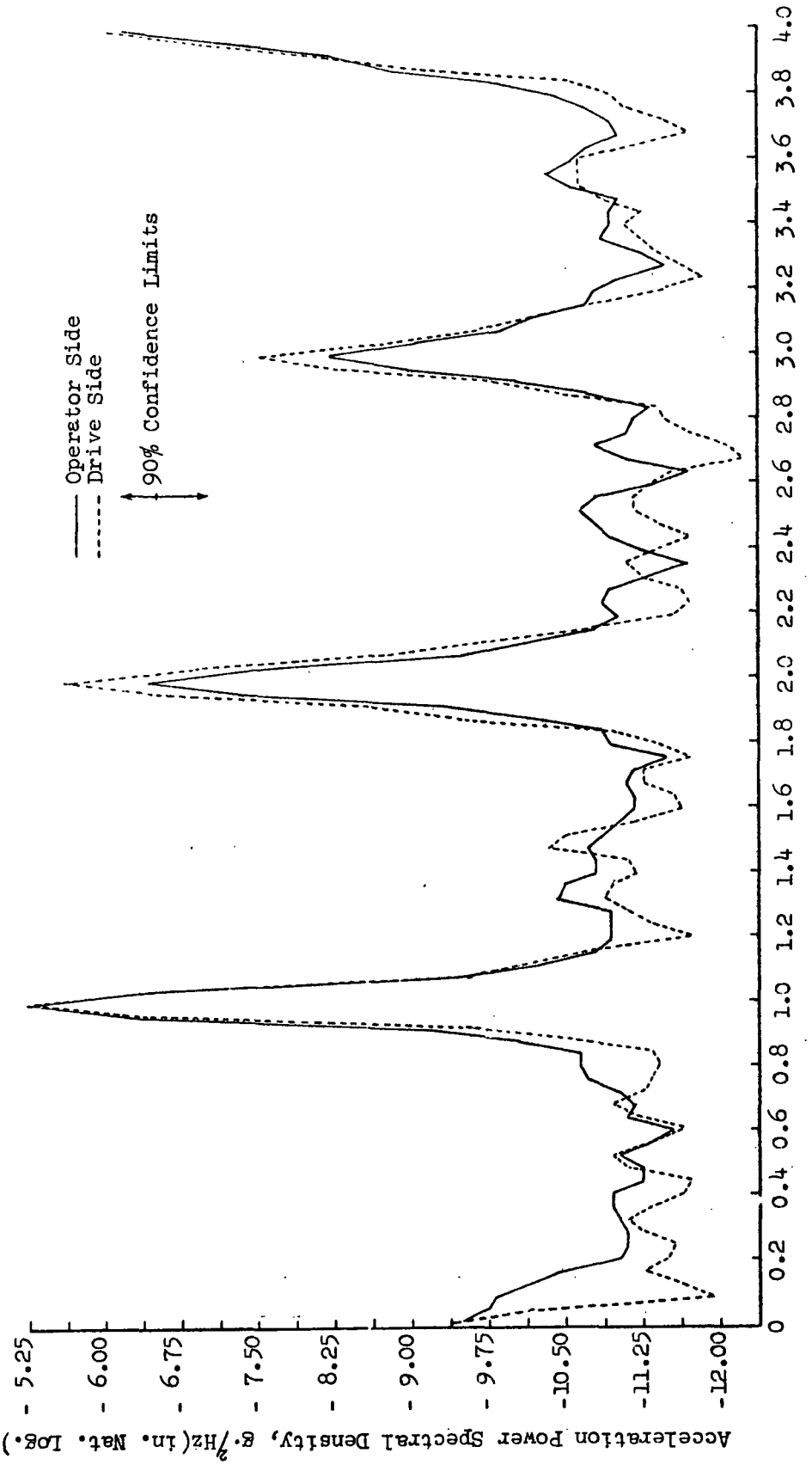

Figure 16. Top Roll Acceleration Power Spectrum for Run 3 (300 f.p.m. Corrugating Speed)

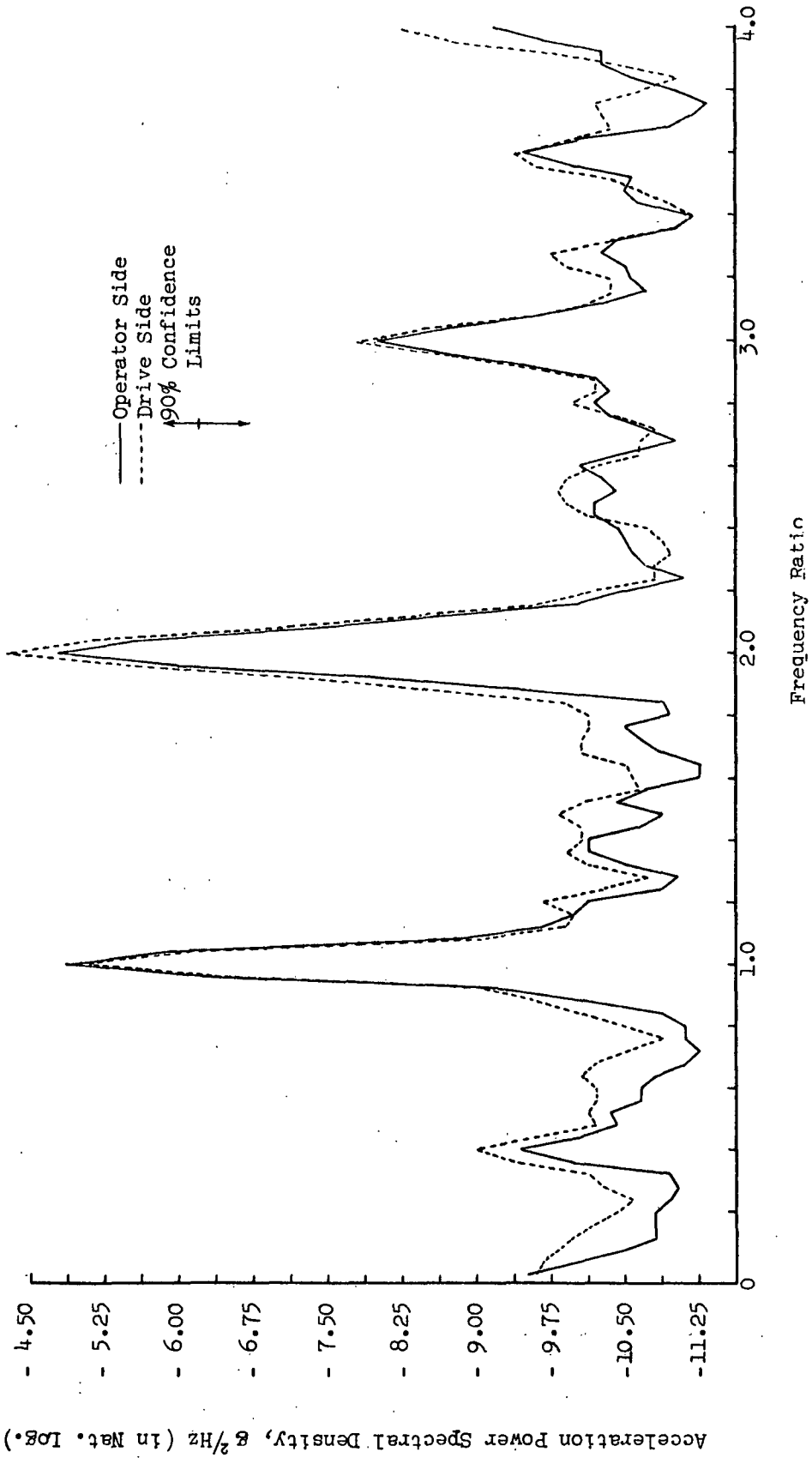

Figure 17. Top Roll Acceleration Power Spectrums for Run 5 (450 f.p.m. Corrugating Speed)

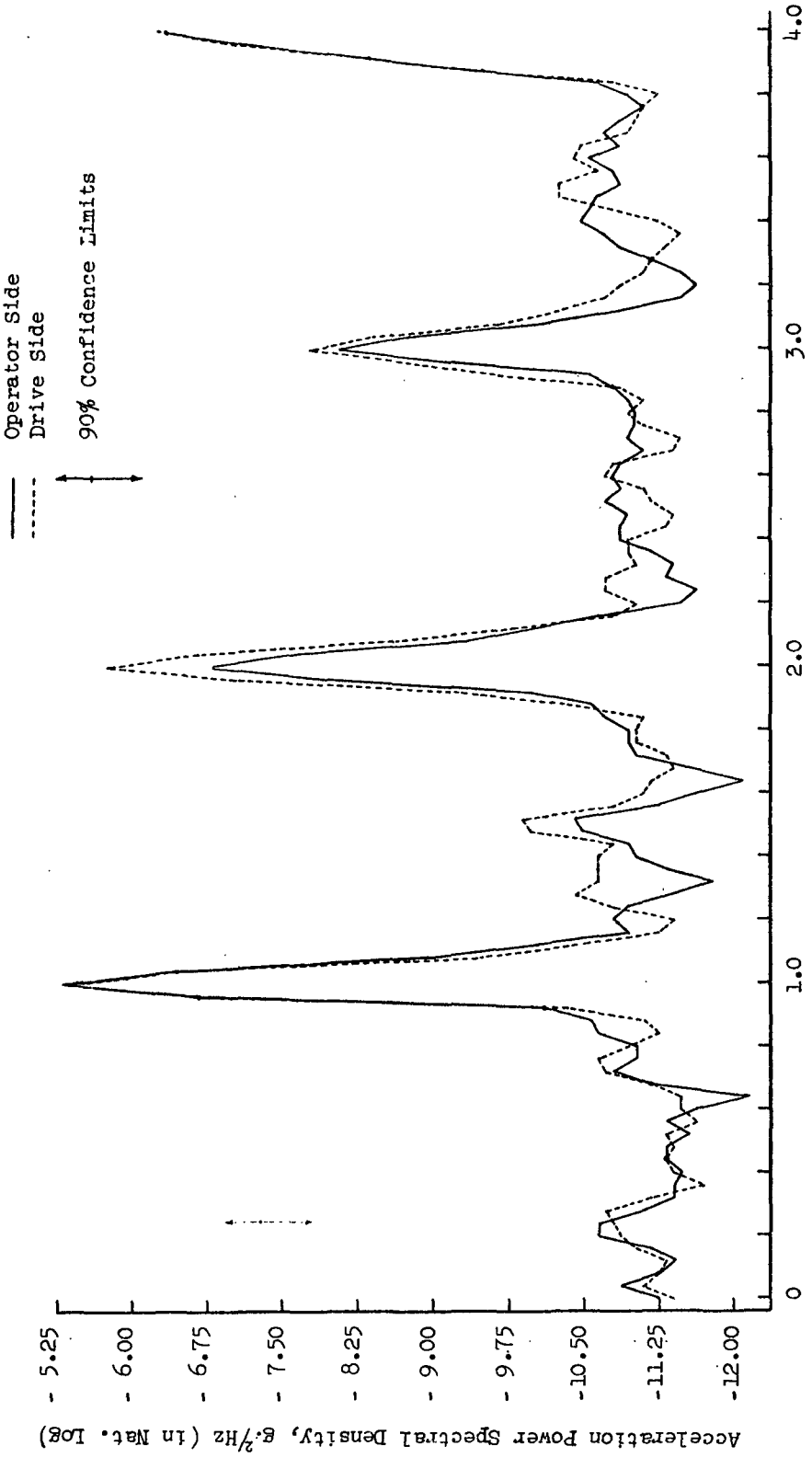

Figure 18. Top Roll Acceleration Power Spectrum for Run 6 Corrugated at 300 f.p.m. Under Standard Conditions

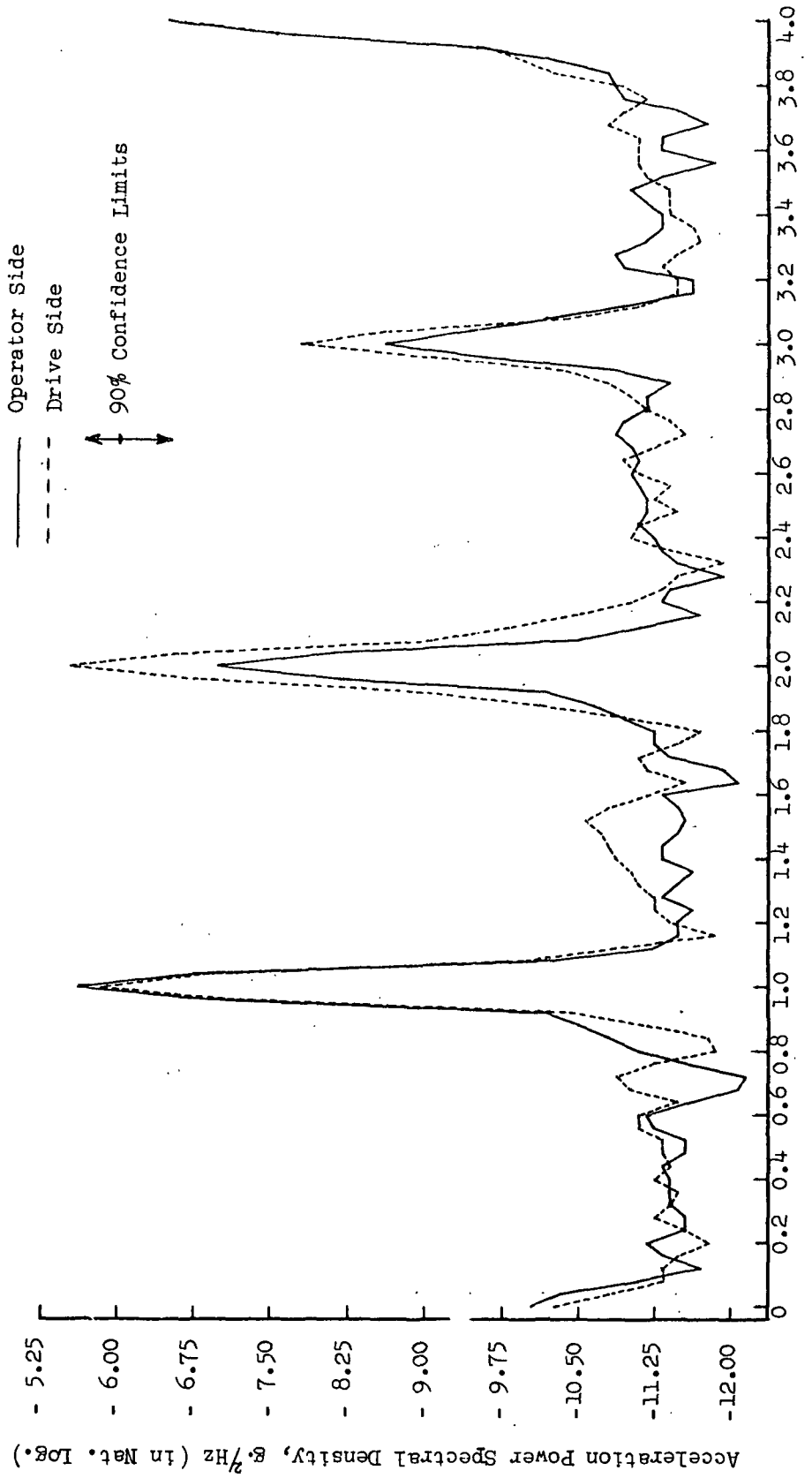

Figure 19. Top Roll Acceleration Power Spectrum for Run 7 Corrugated at 300 f.p.m. at Increased Web Tension

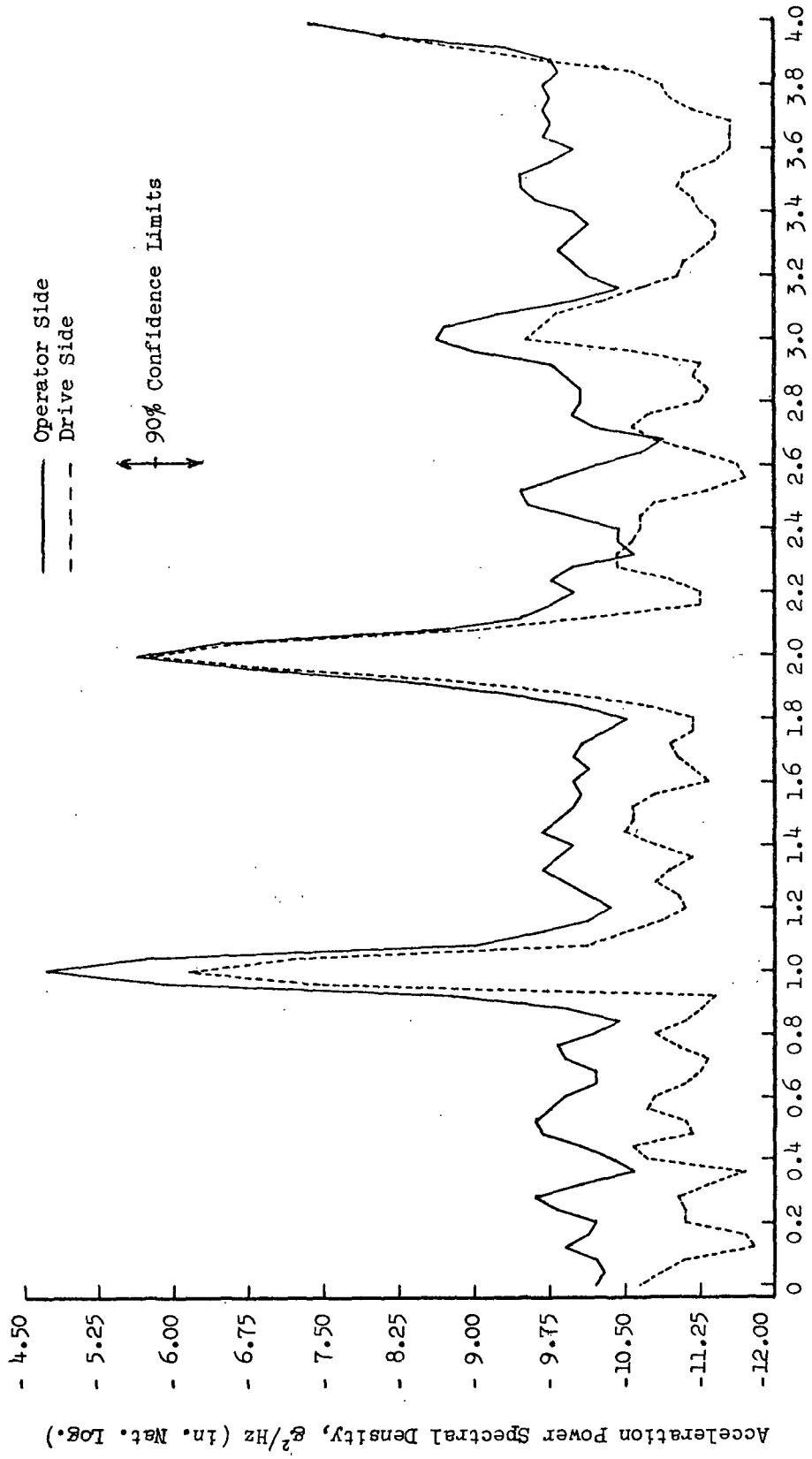

Figure 20. Top Roll Acceleration Power Spectrums for Run 8 Corrugated at 300 f.p.m. at Decreased Top Roll Pressure

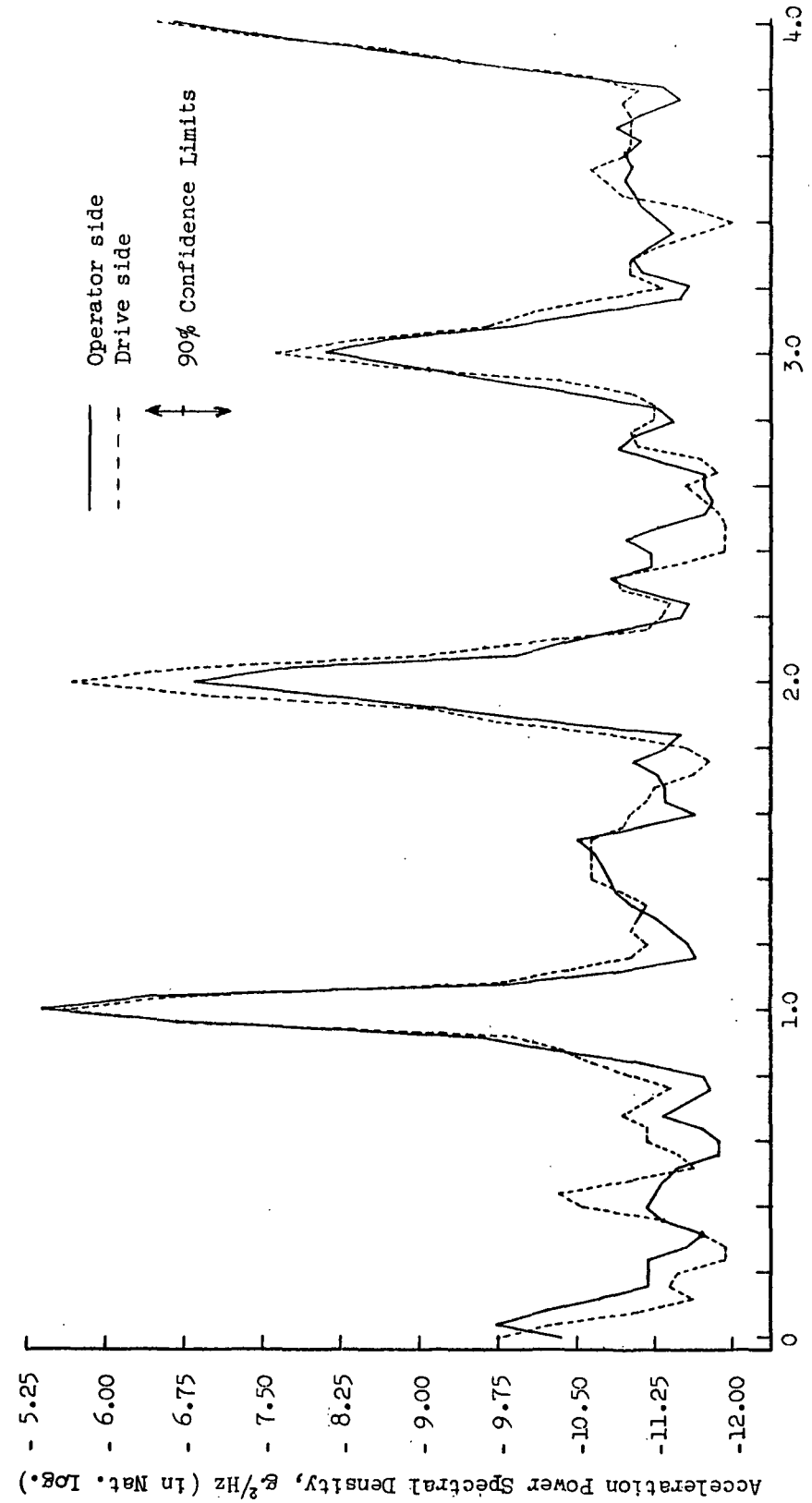

Figure 21. Top Roll Acceleration Power Spectrums for Run 9 Corrugated at 300 f.p.m. Using no Steam Shower

Table VI tabulates the peak acceleration spectral densities for the harmonic components for all runs. Inspection of the table reveals that the relative importance of the harmonic components in terms of peak spectral densities varies substantially from run-to-run. On the operator side, the flute-forming frequency exhibits the highest spectral density in 10 of the 13 runs; however, in two runs (Runs 1 and 5), the second harmonic is the greatest component and in Run 3, the fourth harmonic is the greatest. Also on the operator side, the component at the flute-forming frequency component exhibited the second highest peak in three runs; the second harmonic was second highest in six runs and the fourth harmonic was second highest in four runs.

These variations in relative importance are probably related to specific vibration frequencies or frequency ranges. In Table VII the nominal frequencies of the highest and second highest components are tabulated. While the data at various speeds are limited, it appears that significant harmonic components can be excited for frequencies near 180 Hz or multiples thereof. For example, for Run 1, the 180 Hz component is higher than the flute-forming frequency component (90 Hz). For Run 2, the first multiple of the flute-forming frequency (135 Hz) which is also a multiple of 180 Hz is 540 Hz and this component was the largest harmonic component in the Run 2 signal. In the case of the runs at 300 f.p.m., the fourth harmonic near 720 Hz was a fairly important component on the operator side in five of the six runs carried out with 26-lb. medium. In the case of Run 5, the second harmonic at 540 Hz (a multiple of 180 Hz) was higher than the flute frequency component (270 Hz). The other run at 450 f.p.m. (Run 14) reversed the order but the 540 Hz component was still a major term.

During the course of the work, a very limited trial indicated that machine vibrations were much greater in certain speed ranges. For example, it

TABLE VI

POWER SPECTRAL DENSITY RESULTS FOR TOP CORRUGATING ROLL ACCELERATION SIGNALS

Run No.	Medium	Corr. Cond.	Nominal Speed, f.p.m.	Flute Freq., Hz: Nominal (F_n)	Flute Freq., Hz: Actual (F)	Mean Square, g.^{2}: Op. Side	Mean Square, g.^{2}: Dr. Side	Power Spectral Density, g.^{2}/Hz (x 10^{+4}): Operator Side: F	Operator Side: $2F$	Operator Side: $3F$	Operator Side: $4F$	Drive Side: F	Drive Side: $2F$	Drive Side: $3F$	Drive Side: $4F$
1	26 lb. Mill A	Std.	150	90	87.9	0.4582	0.2419	21.22	67.20	5.16	--	7.25	29.04	6.55	--
2	" "	"	225	135	138.3	0.3942	--	19.39	7.44	5.38	34.60	--	--	--	--
3	" "	"	300	180	184.6	0.7517	0.8961	53.52	15.85	2.65	19.71	49.19	36.64	5.05	22.43
4	" "	"	375	225	227.3	1.9008	--	95.93	44.11	10.38	4.62	--	--	--	--
5	" "	"	450	270	279.6	3.2075	4.1237	107.63	120.37	4.73	1.48	89.06	195.22	6.00	3.68
6	" "	"	300	180	186.3	0.6456	0.8250	46.89	11.39	3.12	16.69	19.14	13.43	1.79	7.86
7	" "	Inc. tens.	300	180	178.6	0.4578	0.6502	35.75	9.17	1.78	14.24	29.01	38.12	3.96	12.28
8	" "	Low pres.	300	180	184.6	1.2644	0.5441	92.02	36.24	1.85	6.40	21.55	32.02	0.74	5.96
9	" "	No shower	300	180	185.7	0.6008	0.7290	44.46	11.04	3.05	12.88	36.85	32.34	4.90	14.95
12	26 lb. Mill B	Std.	300	180	184.0	0.9691	1.0678	78.37	17.50	1.41	14.82	46.73	61.31	5.30	13.96
14	" "	"	450	270	280.0	2.5772	3.4438	143.15	53.87	3.51	1.28	149.04	108.49	5.18	4.02
16	33 lb. Mill A	"	300	180	185.0	0.6346	0.5912	68.41	7.41	1.50	2.86	31.33	34.55	2.69	3.99
18	33 lb. Mill B	"	300	180	188.0	0.5377	0.5166	55.91	5.79	1.23	1.76	33.65	24.41	2.53	1.26

Note: Power spectral density values are reported at the flute frequency F and its first three harmonics ($2F$, $3F$, and $4F$).

appeared that the amplitudes become markedly greater in certain speed ranges, e.g., near 300 and 375 f.p.m. These may be termed critical speeds. The higher vibration amplitudes in such speed ranges may occur because one of the higher harmonics is excited, e.g., the 720 Hz component at 300 f.p.m. It appears likely that operation of the corrugator at such speed would affect the tendency to form high-low flutes.

TABLE VII

NOMINAL ACCELERATION FREQUENCY COMPONENTS

Run	Nom. Speed	Nom. Freq., Hz	Corr. Cond. and Medium	Nominal Frequency, Hz — Operator Side: Highest Comp.	Operator Side: Second Highest Comp.	Drive Side: Highest Comp.	Drive Side: Second Highest Comp.
1	150	90	Std. (26-A)	180 (2F)	90 (F)	180 (2F)	90 (F)
2	225	135	" "	540 (4F)	135 (F)	--	--
3	300	180	" "	180 (F)	720 (4F)	180 (F)	360 (2F)
4	375	225	" "	225 (F)	450 (2F)	--	--
5	450	270	" "	540 (2F)	270 (F)	540 (2F)	270 (F)
6	300	180	" "	180 (F)	720 (4F)	180 (F)	360 (2F)
7	300	180	Inc. tens. "	180 (F)	720 (4F)	360 (2F)	180 (F)
8	300	180	Low. pres. "	180 (F)	360 (2F)	360 (2F)	180 (F)
9	300	180	No shower "	180 (F)	720 (4F)	180 (F)	360 (2F)
12	300	180	Std. (26-B)	180 (F)	360 (2F)	360 (2F)	180 (F)
14	450	270	" "	270 (F)	540 (2F)	270 (F)	540 (2F)
16	300	180	" (33-A)	180 (F)	360 (2F)	360 (2F)	180 (F)
18	300	180	" (33-B)	180 (F)	360 (2F)	180 (F)	360 (2F)

Note: Figures in parentheses refer to harmonic number relative to flute-forming frequency.

The occurrences of critical speeds will, no doubt, vary for different corrugators. This would depend on design, mechanical condition, etc. Information relative to the factors affecting commercial corrugator critical speeds and the amplitudes of variations in top and pressure roll pressure, etc., may be helpful in reducing high-lows in production.

In addition to the flute-forming frequencies and their harmonics, the power spectrums do suggest that other frequency components may be present. For example, in Fig. 17, there appears to be an apparently significant component with a frequency near 0.4, the flute-forming frequency. It appears in both the operator and drive side spectrums. In this run the flute-forming frequency is 279.6 flutes per sec. Therefore, the lower corrugating roll is revolving at a rate of 2.50 r.p.s. (279.6 divided by 112 flutes per revolution). The pressure roll is driven by two 48-tooth gears. Because the pressure roll revolves at the same rate as the lower corrugating roll, the tooth engagement rate of the pressure roll gears would be about 120 Hz — or about 0.43 times the flute frequency. It appears likely, therefore, that at the spectrum peak near 0.4 the flute frequency may be associated with vibrations induced by the pressure roll gearing in this instance.

In Fig. 17, there are also possibly significant peaks in the power spectrum near frequency ratios of 1.4-1.5, 2.4-2.6, and 3.6. In Fig. 15, there are small but possibly significant peaks at frequency ratios near 1.5, 2.5, and 3.5 on one side or the other. It is speculated that vibrations at such frequencies could be associated with harmonics of the pressure and corrugating drive gear tooth contact rates. For the Institute's A-flute corrugator, the fundamental gearing frequencies as ratios of the flute-forming frequency, would be about 0.43 and 0.71 for the pressure and corrugator roll gearing, respectively. However, the spectral densities in these frequency regions were usually low and near the noise level. Hence, in most runs it was not possible to accurately identify the significant frequency components in the regions between the flute frequency peaks in the power spectrums. More accurate, high resolution spectrums would be required for this purpose.

It is not certain that these frequency components are meaningful to high-low flute formation. The low magnitudes of the spectral densities relative to those

at the flute-forming frequency suggest that they might not induce enough variation in the forming conditions from flute-to-flute to directly produce high-lows. Nevertheless, components having frequency ratios near 0.5 or 1.5 would cause the forming conditions to vary from flute-to-flute and tend to produce a high-low pattern. Further work on this aspect of the problem may be warranted.

Table VI also shows the acceleration mean square values for each run. The mean square value is obtained by squaring each value, summing over the entire time period and dividing by the time. Thus, it is a measure of the variance of the series and provides an overall measure of the intensity of the variations. As speed is increased (see Runs 1-5, 12, and 14) it may be noted that the mean square value increases rapidly. For the threefold increase in speed, the mean square increased by about eightfold. This means that the amplitudes of the force fluctuations on the medium due to transverse acceleration of the upper roll increase as the speed increases. If the motion of the upper roll were simple harmonic, the acceleration amplitudes would increase as the square of the speed, hence the mean square values would increase as the fourth power of the speed. Figure 22 shows that the top roll acceleration mean squares approximately increase as the third power of the speed for the runs made at standard conditions with 26-lb. medium. Apparently, the cushioning or dampening characteristics of the medium reduce the growth in the forces due to motion of the top roll as speed increases.

It also may be noted on Table VI that the acceleration mean square values on the drive side were greater than on the operator side in seven of the eleven comparisons. This may be related to the tendency for greater high-lows to occur on the drive side.

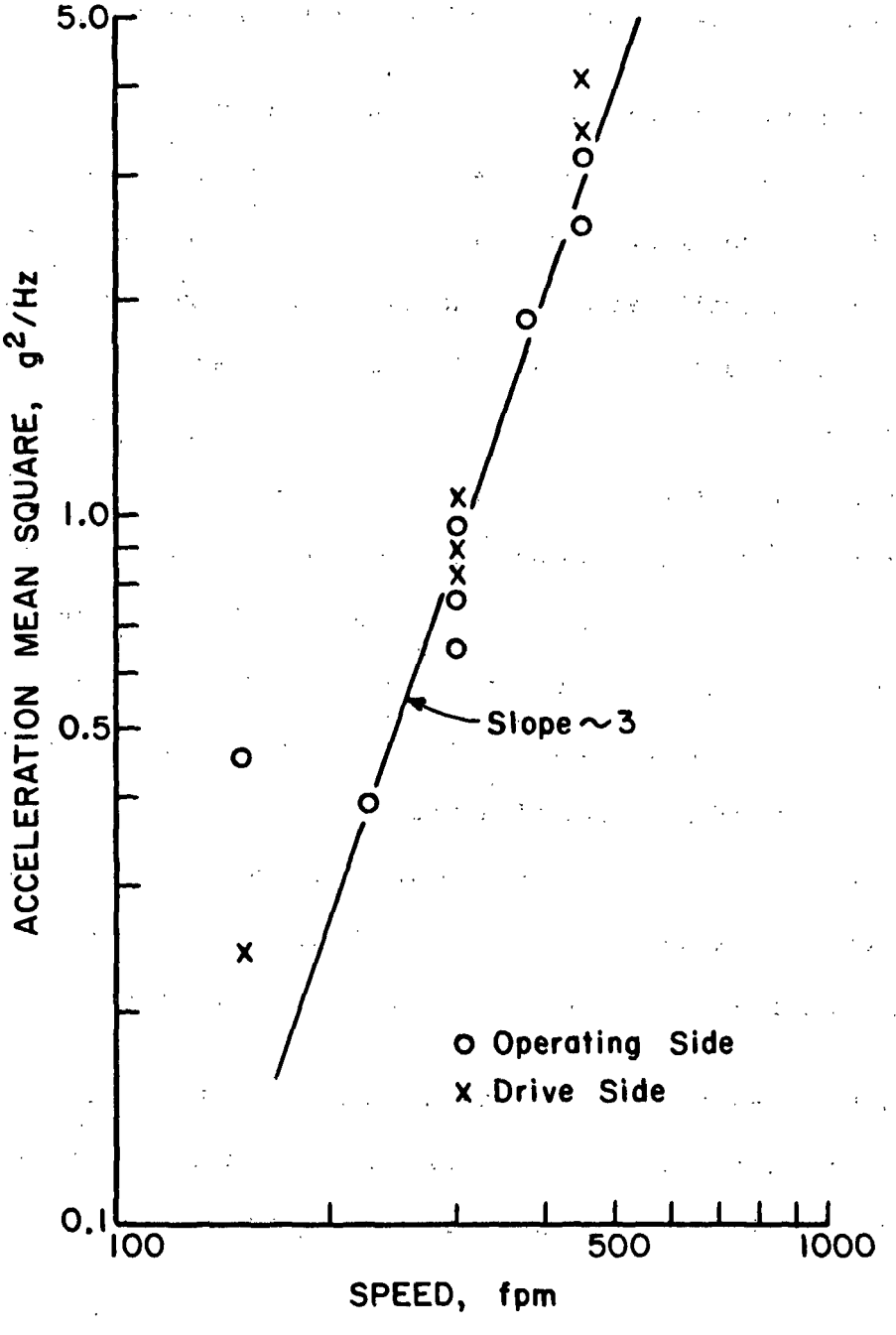

Figure 22. Relationship Between Acceleration Mean Square Values and Corrugating Speed (26-lb. Medium, Standard Corrugating Conditions)

Top Corrugating Roll Pressure Power Spectrums

The pressure spectral densities at the flute-forming frequency, F, and its harmonics up to 4F, are tabulated in Table VIII. The pressure power spectrums obtained at 300 f.p.m. (Run 3) are illustrated in Fig. 23. Figures 24 and 25 show the operator and drive side pressure spectrums obtained at 450 f.p.m. (Run 5).

The figures show that the top corrugating roll pressure fluctuations exhibit major peaks at the flute-forming frequency and harmonics (frequency ratios of 1.0, 2.0, 3.0, and 4.0 in the figures). Thus, as in the case of the acceleration signals, the vibration amplitudes at these frequencies account for the major proportion of the fluctuations in top roll pressure.

As in the case of the acceleration signals, the relative importance of the harmonic components changes from run-to-run — depending on speed and other factors. For example, on the operator side, the fourth harmonic component (frequency near 720 Hz) exhibited a greater spectral density than the second harmonic in five of the six runs made at 300 f.p.m. when 26-lb. medium was employed. The exception was Run 8 but, in this run, a low top roll pressure was employed. The behavior of the acceleration signals was somewhat similar and indicates that the phenomena were not due to the transducers themselves. It appears that near 300 f.p.m. there is a tendency to excite top roll pressure vibrations at about 720 Hz for the Institute's corrugator. This may be a critical speed level for the Institute's corrugator. A similar situation may prevail at speeds near 375 f.p.m. where the spectral density of the third harmonic (about 675 Hz) is greater than even the fundamental flute-frequency component.

While the acceleration mean square values increased with increasing corrugating speed, the pressure mean square values varied erratically as speed

TABLE VIII

POWER SPECTRAL DENSITY RESULTS FOR TOP CORRUGATING ROLL PRESSURE SIGNALS

Run No.	Medium	Corr. Cond.	Nominal Speed, f.p.m.	Flute Freq., Hz		Mean Square, p.s.i.^{2}		Power Spectral Density, p.s.i.^{2}/Hz ($\times 10^{+3}$)							
				Nominal (F_n)	Actual (F)	Op. Side	Dr. Side	Operator Side				Drive Side			
								F	$2F$	$3F$	$4F$	F	$2F$	$3F$	$4F$
1	26 lb. Mill A	Std.	150	90	87.9	19.43	2.13	24.51	365.69	1.07	--	8.72	4.97	5.36	--
2	" "	"	225	135	138.3	2.71	--	17.82	12.42	2.47	3.81	--	--	--	--
3	" "	"	300	180	184.6	14.36	2.35	116.18	5.54	3.04	29.41	9.08	8.46	0.21	0.73
4	" "	"	375	225	227.3	51.42	--	91.64	25.94	247.67	4.15	--	--	--	--
5	" "	"	450	270	279.6	12.52	19.82	46.51	28.46	0.51	3.35	82.46	25.94	1.51	0.23
6	" "	"	300	180	186.3	12.18	2.92	77.02	3.45	1.60	79.89	14.91	10.02	0.12	1.39
7	" "	Inc. tens.	300	180	178.6	12.58	2.28	66.69	5.08	1.35	109.82	8.40	8.52	0.31	0.44
8	" "	Low pres.	300	180	184.6	5.58	4.84	28.23	27.68	0.19	0.27	58.31	0.52	0.14	0.16
9	" "	No shower	300	180	185.7	11.13	2.95	77.58	3.05	0.75	49.02	15.42	11.57	0.20	0.81
12	26 lb. Mill B	Std.	300	180	184.0	38.07	15.84	385.60	14.58	23.70	27.95	182.68	6.49	0.31	3.84
14	" "	"	450	270	280.0	12.71	12.75	81.86	7.14	9.94	85.99	66.11	8.38	11.59	1.14
16	33 lb. Mill A	"	300	180	185.0	10.77	9.69	106.79	4.10	4.90	3.73	99.24	4.45	0.45	13.12
18	33 lb. Mill B	"	300	180	188.0	6.99	10.94	70.76	3.20	1.35	1.45	112.20	4.45	0.33	17.48

Note: Power spectral density values are reported at the flute frequency F and its harmonics ($2F$, $3F$, and $4F$).

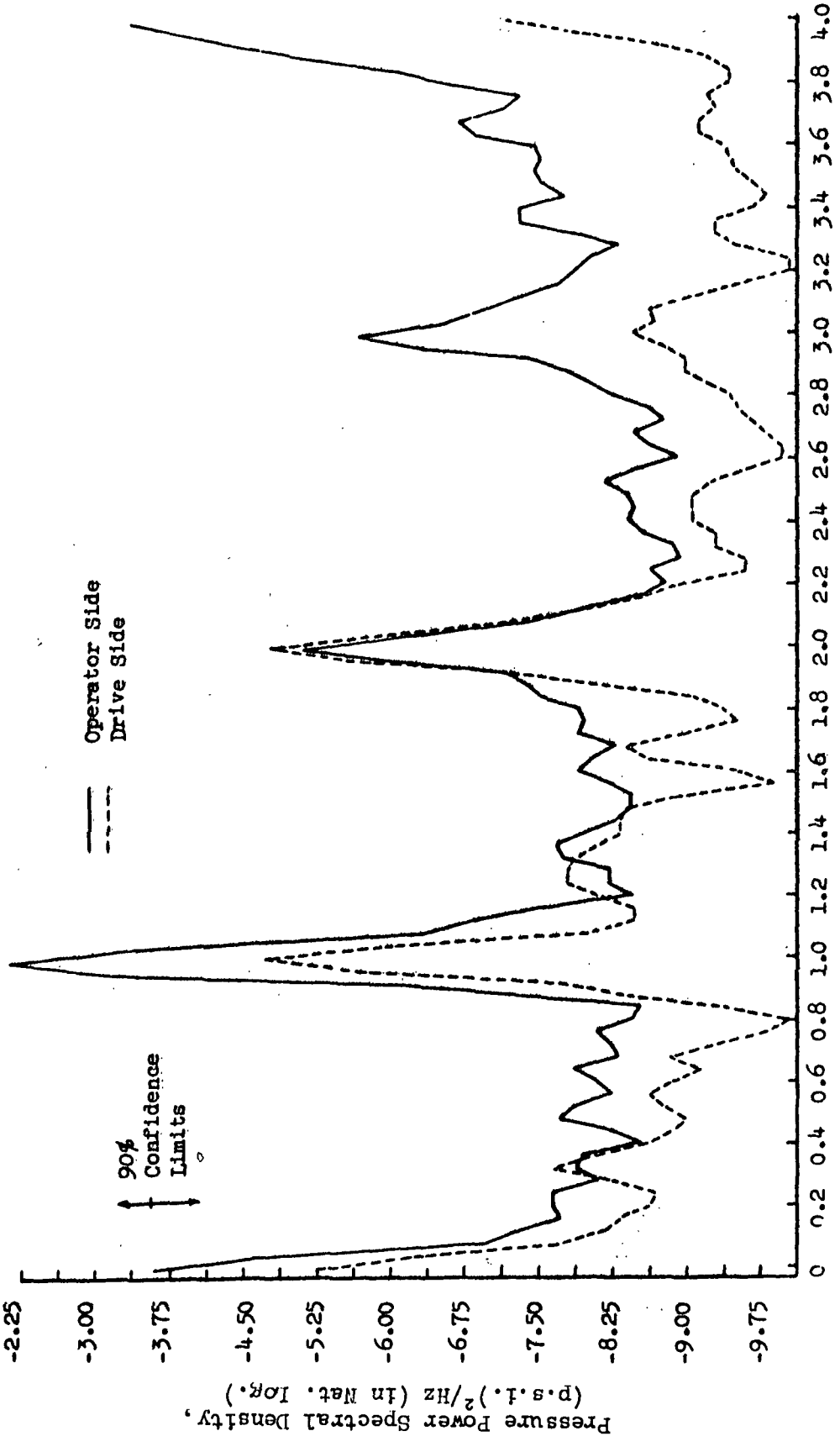

Figure 23. Top Roll Pressure Power Spectrums for Run 3 Corrugated at 300 f.p.m. Under Standard Conditions

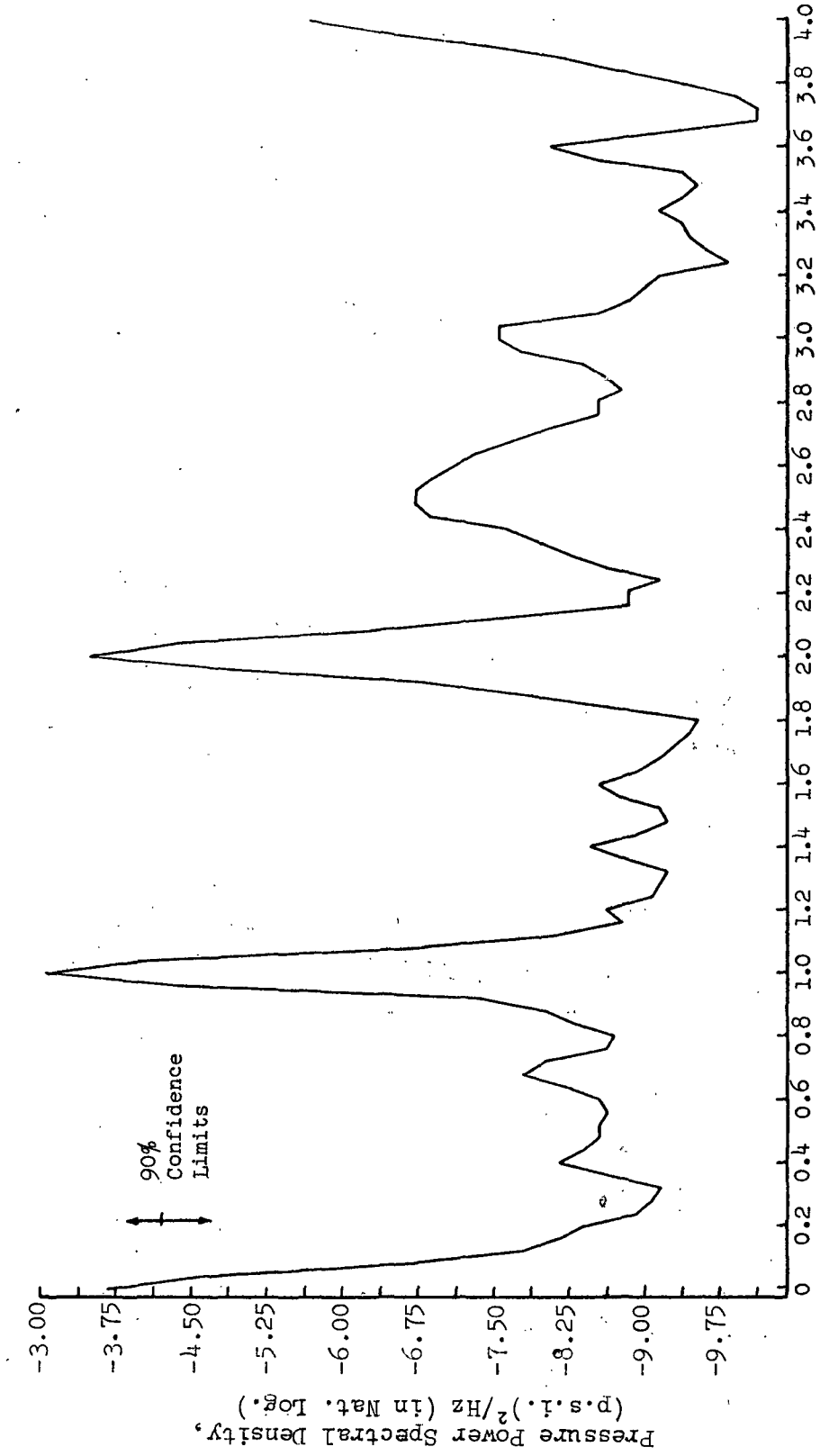

Figure 24. Operator Side Top Roll Pressure Power Spectrum for Run 5
Corrugated at 450 f.p.m. Under Standard Conditions

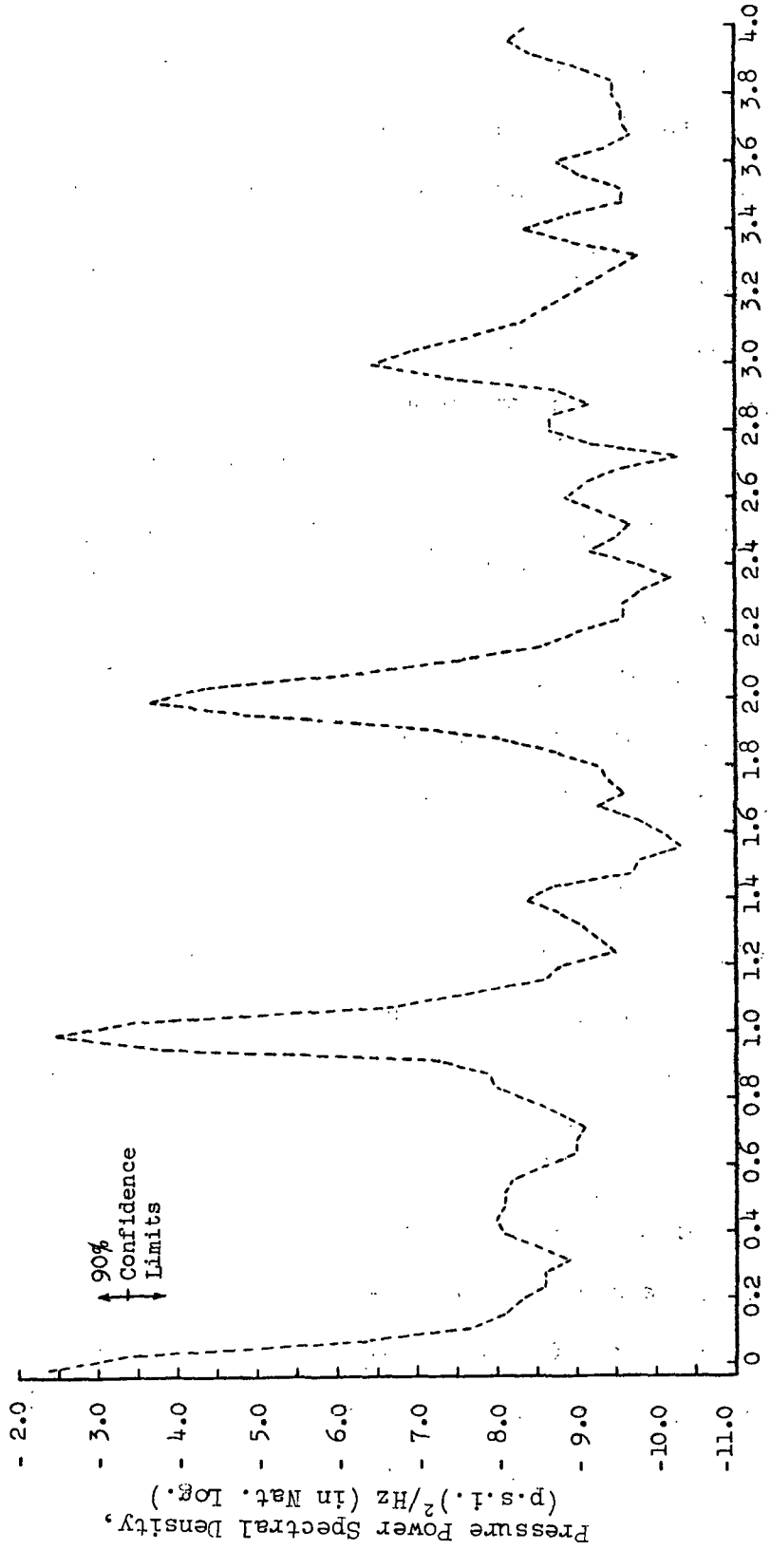

Figure 25. Drive Side Top Roll Pressure Power Spectrum for Run 5 Corrugated at 450 f.p.m. Under Standard Conditions

was changed. Possibly the pressure fluctuations occurring in the neighborhood of critical speed ranges are sufficiently great as to obscure speed effects.

In most cases higher pressure mean square values were obtained on the operator side. This may indicate that the accumulator on the drive side was more effective in reducing pressure fluctuations than the accumulator on the drive side.

Figures 23-25 also indicate that there are no large components having frequencies in the F/2, 3F/2, etc., range. Such components, if present, must have relatively small amplitudes relative to the components at F, 2F, etc. Thus, high-lows are more likely to be related to variations in the amplitudes at F, 2F, etc., of the pressure fluctuations from flute-to-flute.

Web Tension Power Spectrums

Tension spectral densities at the flute-forming frequency and its harmonics are summarized in Table IX. The power spectrums obtained at corrugating speeds of 225, 300, and 375 f.p.m. (Runs 2, 3, and 4) are shown in Fig. 26-28, respectively.

In general, the tension power spectrums for all runs were similar to those for top corrugating roll pressure and acceleration. In all cases, the spectrums were dominated by the components at the flute frequency and its higher harmonics.

As mentioned previously, an examination of the tension signals obtained at 450 f.p.m. suggested the tension arm was in resonant vibration at a frequency of about 540 Hz. For example, the dominant frequency component in Run 14 carried out at 450 f.p.m. was the second harmonic near 540 Hz. Although the tension signal for Run 5 also carried out at 450 f.p.m. was not digitized or analyzed, its

TABLE IX

POWER SPECTRAL DENSITY RESULTS FOR WEB TENSION SIGNALS

Run No.	Medium	Corr. Cond.	Nominal Speed, f.p.m.	Flute Freq., Hz		Mean Square, lb.^{2}/in.^{2}	Power Spectral Density, lb.^{2}/in.^{2}/Hz (x 10^{+5})			
				Nominal (F_n)	Actual (F)		F	$2F$	$3F$	$4F$
1	26 lb. Mill A	Std.	150	90	87.9	0.1297	73.95	13.89	2.21	--
2	" "	"	225	135	138.3	0.2040	21.68	41.33	1.79	277.86
3	" "	"	300	180	184.6	0.1784	25.44	15.96	115.87	0.83
4	" "	"	375	225	227.3	0.1312	43.19	36.97	1.83	0.10
5	" "	"	450	270	279.6	--	--	--	--	--
6	" "	"	300	180	186.3	0.2796	38.3	16.5	185.8	2.0
7	" "	Inc. tens.	300	180	178.6	0.1394	52.4	16.3	17.3	0.1
8	" "	Low pres.	300	180	184.6	0.2471	102.85	81.6	19.1	12.2
9	" "	No shower	300	180	185.7	0.2720	33.9	12.4	158.4	0.03
12	26 lb. Mill B	Std.	300	180	184.0	0.2036	26.06	17.41	114.0	0.39
14	" "	"	450	270	280.0	1.8527	24.08	1213.15	4.04	7.36
16	33 lb. Mill A	"	300	180	185.0	0.4553	57.56	22.31	261.77	1.97
18	33 lb. Mill B	"	300	180	188.0	0.1718	55.32	6.68	77.03	1.13

Note: Power spectral density values are reported at the flute frequency (F) and its harmonics ($2F$, $3F$, and $4F$).

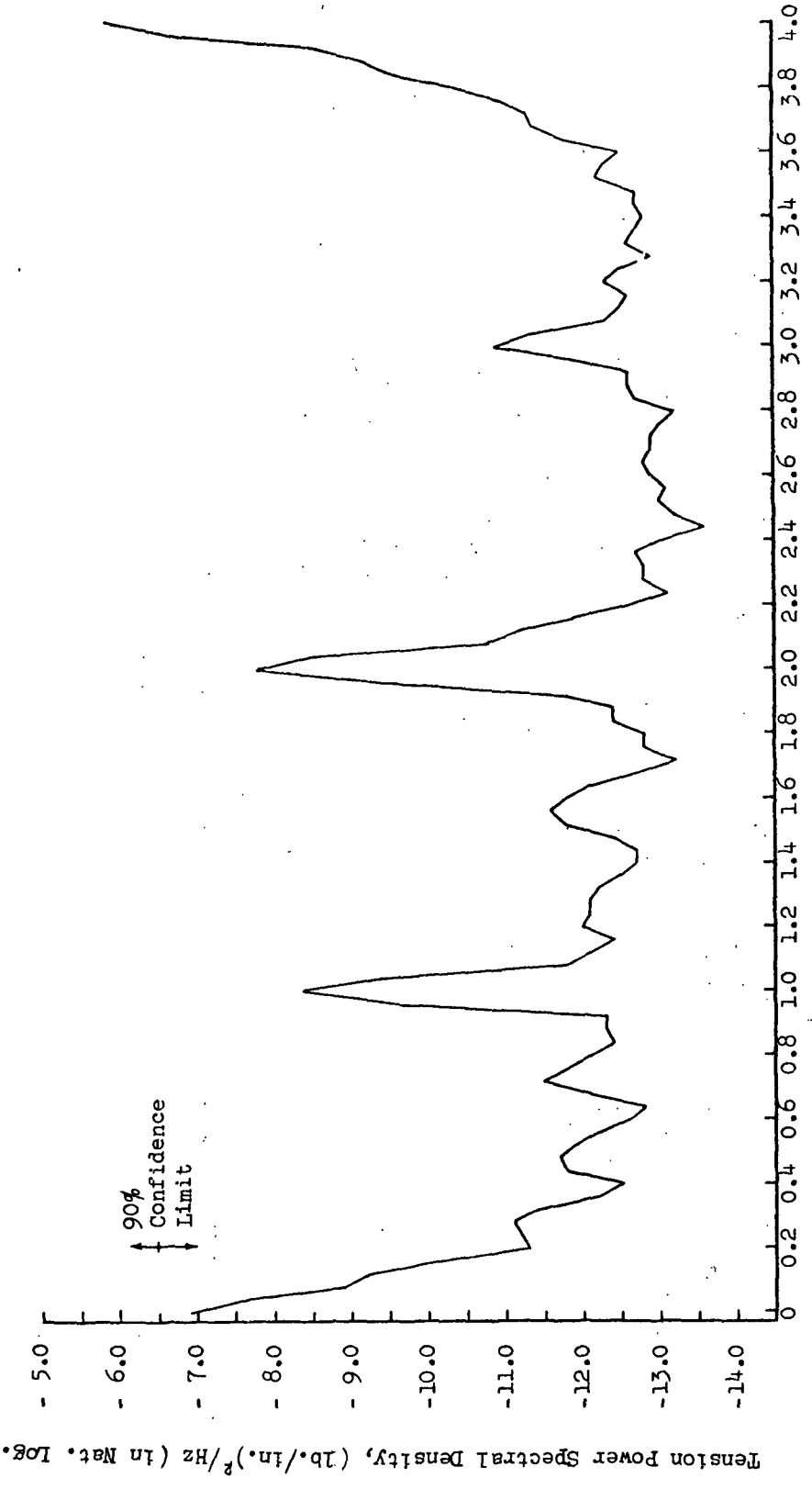

Figure 26. Web Tension Power Spectrum for Run 2 (Speed 225 f.p.m.)

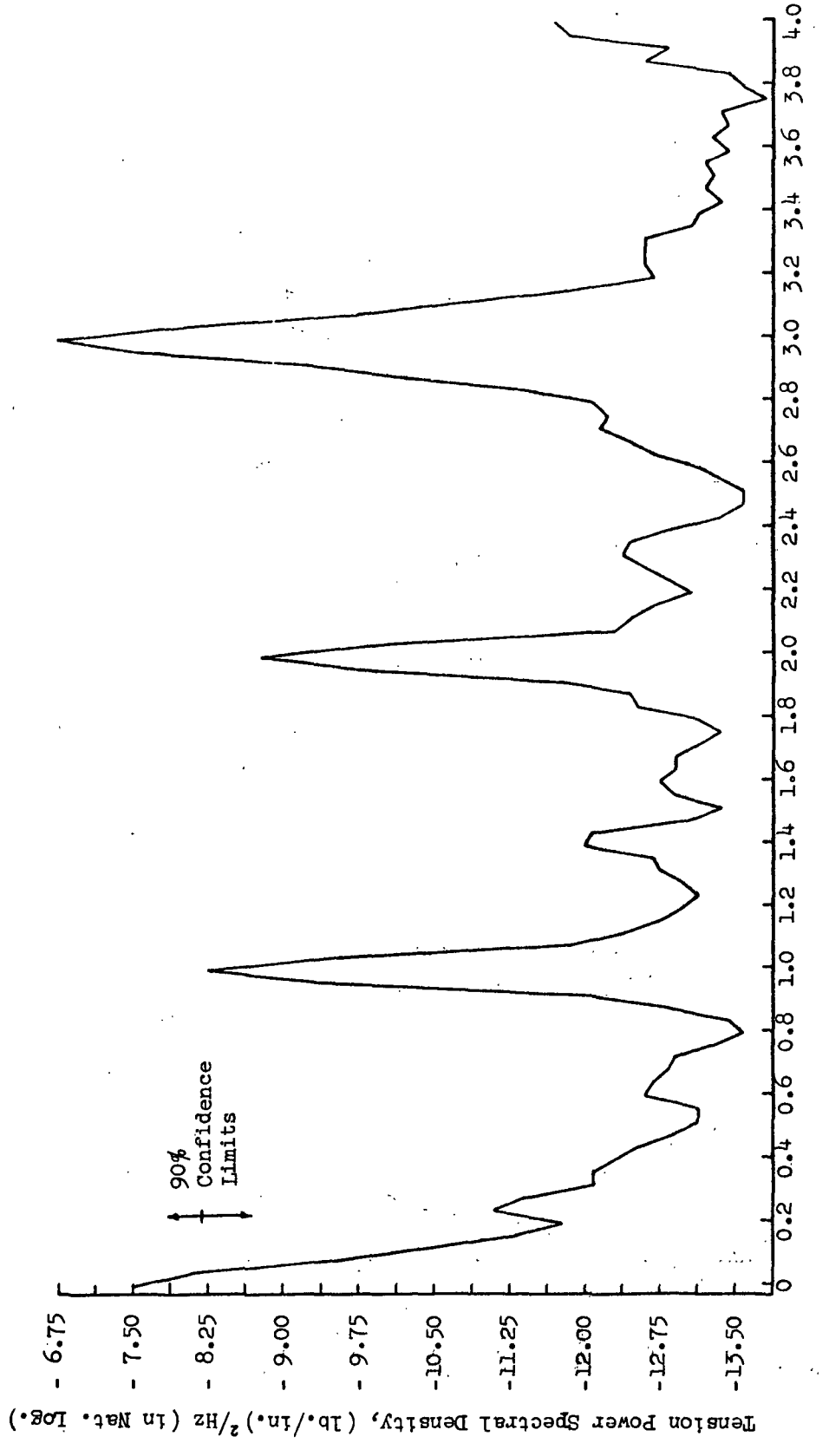

Figure 27. Web Tension Power Spectrum for Run 3 (Speed 300 f.p.m.)

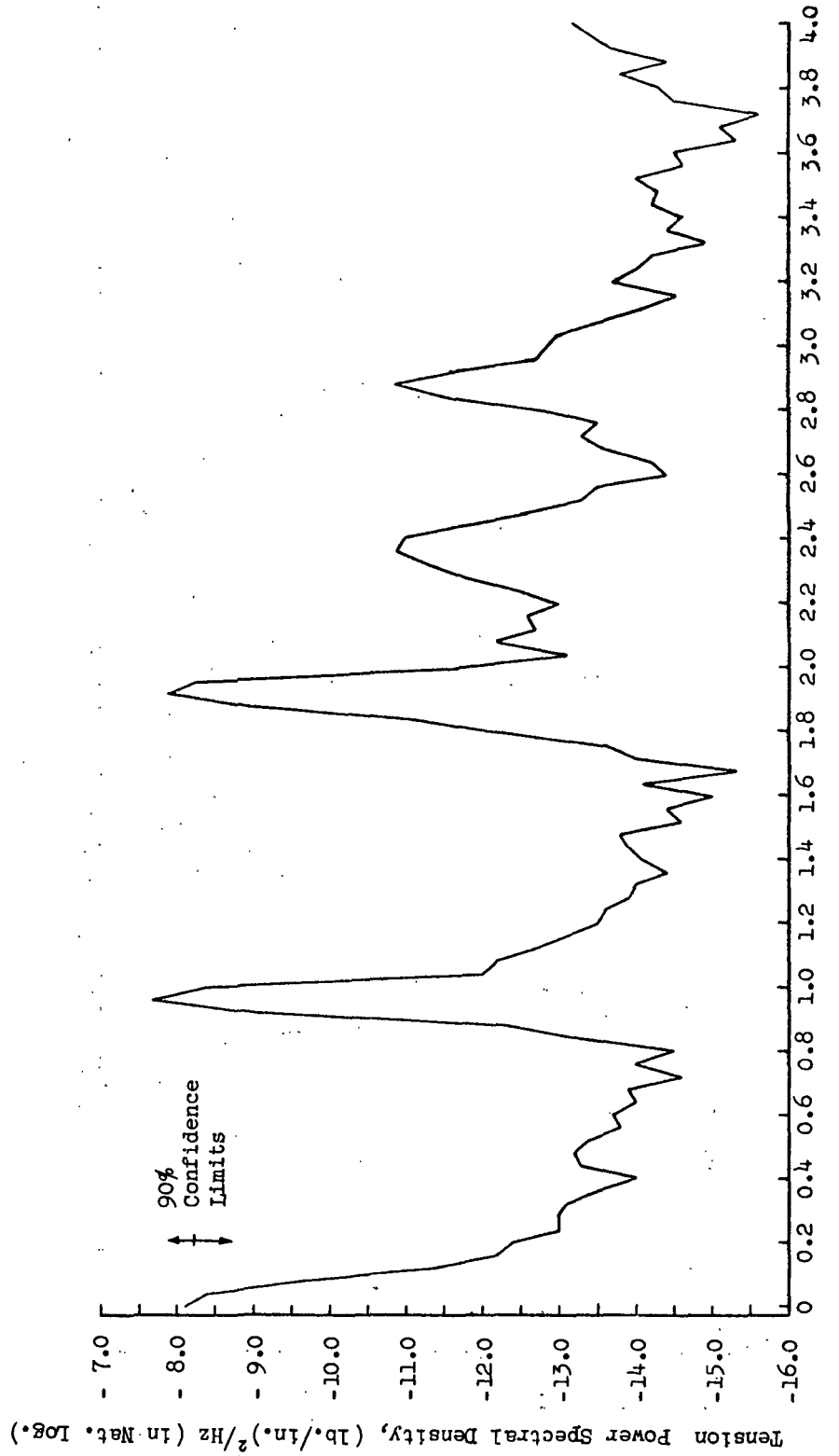

Figure 28. Web Tension Power Spectrum for Run 4 (Speed 375 f.p.m.)

appearance indicated a similar result would have been obtained. The 540 Hz component is also quite large in most of the runs carried out at 300 f.p.m. where it appears as the third harmonic. It also appears as the fourth harmonic in Run 2. In preparing the tensiometer for use in this study, measurements indicated its natural frequency of vibration was in excess of 1000 Hz and no vibration mode near 540 Hz was evident. Nevertheless, the data suggest a resonant mode in this frequency range. Therefore, the tension data must be viewed with caution.

With this in mind, it may be noted that the tension mean square values did not exhibit any obvious trend to increase as the corrugating speed increased in Runs 1-4. Its behavior in this regard was similar to the top roll pressure mean square values.

When the web tension was increased (Run 7) the mean square was lower than in Run 6 (control) even though the tension was at a higher level. The increased web tension did tend to suppress the third harmonic component which may account, in part, for the lower mean square obtained at the higher tension level. Normally, increasing the web tension increases high-lows. However, in this study, Run 7 (made with increased web tension) gave operator and drive side flute height differences of 1.13 and 2.11 pt. The corresponding flute height differences for the control (Run 6) made with normal tension were 1.53 and 1.91 pt. Thus, despite the greater web tension in Run 7, lower high-lows were obtained on the operator side and the high-lows on the drive side were only modestly greater than in Run 6. The lower tension mean square value for Run 7 relative to Run 6 suggests the variations in tension amplitude were somewhat lower in Run 7. It is conjectured that lower tension amplitudes in Run 7 may account in part for the decreases in high-lows on the operator side and the relatively modest increase in high-lows on the drive side.

Top Roll Molding Force Power Spectrums

The molding force on the medium at any instant in the labyrinth should be dependent on (a) the top corrugating roll pressure and (b) the inertial force due to upper roll motion. The latter is equal to the mass of the upper roll times its acceleration at a given instant in time.

For this study, molding forces were calculated in two ways and termed (1) translational and (2) rocking force.

The translational force on each side of the machine was calculated from the following equations:

$$F_o = P_o A_p + (W/2g)\, a_o \qquad (8)$$

$$F_d = P_d A_p + (W/2g)\, a_d \qquad (9)$$

when

$\underline{F_o}$, $\underline{F_d}$ = molding force on operator and drive sides, respectively, lb.

$\underline{P_o}$, $\underline{P_d}$ = top corrugating roll pressure on operator and drive sides, respectively, p.s.i.

$\underline{a_o}$, $\underline{a_d}$ = top corrugating roll acceleration on operator and drive sides, respectively, in./sec.^{2}

$\underline{A_p}$ = area of piston on hydraulic system, in.^{2}

$\underline{W}$ = weight of upper roll and bearing blocks, lb.

g = acceleration of gravity, in./sec.^{2}

The above equations assume that the upper roll motion corresponds to that of a simple one degree of freedom vibration system. One-half the mass ($\underline{W}/2g$) of the upper roll is assumed to act on each side of the machine. They also neglect the static component of the top corrugating roll pressure, i.e., the average operating pressure, in order to estimate the fluctuating or dynamic oscillations about the average pressure.

The above model is highly oversimplified. One objection that immediately comes to mind is that the force exerted by the upper roll is distributed across the roll face in a complex way depending on the nature and magnitude of the pressures and motions on each end of the roll. For this reason, a second model was derived to allow for a rocking motion of the upper roll, i.e., to allow for rotation of the upper roll about an axis perpendicular to the length of the roll. Assuming no flexure of the upper roll, the following equations were derived (see Appendix II for the derivation):

$$F_o = 0.608\ a_o - 0.385\ a_d + 4.17\ P_o - 2.99\ P_d \qquad (10)$$

$$F_d = -0.385\ a_o + 0.608\ a_d - 2.99\ P_o + 4.17\ P_d \qquad (11)$$

where

$\underline{F}$ = molding force, lb./in.

$\underline{a}$ = top roll acceleration, in./sec.^{2}

$\underline{P}$ = top roll pressure, p.s.i.g.

Subscripts $\underline{o}$, $\underline{d}$ = operator and drive side, respectively

As in the case of the translational forces, the average component of the top corrugating roll pressure is neglected in order to estimate the dynamic force oscillations about the average. Essentially the rocking force model allows for side-to-side rotational motions of the upper roll considered as a rigid number. For a narrow width machine such as the Institute's corrugator, the assumption of rigid body rotation may be a fair approximation. However, for wider machines, flexure of the upper roll may take place requiring a more complex model.

The power spectrums for the forces calculated using Equations (8) to (11) were similar in form to those for the base signals. Thus, the most important

components in the force spectrums were those occurring at the flute-forming frequency and its harmonics.

Tables X and XI show the mean square values and the spectral densities at F, 2F, etc., for the translational and rocking forces, respectively. In general, the components of the forces due to the accelerations of the top roll overshadowed the components due to top roll pressure. As a consequence, the force mean square values increase with increasing corrugator speed (e.g., see Run 1-5) as occurred in the case of the acceleration mean square values. Figure 29 shows that the translational force mean square values were linearly related to the acceleration mean square values. This means that the translational forces are primarily dependent on the acceleration of the upper roll because the pressure fluctuations were relatively small in these studies. Figure 30 shows that the rocking forces mean square values were also well related to the acceleration mean square values; however, the 450 f.p.m. points fall on a line to the right of the line for the other speeds. Apparently, the interaction between the motion on operating and drive sides reduced the rocking force intensities at the higher speed.

CORRELATIONS BETWEEN POWER SPECTRUM RESULTS AND FLUTE HEIGHT DIFFERENCES

Correlations were carried out to determine the degree of relationship between the mean square and/or spectral density values for the measured variables and average flute height differences. The analysis was restricted to the eleven runs for which both operator and drive side pressure and acceleration data were available. A dummy variable technique was used to allow for the difference in high-low levels between operator and drive sides. The tension data for Run 14 (corrugating speed of 450 f.p.m.) were also employed for Run 5 which was fabricated at the same speed.

TABLE X

POWER SPECTRAL DENSITY VALUES FOR TRANSLATIONAL MOLDING FORCE

Run No.	Medium	Corr. Cond.	Nominal Speed, f.p.m.	Flute Freq., Hz		Mean Square, lb.^{2} (x 10^{-2})		Power Spectral Density, lb.^{2}/Hz (x 10^{-2})							
				Nominal (F_n)	Actual (F)	Op. Side	Dr. Side	Operator Side				Drive Side			
								F	$2F$	$3F$	$4F$	F	$2F$	$3F$	$4F$
1	26 lb. Mill A	Std.	150	90	87.9	1088	632	5.45	14.91	1.52	--	1.88	7.56	2.05	--
2	" "	"	225	135	138.3	1031	--	5.10	1.82	1.43	9.14	--	--	--	--
3	" "	"	300	180	184.6	1921	2353	13.28	4.09	0.69	5.47	13.05	9.44	1.34	5.93
4	" "	"	375	225	227.3	6270	--	23.58	11.19	3.27	23.57	--	--	--	--
5	" "	"	450	270	279.6	8534	--	28.60	32.04	1.26	0.39	--	--	--	--
6	" "	"	300	180	186.3	1685	2160	11.65	2.92	0.83	5.17	12.06	8.11	1.13	4.88
7	" "	Inc. tens.	300	180	178.6	1191	1680	9.08	2.35	0.46	4.11	7.40	9.80	1.07	3.24
8	" "	Low pres.	300	180	184.6	3243	1426	23.43	9.12	0.50	1.70	5.34	8.61	0.19	1.58
9	" "	No shower	300	180	185.7	1560	1910	11.16	2.84	0.79	3.79	9.88	8.23	1.30	3.92
12	26 lb. Mill B	Std.	300	180	184.0	2338	2661	17.95	4.36	0.41	3.91	10.47	15.97	1.41	3.59
14	" "	"	450	270	280.0	6578	8862	35.91	14.14	0.94	0.36	37.76	28.33	1.34	1.06
16	33 lb. Mill A	"	300	180	185.0	1621	1482	17.48	1.88	0.38	0.71	7.25	8.99	0.73	1.18
18	33 lb. Mill B	"	300	180	188.0	1407	1257	14.65	1.46	0.33	0.45	7.66	6.29	0.68	0.28

Note: Power spectral density values are reported at the flute frequency F and its first three harmonics ($2F$, $3F$, and $4F$).

TABLE XI

POWER SPECTRAL DENSITY VALUES FOR ROCKING MOLDING FORCE

Run No.	Medium	Corr. Cond.	Nominal Speed, f.p.m.	Flute Freq., Hz		Mean Square, lb.²/in.²		Power Spectral Density, lb.²/in.²/Hz							
				Nominal (F_n)	Actual (F)	Op. Side	Dr. Side	Operator Side				Drive Side			
								F	$2F$	$3F$	$4F$	F	$2F$	$3F$	$4F$
1	26 lb. Mill A	Std.	150	90	87.9	11610	6346	46.8	130.7	13.2	--	3.1	49.1	15.6	--
3	" "	"	300	180	184.6	24501	29208	105.6	42.1	10.7	111.8	76.6	110.0	21.3	133.8
5	" "	"	450	270	279.6	53994	77636	144.6	107.6	18.7	11.3	53.1	332.1	22.4	18.6
6	" "	"	300	180	186.3	17066	23049	47.6	75.6	4.2	20.7	57.5	139.2	7.9	13.1
7	" "	Inc. tens.	300	180	178.6	15115	21166	65.6	63.7	8.6	22.7	46.0	155.7	16.3	9.9
8	" "	Low pres.	300	180	184.6	41251	18960	289.9	44.1	7.6	20.6	65.4	40.9	3.8	19.1
9	" "	No shower	300	180	185.7	16832	21313	52.6	74.3	7.3	20.0	41.0	140.3	13.6	19.8
12	26 lb. Mill B	Std.	300	180	184.0	25740	29998	155.6	33.4	9.5	17.6	66.0	177.9	21.9	13.1
14	" "	"	450	270	280.0	31575	59815	97.0	11.2	32.2	11.7	121.3	185.9	36.8	20.4
16	33 lb. Mill A	"	300	180	185.0	18421	16549	191.4	14.1	2.9	15.9	62.4	102.1	7.4	22.1
18	33 lb. Mill B	"	300	180	188.0	16461	14231	137.6	38.5	2.5	3.7	46.5	98.0	6.8	1.3

Note: Power spectral values are reported at the flute frequency F and its first three harmonics ($2F$, $3F$, and $4F$).

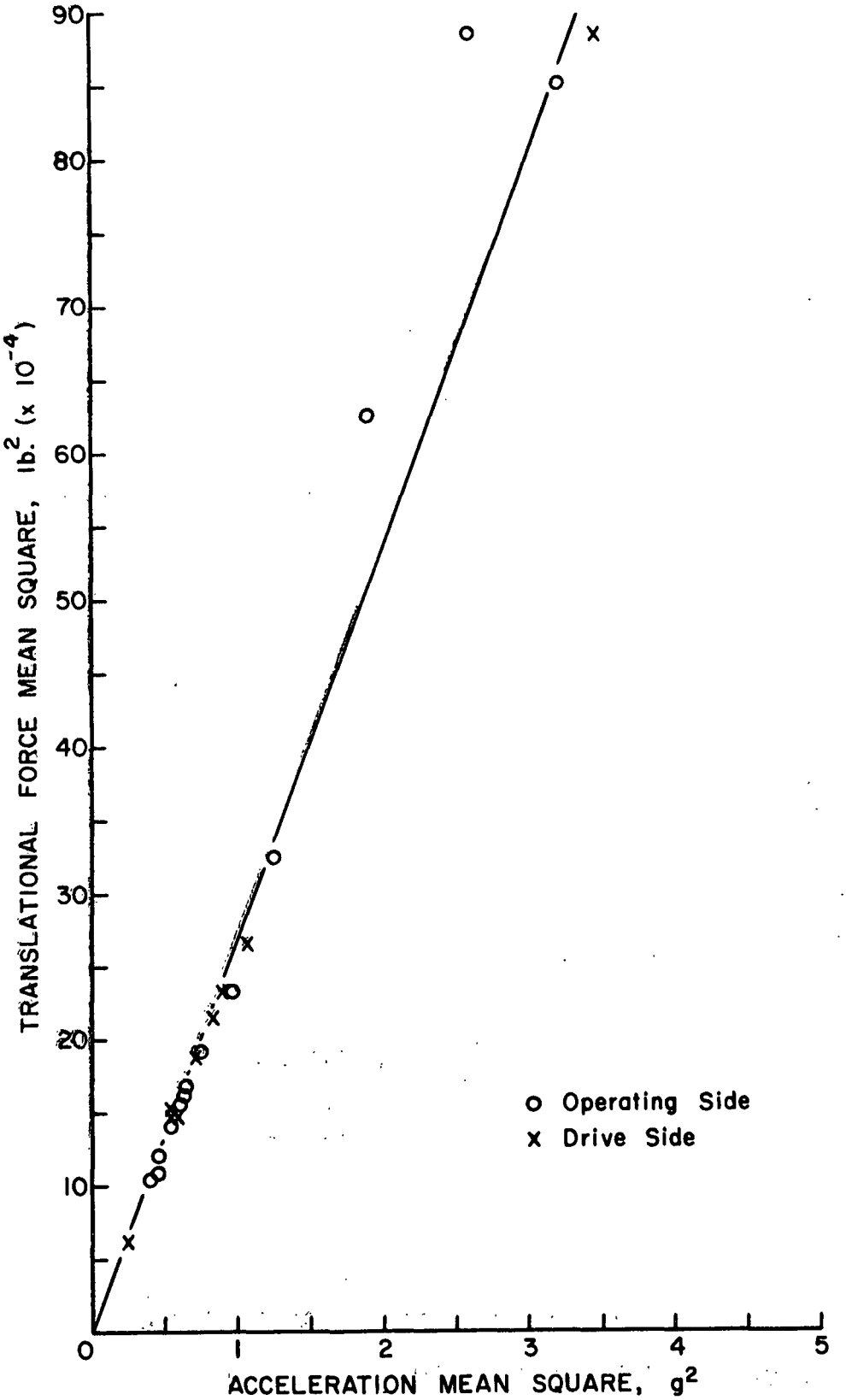

Figure 29. Relationship Between Translational Force and Acceleration Mean Square Values

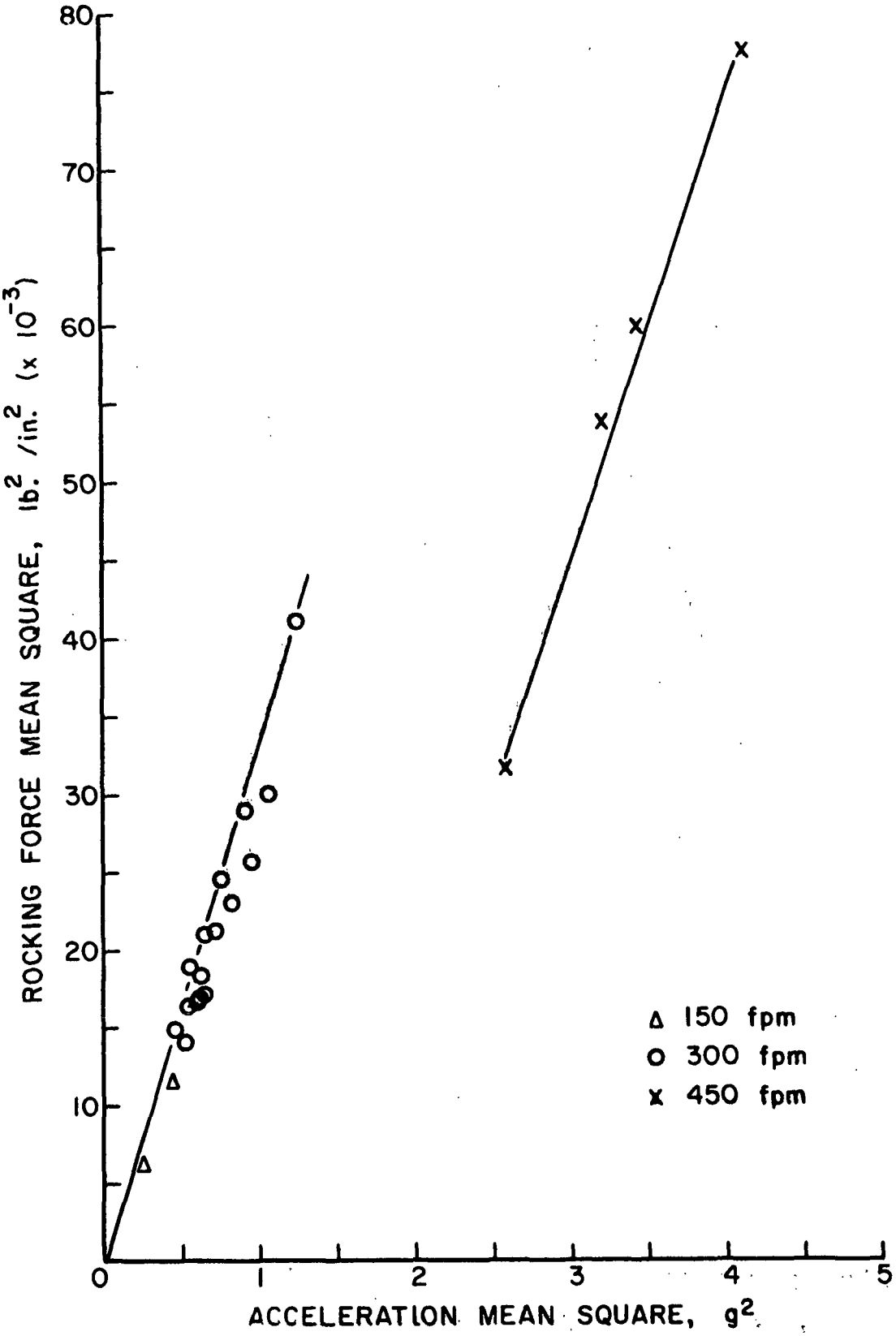

Figure 30. Relationship Between Rocking Force and Acceleration Mean Square Values

The two best regression equations are shown in Table XII. The first regression equation involved the following variables: (1) corrugator speed, (2) the mean square values for pressure, (3) the mean square values for acceleration, and (4) an interaction term involving the pressure mean square and tension spectral density at the flute-forming frequency. The speed, pressure, and acceleration terms were significant at either of the 0.05 levels. The pressure times tension interaction term was significant at the 0.10 level. A multiple correlation coefficient of 0.88 was obtained for the relationship.

The regression coefficient for speed was positive. This indicates average high-lows increase with speed which is in agreement with experience and past results.

A negative regression coefficient was obtained for the mean square value of the top roll acceleration. This indicates that, at a given speed, average high-lows tended to decrease as the acceleration mean square value increased. It may be recalled that the mean square value is a measure of the variance of the series. Inasmuch as the power spectrums showed that the main signal components were those occurring at the flute-forming frequency and its harmonics, the acceleration mean square values should be essentially proportional to the sum of the squares of the amplitudes at these frequencies.

Higher acceleration amplitudes imply that the medium is exposed to greater fluctuations in force about the mean level during the formation of each flute. At a given speed, changes in operating conditions which increase the amplitudes of the inertial force (higher acceleration mean square values) could lead to better molding of the flute arches on the average. This, in turn, could give rise to lower high-lows. Another way of viewing the cause for the negative coefficient for the acceleration mean square value is in terms of top roll displacement. For simple harmonic

TABLE XII

RELATIONSHIPS BETWEEN HIGH-LOWS AND POWER SPECTRAL ANALYSIS RESULTS

No.	Side	Regression Equation	t Value Var. 1	t Value Var. 2	t Value Var. 3	t Value Var. 4	Mult. Corr. Coeff.
1	Operator	$\underline{D} = -0.20 + 0.0067\underline{S} - 0.27\underline{P}_o - 0.40\underline{A}_o + 0.06\underline{P}_o\underline{T}_f$	4.53[a]	-2.58[b]	-4.02[a]	1.95[c]	0.88
	Drive	$\underline{D} = 0.34 + 0.0067\underline{S} - 0.27\underline{P}_d - 0.40\underline{A}_d + 0.06\underline{P}_d\underline{T}_f$					
2	Operator	$\underline{D} = 0.15 + 0.0077\underline{S} - 0.0000294\underline{F}_d$	5.30[a]	-5.28[a]	--	--	0.87
	Drive	$\underline{D} = 0.34 + 0.0077\underline{S} - 0.0000294\underline{F}_d$					

[a]Significant at 0.01 level.

[b]Significant at 0.05 level.

[c]Significant at 0.10 level.

Note: Symbols are as follows:

$\underline{F}_d$ = Mean square value of drive side rocking force

$\underline{P}_o, \underline{P}_d$ = Mean square value of operator and drive side top roll pressure, respectively.

$\underline{A}_o, \underline{A}_d$ = Mean square value of operator and drive side acceleration, respectively.

$\underline{T}_f$ = Spectral density of web tension at flute-forming frequency.

$\underline{S}$ = Corrugator speed, f.p.m.

$\underline{D}$ = Average flute height difference, pt.

motion, displacement is proportional to acceleration divided by the square of the frequency. At a given speed, changes in operating conditions which result in lower "average" acceleration amplitudes (lower mean square values) would give rise to smaller displacements of the top roll. This could result in poorer molding of the medium and, hence, in increased high-lows.

Similar explanations may explain the negative coefficient for the pressure mean square value in so far as the pressure variations are associated with top roll motion.

Web tension mean square values did not enter into the regression equation as a very significant factor. However, the tendency for the tension transducer to exhibit resonant vibrations near 540 Hz probably was an interfering factor in the regression analysis.

With these considerations in mind, the results indicate that high-lows are affected by the vibration amplitudes of the pressure and acceleration signals. Better tension measurements are needed to determine the degree of relationship between tension fluctuations and high-lows.

The correlations between the force mean square values and average flute height differences were also investigated. The best regression equation was obtained with the rocking force values and is shown in Table XII as Equation (2). Curiously, the results appeared to indicate that high-lows were best related to corrugator speed and the rocking force mean square values on the drive side, though the latter is dependent on both operator and drive acceleration and pressure values due to the method of calculation. The negative regression coefficient corresponded to that of the pressure and acceleration mean square values in Equation (1). It appears to imply that, at a given speed, operating conditions which increase the amplitudes

of the molding force fluctuations (higher mean square values) could lead to better molding of the medium arches and, hence, result in lower high-lows.

In addition to the above, an analysis was made to investigate, in a limited way, the degree of relationship (coherence) between individual flute height differences and variations in the pressure, tension, and acceleration signals. This was done for a few selected runs. In time series analysis, coherence is analogous to the square of the correlation coefficient in regression analyses.

For Run 9 which exhibited appreciable high-lows, a preliminary analysis indicated there was little or no coherence at the high-low frequency ($F/2$) between flute heights and the "average," maximum, or minimum level of a given signal prevailing during the formation of each flute.

Attention was then directed to using digital filters to approximately separate out signal components having frequencies near $F/2$, $3F/2$, etc., i.e., the frequencies near the high-low frequency ($F/2$) or multiples thereof. The filtered signals were then analyzed in conjunction with flute height data to determine the degree of coherence at or near the high-low frequency. Extensive calculations were required; hence, only three runs were analyzed in this way. The selected runs are listed below:

Run	Corrugating Conditions	Av. Flute Height Diff., pt.	
		Operator Side	Drive Side
6	Standard conditions	1.53	1.91
7	High web tension	1.13	2.11
9	No steam shower	1.44	2.63

The following results were obtained:

1. For Run 9, fairly favorable results were obtained, particularly on the operator side. The F/2 and/or 3F/2 components of the pressure and tension signals associated with certain positions in the flute exhibited statistically significant coherences ranging from 0.58 to 0.70 with operator side flute heights. The drive side flute heights exhibited lower coherences with the same frequency components but except for one pressure signal component were not significant at the 90% confidence level.
2. For Runs 6 and 7, less favorable results were obtained. In the case of Run 7, the F/2 components of the drive side pressure and tension exhibited coherences of about 0.52 with drive side flute heights. This level of coherence approached significance at the 0.05 level. Lower coherences were obtained for the operator side results for Run 7 — perhaps because the operator side did not exhibit appreciable high-lows. In the case of Run 6, the highest coherences were obtained with the pressure signals and the magnitudes (ca. 0.48) were at about the 90% confidence level.

Examination of the results suggests that the meaningful signal components were near the "noise" level of the experiment. The digital filtering techniques do permit focusing attention on selected vibration frequency bands. However, random vibrations and electrical "noise" having similar frequencies are also accentuated. Hence, the resulting "noise" may have obscured relationships between the variables and high-lows. These problems may be accentuated due to the aliasing

of higher frequency components involved in reducing the signals to a form suitable for direct analysis with flute heights.

FOURIER ANALYSES — ALL RUNS

Fourier analyses were carried out to estimate the amplitudes and phases of the flute-forming frequency component and its second and third harmonics for all signals and runs. The analyses were based on the data for the first 12 flutes in each instance, i.e., 12 replicates of eight data points each. It was restricted to 12 flutes to reduce possible cumulative errors due to digitizing. Because there were only eight data points per flute cycle, it was not possible to estimate fourth or higher harmonic components.

As one consequence, when important fourth harmonic components (or higher components) were present in a given signal, large prediction errors were commonly obtained indicating a poor fit to the data. Also, the statistical tests of significance for the harmonic coefficients and differences between replicates were not very sensitive.

The results obtained are summarized in Table XIII and XIV for operator and drive side top roll acceleration, respectively; in Tables XV and XVI for operator and drive side top roll pressure, respectively; and in Table XVII for web tension. As would be expected, the semiamplitudes exhibit trends similar to those obtained in the power spectral analyses.

The overall average magnitudes of the components at the flute-forming frequency are shown as follows:

TABLE XIII

FOURIER ANALYSIS OF OPERATOR SIDE TOP
CORRUGATING ROLL ACCELERATION SIGNALS

Run No.	Nominal Speed, f.p.m.	Corr. Cond.	Flute Freq., Hz	Semiamplitude, g. Flute Freq.	Second Harm.	Third Harm.	Semiamplitude, % Second Harm.	Third Harm.	Phase, ° Flute Freq.	Second Harm.	Third Harm.	Average Error, % [a]
					26 lb. S. C. Medium, Mill A							
1	150	Std.	87.9	0.40	0.24	0.12	60.0	30.0	154	27	238	11.6
2	225	Std.	138.3	0.53	0.28	0.24	52.8	45.3	237	106	219	356.0
3	300	Std.	184.6	0.89	0.46	0.12	51.7	13.5	232	78	220	175.5
4	375	Std.	227.3	0.82	0.29	0.12	35.4	14.6	240	139	348	26.5
5	450	Std.	279.6	1.66	1.68	0.45	101.2	27.1	134	139	267	19.9
					26 lb. S. C. Medium, Mill A							
6	300	Std.	186.3	0.88	0.49	0.14	55.7	15.9	226	88	281	177.8
7	300	Inc.Tens.	178.6	0.81	0.49	0.20	60.5	24.7	222	44	199	21.1
8	300	Low Press.	184.6	1.20	1.04	0.26	86.7	21.7	255	93	312	53.3
9	300	No Shower	185.7	1.00	0.55	0.31	55.0	31.0	202	31	176	35.1
					26 lb. S. C. Medium, Mill B							
12	300	Std.	184.0	1.16	0.52	0.20	44.8	17.2	247	137	270	38.5
14	450	Std.	280.0	1.81	0.93	0.17	51.4	9.4	101	105	181	5.4
					33 lb. S. C. Medium — Run 16, Mill A — Run 18 Mill B							
16	300	Std.	185.0	1.11	0.29	0.14	26.1	12.6	255	147	312	38.8
18	300	Std.	188.0	0.99	0.38	0.16	38.4	16.2	236	108	335	46.4
Av.				1.02	.59	0.20	55.4	21.5				

[a]High prediction errors indicate presence of components not accounted for in analysis — probably fourth or higher harmonics.

TABLE XIV

FOURIER ANALYSIS OF DRIVE SIDE TOP
CORRUGATING ROLL ACCELERATION SIGNALS

Run No.	Nominal Speed, f.p.m.	Corr. Cond.	Flute Freq., Hz	Semiamplitude, g. Flute Freq.	Second Harm.	Third Harm.	Semiamplitude, % Second Harm.	Third Harm.	Phase, ° Flute Freq.	Second Harm.	Third Harm.	Average Error, %[a]
				26 lb. S. C. Medium, Mill A								
1	150	Std.	87.9	0.22	0.17	0.04	77.3	18.2	176	9	155	5.7
3	300	Std.	184.6	0.97	0.58	0.20	59.8	20.6	209	100	225	37.9
5	450	Std.	279.6	1.24	2.20	0.02	177.4	1.6	130	118	40	19.1
				26 lb. S. C. Medium, Mill A								
6	300	Std.	186.3	0.90	0.85	0.30	94.4	33.3	203	127	270	267.3
7	300	Inc.Tens.	178.6	0.74	0.78	0.29	105.4	39.2	195	99	226	10.2
8	300	Low Press.	184.6	0.62	0.83	0.11	133.9	17.7	212	103	300	144.3
9	300	No Shower	185.7	0.97	0.77	0.29	79.4	29.9	179	89	156	130.0
				26 lb. S. C. Medium, Mill B								
12	300	Std.	184.0	1.05	0.97	0.32	92.4	30.5	221	175	276	82.1
14	450	Std.	280.0	1.72	1.46	0.46	84.9	26.7	94	90	84	45.0
				33 lb. S. C. Medium — Run 16, Mill A — Run 18, Mill B								
16	300	Std.	185.0	0.74	0.69	0.23	93.2	31.1	218	171	280	114.2
18	300	Std.	188.0	0.83	0.59	0.19	71.1	22.9	208	148	287	175.7
Av.				0.91	0.90	0.22	97.2	24.7				

[a]High prediction errors indicate presence of components not accounted for in analysis — probably fourth or higher harmonics.

TABLE XV

FOURIER ANALYSIS OF OPERATOR SIDE TOP CORRUGATING ROLL PRESSURE SIGNALS

Run No.	Nominal Speed, f.p.m.	Corr. Cond.	Flute Freq., F, Hz	Semiamplitude, p.s.i.g.			Semiamplitude, %[a]		Phase, °			Average Error, %[a]
				Flute Freq.	Second Harm.	Third Harm.	Second Harm.	Third Harm.	Flute Freq.	Second Harm.	Third Harm.	
						26 lb. S. C. Medium, Mill A						
1	150	Std.	87.9	1.47	1.95	0.36	132.7	24.5	257	176	37	3.1
2	225	Std.	138.3	1.85	1.23	0.31	66.5	16.8	323	297	17	18.6
3	300	Std.	184.6	3.57	0.90	0.30	25.2	8.4	1	252	78	498.2
4	375	Std.	227.3	2.64	0.27	1.97	10.2	74.6	46	333	226	41.0
5	450	Std.	279.6	3.42	1.85	0.42	54.1	12.3	332	293	72	13.4
						26 lb. S. C. Medium, Mill A						
6	300	Std.	186.3	3.80	1.06	0.61	27.9	16.1	357	254	108	44.8
7	300	Inc.Tens.	178.6	3.25	0.86	0.56	26.5	17.2	339	250	84	204.3
8	300	Low Press.	184.6	2.01	2.57	0.12	127.9	6.0	77	304	206	50.4
9	300	No Shower	185.7	4.02	0.69	0.52	17.2	12.9	333	206	51	529.2
						26 lb. S. C. Medium, Mill B						
12	300	Std.	184.0	9.26	1.71	2.24	18.5	24.2	31	359	359	43.2
14	450	Std.	280.0	3.81	1.12	0.42	29.4	11.0	301	233	133	25.5
						33 lb. S. C. Medium — Run 16, Mill A — Run 18, Mill B						
16	300	Std.	185.0	4.97	0.73	0.33	14.7	6.6	9	327	129	14.8
18	300	Std.	188.0	3.88	0.87	0.79	22.4	20.4	4	308	91	47.9
Av.				3.69	1.22	0.69	44.1	19.3				

[a]High prediction errors indicate presence of components not accounted for in analysis — probably fourth or higher harmonics.

TABLE XVI

FOURIER ANALYSIS OF DRIVE SIDE TOP
CORRUGATING ROLL PRESSURE SIGNALS

Run No.	Nominal Speed, f.p.m.	Corr. Cond.	Flute Freq., F, Hz	Semiamplitude, p.s.i.g. Flute Freq.	Semiamplitude, p.s.i.g. Second Harm.	Semiamplitude, p.s.i.g. Third Harm.	Semiamplitude, % [a] Second Harm.	Semiamplitude, % [a] Third Harm.	Phase, ° Flute Freq.	Phase, ° Second Harm.	Phase, ° Third Harm.	Average Error, %[a]
				26 lb. S. C. Medium, Mill A								
1	150	Std.	87.9	0.85	0.22	0.11	25.9	12.9	273	136	37	14.4
3	300	Std.	184.6	1.36	1.08	0.10	79.4	7.4	298	281	29	36.5
5	450	Std.	279.6	4.21	2.00	0.46	47.5	10.9	328	324	84	6.8
				26 lb. S. C. Medium, Mill A								
6	300	Std.	186.3	1.73	1.76	0.16	101.7	9.2	297	298	181	32.6
7	300	Inc.Tens.	178.6	1.54	1.12	0.28	72.7	18.2	23	301	130	13.1
8	300	Low Press.	184.6	3.04	0.23	0.15	7.6	4.9	97	67	76	12.6
9	300	No Shower	185.7	1.87	1.11	0.08	59.4	4.3	260	238	91	70.2
				26 lb. S. C. Medium, Mill B								
12	300	Std.	184.0	5.85	0.94	0.26	16.1	4.4	60	31	74	8.7
14	450	Std.	280.0	3.39	1.19	1.46	35.1	43.1	307	279	21	11.6
				33 lb. S. C. Medium — Run 16, Mill A — Run 18, Mill B								
16	300	Std.	185.0	4.14	0.68	0.40	16.4	9.7	62	16	323	59.7
18	300	Std.	188.0	4.85	0.94	0.42	19.4	8.7	46	348	28	43.4
Av.				2.98	1.02	0.35	43.7	12.2				

[a]High prediction errors indicate presence of components not accounted for in analysis — probably fourth or higher harmonics.

TABLE XVII

FOURIER ANALYSIS OF TOP CORRUGATING ROLL TENSION SIGNALS

Run No.	Nominal Speed, f.p.m.	Corr. Cond.	Flute Freq., Hz	Semiamplitude, lb./in. Flute Freq.	Second Harm.	Third Harm.	Semiamplitude, % [a] Second Harm.	Third Harm.	Phase, ° Flute Freq.	Second Harm.	Third Harm.	Average Error, %[a]
						26 lb. S. C., Mill A						
1	150	Std.	87.9	0.21	0.03	0.02	14.3	9.5	102	290	131	10.9
2	225	Std.	138.3	0.16	0.21	0.04	131.2	25.0	145	107	193	200.8
3	300	Std.	184.6	0.16	0.16	0.42	100.0	26.2	90	298	119	4.7
4	375	Std.	227.3	0.19	0.08	0.02	42.1	10.5	83	338	87	10.6
						26 lb. S. C., Mill A						
6	300	Std.	186.3	0.23	0.15	0.50	65.2	21.7	79	338	197	17.8
7	300	Inc.Tens.	178.6	0.25	0.17	0.10	68.0	40.0	74	280	65	2.2
8	300	Low Press.	184.6	0.38	0.13	0.26	34.2	68.4	33	322	231	3.1
9	300	No Shower	185.7	0.22	0.18	0.45	81.8	204.5	57	264	114	2.4
						26 lb. S. C., Mill B						
12	300	Std.	184.0	0.18	0.20	0.46	111.1	255.6	84	357	157	2.3
14	450	Std.	280.0	0.13	1.92	0.05	1476.9	38.5	46	90	100	2.5
						33 lb. S. C. — Run 16, Mill A — Run 18, Mill B						
16	300	Std.	185.0	0.33	0.23	0.62	69.7	187.9	113	1	202	29.6
18	300	Std.	188.0	0.40	0.10	0.46	25.0	115.0	65	308	220	7.9
Av.[b]				0.25	0.15	0.30	67.5	87.7				

[a] High prediction errors indicate presence of components not accounted for in analysis — probably fourth or higher harmonics.

[b] Omitting Run 14.

	Semiamplitude	
	Operator Side	Drive Side
Top roll acceleration, g	± 1.02	± 0.91
Top roll pressure, p.s.i.	± 3.69	± 2.98
Web tension, lb./in.	± 0.25	

Relative to the average top roll pressures of 260 and 240 p.s.i. (operator and drive sides, respectively) which prevailed in all but one run, the pressure semiamplitudes are relatively small. Therefore, it appears likely that the oscillations in top roll pressure are not great enough to directly cause high-lows.

Assuming that half the top roll mass (103#/g) acts on each side of the machine, the average force semiamplitudes due to top roll acceleration, would be about 530 and 470 lb. for the operator and drive sides, respectively. This is about 86 and 78 lb./in., respectively. For a top roll pressure of 260 p.s.i., the line load is estimated at about 350 lb./in. for the Institute's corrugator. Thus, the acceleration semiamplitudes at the flute-forming frequency correspond to a fluctuating force of about ± 25% of the average top roll force. Consequently, the up-and-down acceleration of the top roll produces a relatively large variation in force on the corrugating medium. It appears possible that variations in the magnitude of this fluctuating force from flute-to-flute could be related to the occurrence of high-lows.

The average semiamplitude of web tension at the flute-forming frequency was 0.25 lb./in. Relative to the average tension level of 0.5 lb./in. used in all but one run, this amounts to a ± 50% variation in tension during the formation of each flute. Inasmuch as tension increases toward the center of the labyrinth due to friction, an initial oscillation semiamplitude of ± 0.25 lb./in. will be much greater near the center. Thus, variations in the magnitude of the web tension

from flute-to-flute could possibly be great enough to influence flute formation and, hence, high-lows.

The acceleration semiamplitudes at the flute frequency increased with increasing corrugating speed as would be expected. Figure 31 shows the relationship between semiamplitude and speed for the runs made with 26-lb. semichemical medium at standard conditions. Fitting a line to the data by eye, indicated the slope was about 1.5. For simple harmonic motion, the slope would be 2.0. The lower slope may be due to the damping action and/or nonlinear elastic behavior of the corrugating medium.

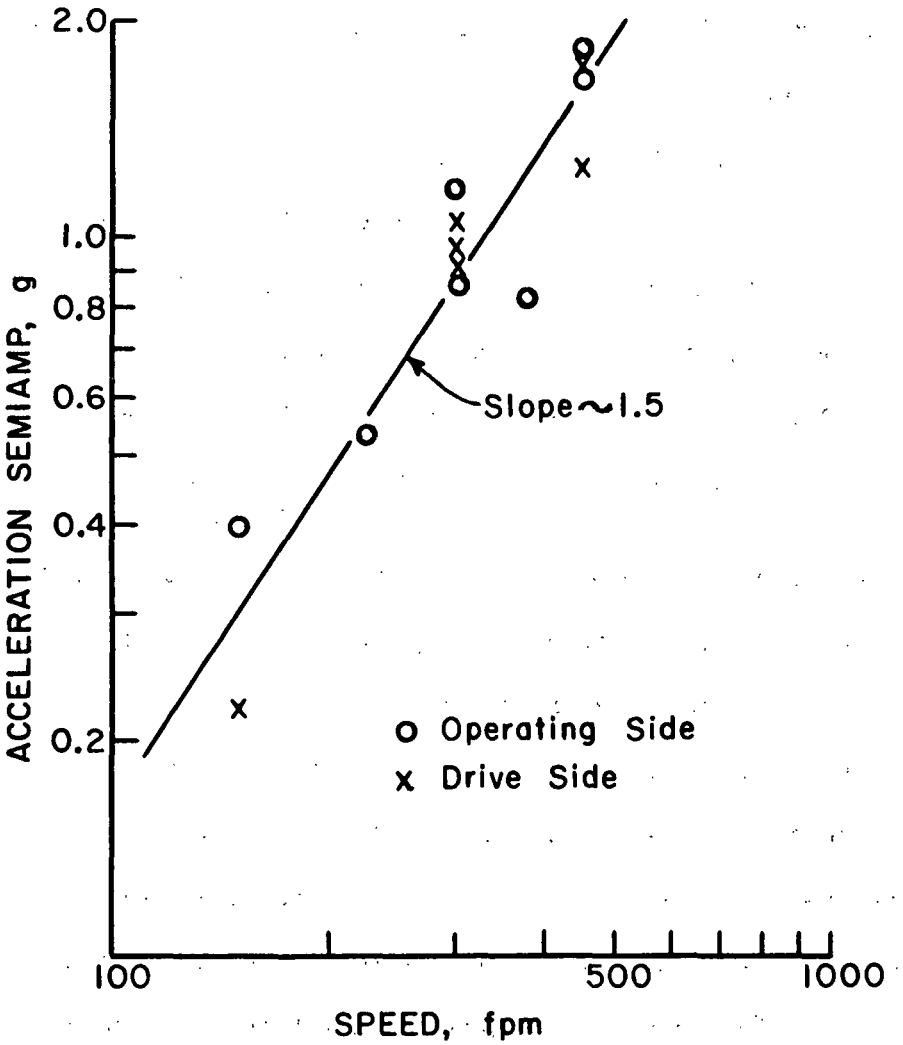

Figure 31. Relationship Between Acceleration Semiamplitude at the Flute-Forming Frequency and Speed (26-lb. Medium, Standard Corrugating Conditions)

The relative magnitudes of the second and third harmonics varied greatly from run-to-run for the acceleration, pressure, and web tension signals. A similar behavior was observed in the cases of the power spectral densities. At certain speeds and depending somewhat on other conditions, certain parts of the corrugator must be excited to vibrate at their natural frequency. These vibrations appear as greater than "normal" high harmonics in the pressure, acceleration, and tension signals. Further work is needed to identify the machine parts giving rise to these vibrations.

Table XVIII shows the average second and third harmonic semiamplitudes as percentages of the semiamplitude of the flute-frequency component. On the average, the drive side acceleration second harmonic was much greater than on the operator side. Thus, the top roll inertial forces on the medium due to the second harmonic were different on the two sides of the corrugator during these runs. The web tension results show that the second and third harmonic semiamplitudes averaged 67.5 and 87.7% of the semiamplitude of the flute-frequency component. Both appear to contribute significantly to the web tension variations. However, the importance of the third harmonic may be caused, in part, by the transducer itself.

The phase values on Tables XIII-XVII show the location in the cycle where the maximum amplitude for the particular frequency is attained relative to the start ($\underline{t} = 0$). For a given run, the digitizing was carried out so that all signals had a common starting time. The starting time was based on the operator side pressure signal. It was selected so that it approximately coincided with a maximum peak in the signal. These peaks occur as an arch of the flute is formed (see Fig. 1). For this reason, the phases at the flute-forming frequency of the operator side pressure signal are near 0° or 360° in most instances. Deviations from these values occurred

because the higher harmonics tended to obscure the true maximum corresponding to the flute-frequency component when the starting time was chosen.

TABLE XVIII

AVERAGE SEMIAMPLITUDES OF SECOND AND THIRD HARMONICS OF FLUTE-FORMING FREQUENCY

Signal	Semiamplitude, %[a]					
	Second Harmonic			Third Harmonic		
	Max.	Min.	Av.	Max.	Min.	Av.
Top roll acceleration, g						
Operator side	101.2	26.1	55.4	45.3	9.4	21.5
Drive side	177.4	59.8	97.2	39.2	1.6	24.7
Top roll pressure, p.s.i.						
Operator side	132.7	10.2	44.1	74.6	6.0	19.3
Drive side	101.7	7.6	43.7	43.1	4.3	12.2
Web tension[b]	131.2	25.0	67.5	204.5	9.5	87.7

[a] Percent of flute frequency semiamplitude.

[b] Run 14 omitted from average.

At the flute-forming frequency, the phase data indicate that the maximum semiamplitude of the acceleration and pressure signal is generally attained somewhat earlier on the drive side during formation of a flute. This was generally true for both pressure and acceleration. There was some indication that the phase difference changed with speed, however, and further data are needed to clarify this aspect.

CORRELATIONS BETWEEN FOURIER SEMIAMPLITUDES AND AVERAGE HIGH-LOWS

Correlations were carried out to determine the degree of relationship between the semiamplitudes of the top roll pressure, acceleration, and web tension signals and average high-lows. The analysis was restricted to the eleven runs for which both pressure and acceleration data were available. A "dummy" variable technique was used to allow for the difference in high-low levels between operator and drive sides. The tension data for Run 14 (corrugating speed of 450 f.p.m.) were also employed for Run 5 which was fabricated at the same speed.

For the semiamplitudes at the flute-forming frequency, the best regression equations obtained with all factors significant at the 0.01 level were as follows:

Operator side: $D = 0.11 + 3.30T + 0.58\ A_d$ (12)

Drive side: $D = 0.50 + 3.30T + 0.58\ A_d$ (13)

where

$\underline{D}$ = average flute height difference, pt.

$\underline{T}$ = tension semiamplitude at flute frequency, lb./in.

$\underline{A_d}$ = drive side acceleration semiamplitude at flute frequency, g

The multiple correlation coefficient was 0.844. These results indicate that greater average fluctuations in web tension and top roll acceleration at the flute-forming frequency cause greater high-lows. Thus, machine conditions and medium properties which affect either web tension or the up-and-down acceleration of the top roll may be expected to affect high-low flute formation. The frictional properties of the medium would be expected to affect the web tension fluctuations. The medium also functions as a nonlinear spring/damper between the top and bottom corrugating roll. Hence, properties of the medium which affect its flow and

deformation under pressure may be expected to affect the up-and-down accelerations of the top roll.

The operator side acceleration semiamplitude did not enter the equation until late in the stepwise regression procedure. This probably occurred because it was highly intercorrelated with the drive side acceleration values.

FOURIER ANALYSES — RUN 6

A more detailed Fourier analysis was carried out on the top roll pressure, web tension, and top roll acceleration signals for Run 6. This run was carried out at 300 f.p.m. under standard corrugating conditions. A more detailed analysis was carried out for this run because the oscillograph records were digitized so as to obtain approximately sixteen data points per flute per signal rather than eight as in the case of the other runs. Thus, the additional data points enhanced the statistical reliability of the Fourier analysis results.

For the analyses, the data for the first twelve flutes were utilized. By treating the data as six replicates of 32 observations (two flutes), estimates were obtained for the average semiamplitude and phase of components at $\underline{F}/2$, $\underline{F}$, $3\underline{F}/2$, — $4\underline{F}$ where $\underline{F}$ is the flute-forming frequency ($\underline{F}$ = 186.3 Hz for this run). The components at $\underline{F}$, $2\underline{F}$, $3\underline{F}$, and $4\underline{F}$ are termed the flute-forming frequency, second, third, and fourth harmonics, respectively. As discussed previously, the procedures outlined by Bliss (10) were used to evaluate the statistical significance of the Fourier terms. It should be mentioned that the analysis was purposely restricted to the data for the first twelve flutes to reduce cumulative digitizing errors. For this run, the digitizing error over 120 flutes (1920 data points per signal) amounted to about 0.2%, i.e., the observations extended over about 120.25 flutes rather than 120 flutes.

The results obtained in the analyses are summarized in Table XIX. In most cases the components at the flute-forming frequency or its harmonics (frequency ratios of 1, 2, 3, and 4) exhibited statistical significance at the 0.01 level. On the other hand, the components at frequency ratios of 0.5, 1.5, 2.5 and 3.5 were not statistically significant at the 0.05 level except in one instance. Their magnitudes were also much lower than the magnitudes of the components at the flute-forming frequency. These results confirm the power spectral analyses results which indicated that the principal vibration components in all the signals were those associated with the flute-forming frequency and/or its harmonics. In view of these results, it appears that high-lows are more likely to be related to variations in amplitude and phase from flute-to-flute of the components at the flute-forming frequency and/or its harmonics.

As would be expected from the power spectrum results, the amplitudes of the harmonics of the flute-forming frequency (F) were in some cases nearly as large as the components at the flute-forming frequency. For example, the fourth harmonic component (frequency ratio = 4.0) on the operator side pressure signal was the second highest component. Its amplitude was 67.5% as great as the component at the flute-forming frequency. In the case of the drive side pressure and the operator and drive side acceleration signals, the amplitudes of the second harmonic (frequency ratio = 2), were 85.6, 53.8, and 90.6% of the amplitudes of the respective flute-forming frequency components. The third harmonic (frequency ratio = 3.0) in the tension signal was more than twice as great as the flute-forming frequency component — possibly due to a resonant vibration at this frequency in the tension transducer. Thus, all the signals were rich in harmonic content. If the analysis was extended to higher frequencies, it is likely that significant higher harmonics could also be detected in some cases. This means

TABLE XIX

FOURIER ANALYSIS OF TOP ROLL PRESSURE, ACCELERATION, AND WEB TENSION RESULTS AT 300 F.P.M.
(Run 6)

Harmonic No.	Nominal Freq., Hz	Freq. Ratio[a]	Top Roll Pressure						Top Roll Acceleration						Web Tension		
			Operator Side			Drive Side			Operator Side			Drive Side					
			Semiamp.			Semiamp.			Semiamp.			Semiamp.			Semiamp.		
			p.s.i.	%[b]	Phase, °	p.s.i.	%[b]	Phase, °	g.	%[b]	Phase, °	g.	%[b]	Phase, °	lb./in.	%[b]	Phase, °
1	90	0.5	0.080	2.1	73	0.251	14.8	340	0.057	6.1	175	0.008	0.9	147	0.008	3.8	27
2	180	1.0	3.828[d]	100.0	0	1.699[d]	100.0	295	0.928[d]	100.0	224	0.866[d]	100.0	205	0.211[d]	100.0	80
3	270	1.5	0.142	3.7	353	0.279	16.4	307	0.080	8.6	120	0.130[c]	15.0	130	0.004	1.9	98
4	360	2.0	0.862[d]	22.5	264	1.455[d]	85.6	296	0.499[d]	53.8	80	0.782[d]	90.3	128	0.164[d]	77.7	327
5	450	2.5	0.164	4.3	12	0.056	3.3	159	0.039	4.2	182	0.012	1.4	209	0.012	5.7	8
6	540	3.0	0.642[d]	16.8	121	0.095	5.6	138	0.225[d]	24.2	265	0.225[d]	25.4	271	0.487[d]	230.8	192
7	630	3.5	0.158	4.1	290	0.034	2.0	246	0.030	3.2	120	0.039	4.5	61	0.010	4.7	84
8	720	4.0	2.586[d]	67.6	110	0.271	16.0	312	0.352[d]	37.9	171	0.416[d]	48.0	153	0.035	16.6	140
Mean	---	--	-1.254			0.331			-0.024			-0.043			-0.217		
Significance level of difference between replicates			0.01			NS			NS			NS			0.01		

[a] Ratio of frequency to nominal flute-forming frequency (180 Hz).

[b] Semiamplitudes expressed in percent of semiamplitudes at flute-forming frequency.

[c] Fourier sine and cosine coefficients significant at 0.05 level.

[d] Fourier sine and cosine coefficients significant at 0.01 level.

Note: Underlined values indicate significant differences in Fourier coefficients between replicate flutes.

that the stress environment during the molding of each flute is the complex result of a number of frequency components. This may be expected to vary with corrugator and operating conditions.

At the flute-forming frequency, the semiamplitudes of the pressure signals were 3.828 and 1.699 p.s.i.g. for the operator and drive sides, respectively. The top roll operating pressure levels were 260 and 240 p.s.i.g. on the operator and drive sides, respectively. Thus, the pressure semiamplitudes were small relative to the average operating levels and it seems unlikely that variations in their magnitude could directly cause high-lows.

At the flute-forming frequency, the acceleration amplitudes were 0.928 and 0.866 g for the operator and drive sides, respectively. Assuming that half the mass of the upper roll including bearing blocks acts on each side, the inertial forces induced by the accelerations of the upper roll are obtained by multiplying the accelerations in g units by half the weight of the upper roll (1034 lb.). On this basis the acceleration semiamplitudes correspond to forces of 480 and 448 lb. or about 80 and 75 lb./in. of width for the operator and drive sides, respectively. The static force on the bottom corrugating roll for a top roll pressure of 260 p.s.i. is about 350 lb./in. Thus, the force semiamplitudes indicated by the upper roll accelerations are about 20-25% of the static component due to average top roll pressure and roll weight. As a consequence, fairly substantial variations in molding force on the medium are caused by the up-and-down accelerations of the upper corrugating roll. It appears possible that variations on the molding force from flute-to-flute could affect high-low flute formation.

The tension semiamplitude at the flute-forming frequency was 0.211 lb./in. or about 40% of the nominal operating level of 0.5 lb./in. for this run. Thus,

the initial tension force on the medium due to the flute frequency component oscillates from about 0.289 to 0.711 lb./in. on the average. A much greater semiamplitude of 0.487 lb./in. was obtained for the third harmonic of the flute frequency implying that the web tension was oscillating from near zero to almost 1 lb./in. However, this semiamplitude may be erroneously great if it is due to the transducer being excited at its natural frequency. Considering only the component at the flute-forming frequency, it may be recalled that the maximum tension in the nip is much higher than the initial tension (14). For example, for coefficients of friction of 0.20 and 0.30, it was estimated in Reference (14) that the ratios of maximum tension near the center of the labyrinth to initial tension would be 4.1 and 8.5, respectively. Hence, the maximum average tension values for these two cases would be 2.1 and 4.25 lb./in., respectively, for an initial average tension of 0.5 lb./in. Superimposed on these average values would be fluctuations of ± 0.87 and ± 1.79 lb./in. due to the tension component at the flute-forming frequency. Hence, fairly large oscillations in web tension occur within the corrugating labyrinth.

The phase values shown in Table XIX indicate the location in the cycle where the maximum amplitude occurs. They are measured relative to an arbitrarily selected common starting time for all signals. The starting time was selected to approximately coincide with a peak in the operator side pressure signal corresponding to the time when an arch of the flute which would later be bonded to the liner was formed. Thus, for the flute frequency component (frequency ratio = 1.0) the phase of the operator side pressure component was 0°. This indicates that the operator side pressure flute frequency component was a maximum at $\underline{t} = 0$ when the arch of the flute which would subsequently be bonded to the liner was formed. The corresponding phase for the drive side pressure signal was 295°. This indicates

that the maximum semiamplitude of the flute-frequency component of the drive side pressure led the operator side pressure by 65° (360-295°).

At the flute-forming frequency, the acceleration phases were 224 and 205° for the operator and drive sides, respectively. Thus, a phase difference of about 19° between operator and drive sides was obtained with the drive side leading the operator side. Thus, it appears that the maximum semiamplitudes of both the top roll pressure and acceleration flute frequency components are attained somewhat earlier during the formation of a flute on the drive side.

At the flute-forming frequency, the maximum tension semiamplitude was attained at 80°, i.e., at about the time a sidewall of the flute was at the center line.

For two of the signals, operator side pressure and web tension, there were significant differences between the six pairs of replicate flutes. Such differences may be associated with trends in the mean value over the 12-flute interval.

In addition, the analyses of variances indicated that in many cases there were highly significant differences in the Fourier coefficients between replicate flutes even over the 12-flute interval. At the flute-forming frequency (frequency ratio = 1.0) this was true for all signals but drive side pressure. The analyses also indicated in these cases that the differences between flutes generally involved both the amplitude and phase of the components. Variations in amplitude and/or phase from flute-to-flute would affect the stresses imposed on the medium. Because such variations might be associated with high-low flute formation, it was decided to investigate the nature and magnitude of the variation. The results obtained are summarized in the following section.

VARIATIONS IN INDIVIDUAL FLUTE HARMONIC COMPONENTS — RUN 6

For this phase of the analysis of Run 6, a Fourier analysis was carried out on a flute-by-flute basis. The amplitude and phase of the flute frequency component and the second, third, and fourth harmonics were determined for each consecutive set of 16 data points per signal, i.e., for each flute.

The semiamplitudes for each harmonic and signal were averaged and the coefficients of variation were calculated. The results are summarized in Table XX. The coefficients of variation for web tension ranged from 16.0 to 52.5%. For top roll acceleration, the coefficients of variation ranged from 13.6 to 37.6 on the operator side and 16.3 and 33.7% on the drive side. Even greater variability was found in the top roll pressure results. Thus, the data indicate that the amplitudes of the main harmonic components exhibit appreciable variability from flute-to-flute.

When the phase results were examined, two trends in the data were discerned. First, the phase values for each signal and harmonic decreased approximately linearly over the 118 flutes. At the flute frequency the change in phase amounted to above 69°. This linear change in phase is believed to be due to the cumulative errors in digitizing over the record length. It amounted to the equivalent of a 0.2% error over 1888 data points or less than 1/4 flute in 120 flutes. Second, it was observed that cyclic changes in phase were superimposed on the linear trend. To better examine these cyclic changes, the phase values for the flute-forming frequency component were adjusted for the linear trend using linear regression and the adjusted values were smoothed using a short moving average. The resulting phase values are graphed in Fig. 32 together with the absolute flute height differences, i.e., the sign of the flute height difference is disregarded.

TABLE XX

SUMMARY OF FOURIER RESULTS FOR INDIVIDUAL FLUTE ANALYSIS

Harmonic No.	Freq., Hz	Top Roll Acceleration, g.				Top Roll Pressure, p.s.i.				Web Tension, lb./in.	
		Operator Side		Drive Side		Operator Side		Drive Side			
		Av.	V	Av.	V	Av.	V	Av.	V	Av.	V
1[a]	186.3	0.92	13.6	0.88	16.3	3.73	15.1	1.62	25.5	0.27	30.7
2	372.6	0.46	31.9	0.76	21.8	0.78	49.8	1.37	25.5	0.19	34.3
3	558.9	0.25	37.6	0.31	33.7	0.62	57.2	0.29	56.5	0.59	16.0
4	745.2	0.44	18.8	0.46	21.1	3.16	22.4	0.44	41.4	0.09	52.5

[a]Flute-forming frequency.

Note: Av. is the average of the semiamplitudes over 118 flutes.

V is the coefficient of variation.

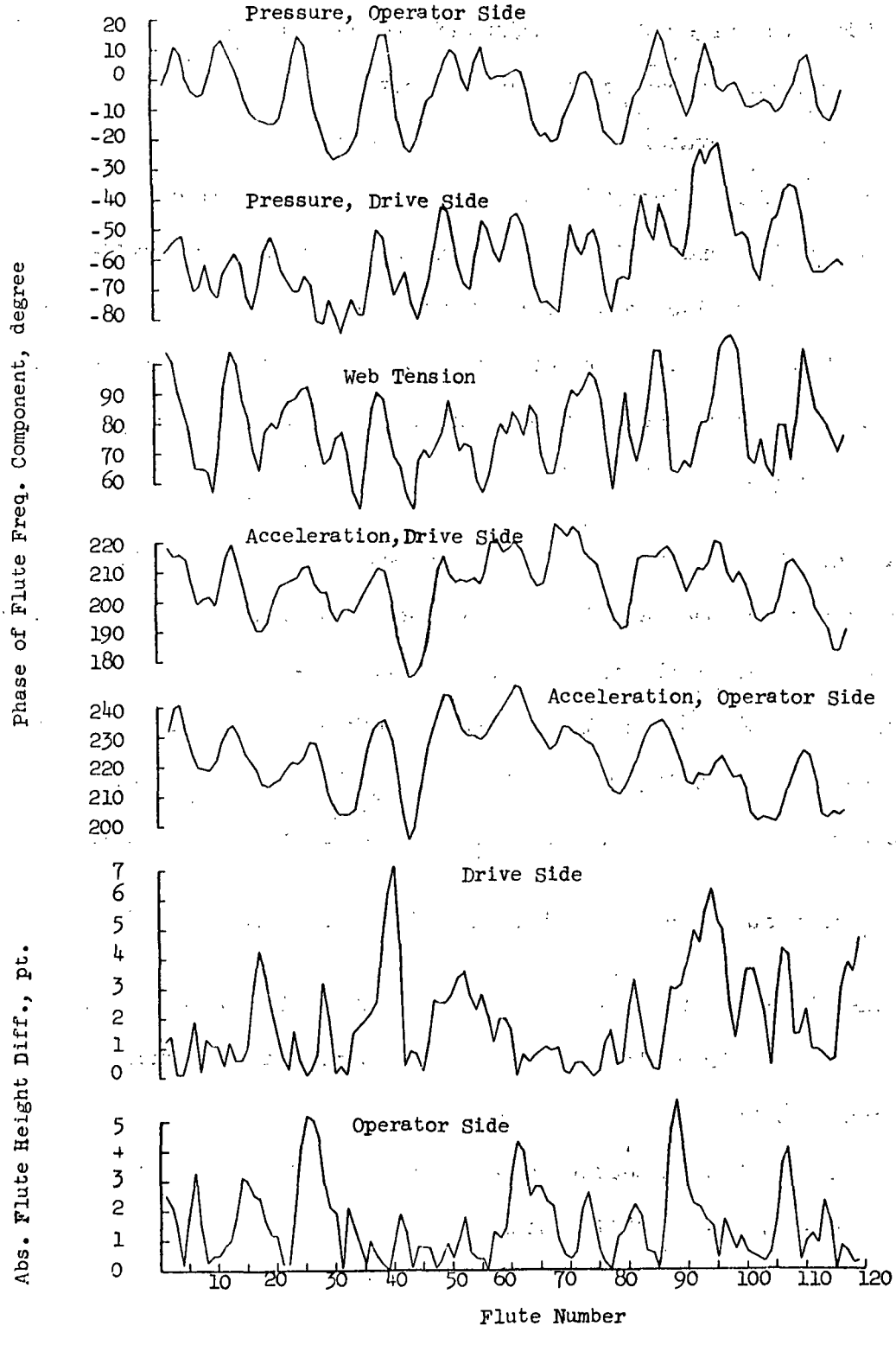

Figure 32. Phase of Flute Frequency Component and Absolute Flute Height Difference vs. Flute Number for Run 6

Figure 32 shows that all signals exhibited an irregular cyclic change in phase having an approximate frequency of 15 Hz. Peaks in phase often but not always appear to coincide with larger flute height differences on one side or the other of the machine. For example, a peak in phase at about Flute 13 or 14 appears to coincide with a peak in the operator side flute height differences at Flute 14. The phases generally peak about Flute 25 or 26 and large operator side flute height differences occur in the same region. The drive side flute height difference peaks near 23 and 28 flutes may also be associated with the phase peaks near 25 or 26. All the phases peak at about the 38th or 39th flute and very large flute height differences were obtained on the drive side in this region. Further points of similarity are also evident in Fig. 31.

As an additional illustration, Fig. 33 shows the average phase for all signals vs. flute number together with the average flute height difference for the two sides of the machine. Peaks in phase were obtained at Flute numbers 4-5, 13, 26, 39, 50, 60, 71-74, 86, 96, and 110. Peaks in flute height differences were obtained at Flute numbers 6, 17, 28, 40, 52, 60-62, 72-73, 81, 88, 94, 100, and 117. A fair degree of correspondence in the two series appears to occur.

The above results appear to indicate the following for this run:

1. The phases of the first harmonic component (flute frequency) exhibit an irregular cyclic behavior having a frequency of about 15 Hz.
2. Peaks in phase appeared to often coincide with regions of greater high-low differences.

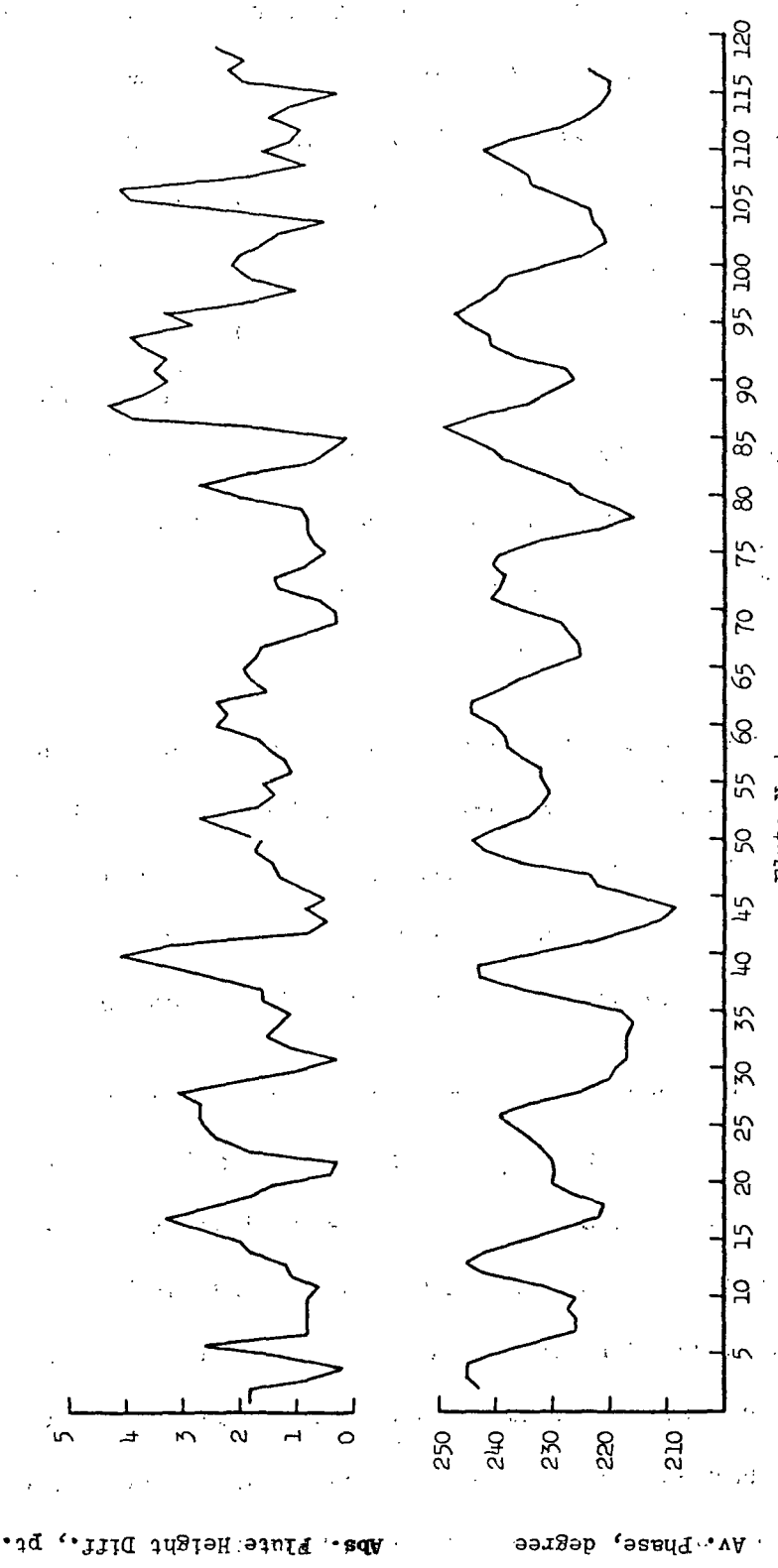

Figure 33. Average Phase of Flute Frequency Component and Average Absolute Flute Height Difference for Operator and Drive Side vs. Flute Number

Phase refers to the location or time during the formation of a flute when the particular signal exhibits its maximum amplitude. As the phase shifts, the maximum amplitude occurs at a different time in the formation of the flute. For example, in the case of the pressure signal on the operator side, Fig. 32 shows that the maximum amplitude shifts back and forth from the leading to the lagging side of the flute arch. Similarly, in the case of web tension, Fig. 31 shows that the maximum amplitude is sometimes attained as early as 60° (1/6 of the flute) or as late as 110° (nearly at 1/3 of the flute). Thus, it may be speculated that high-low flute formation is related in part to the points in time when maximum stresses are applied during the formation of a given flute. This certainly appears to be a fruitful area for future study. The phase shifts in the other harmonic components should be examined. Also, similar analyses should be performed on data obtained at other machine speeds, conditions, etc.

The cause for the phase variation is not known. The fact that all the signals tended to exhibit similar though not identical cycles indicates they have a common cause. Perhaps the phase shifts have their origin in a low frequency vibration common to all signals or a beat frequency induced by two vibration components. Possibly, small but cyclic variation in machine speed occurs.

The nature of the change in semiamplitude of the first harmonic components of the acceleration and tension signals vs. flute number is illustrated in Fig. 34. It may be noted that the acceleration semiamplitudes tend to exhibit a high-low behavior, i.e., the amplitudes frequently vary in a high-low-high, etc., pattern. The power spectrums (not shown) for the semiamplitudes of the flute frequency components also indicated the presence of significant variations at about one-half the flute frequency — a characteristic of a high-low pattern. By comparison with Fig. 32 and 33, it also may be noted that unusually high or low semiamplitudes

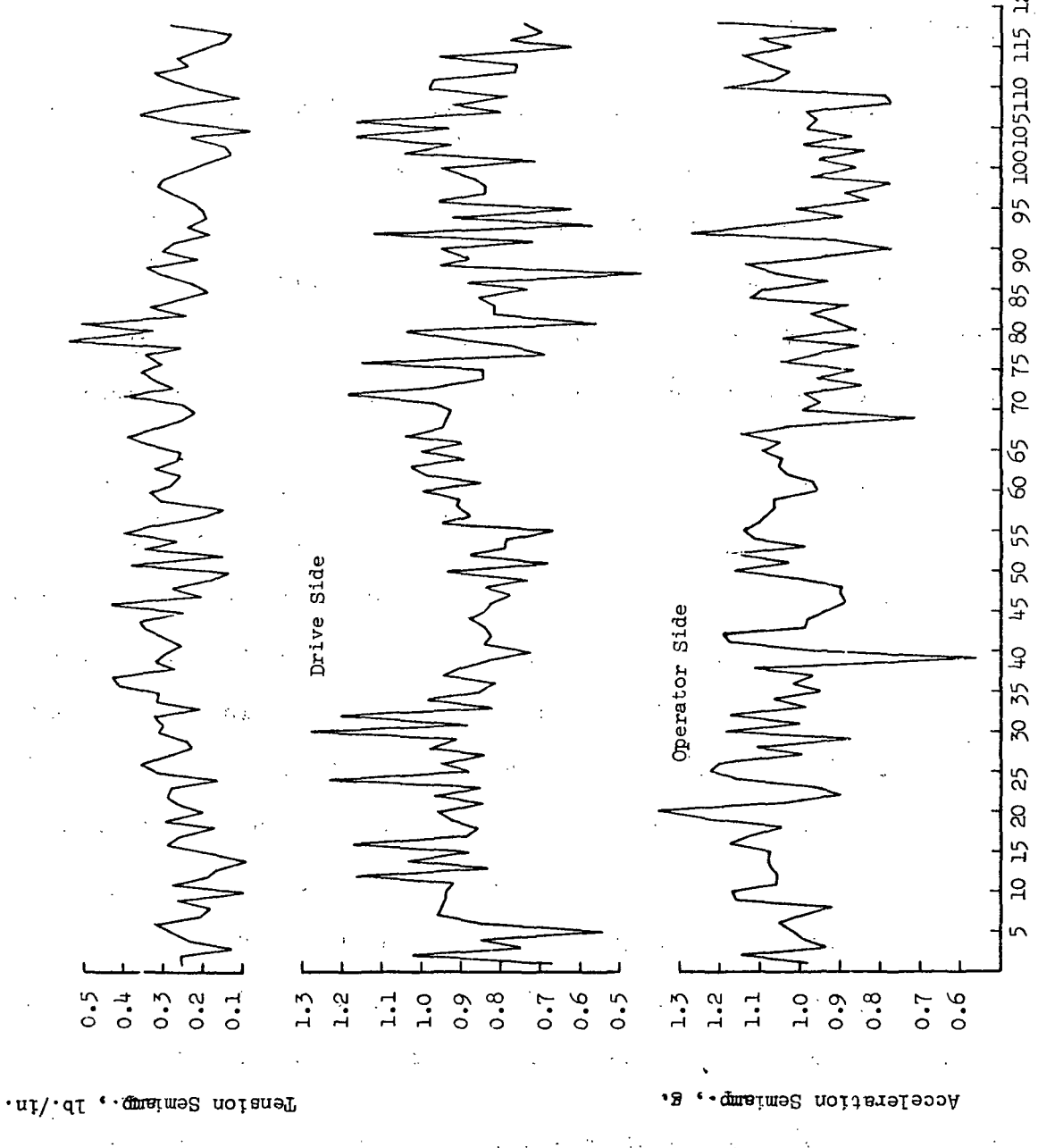

Figure 34. Semiamplitudes of the Flute Frequency Component in Acceleration and Web Tension Signals vs. Flute Number for Run 6

sometimes appear to coincide with unusually large high-lows. For example, Fig. 33 showed that fairly large high-lows were obtained around Flutes number 2, 6, 17, 28, and 40, etc. Fig. 34 shows that either the operator or drive side acceleration semiamplitude was unusually high or low on the following flute numbers: 2, 5, 12-16, 20, 25, 30-32, 39. Thus, excursions in acceleration semiamplitude were associated in some instances with large high-low differences.

However, a multiple linear regression analysis indicated that the semiamplitudes and phases at the flute frequency were not well correlated with either algebraic or absolute flute height differences. This also held true for the semiamplitudes of the harmonic components. The acceleration and pressure semiamplitudes were also converted into forces (translational and rocking) and correlated with flute heights. Low correlations were also obtained following this approach.

A few limited trials were made to determine the degree of coherence between the flute height differences (absolute) and the tension and acceleration amplitudes (first harmonic). Coherence is analogous to the square of the correlation coefficient in time series analyses and is a measure of the relationship between two series as a function of frequency. The tension semiamplitudes exhibited a low but significant (90% level) coherence square of 0.60 at a frequency of 66.8 Hz. The tension phase exhibited coherence squares of 0.42, 0.51, and 0.54 at frequencies of 25.7, 56.6, and 72.0 Hz. However, these coherence values were not significant at the 90% level. The averages of the acceleration semiamplitude differences for the two sides gave coherence squares of 0.40 and 0.50 at 15.4 and 82.3 Hz, respectively. These also approached but did not attain significance at the 90% level.

Possibly this approach would yield better results if several series could be cohered with the flute height differences simultaneously. This would be analogous

to multiple linear regression. Techniques are available to analyze time series in this way but were not available for this work.

Summarizing briefly, the results from this phase of the analysis indicated that:

1. The semiamplitudes of the signals at the flute frequency and its harmonics exhibited considerable variation from flute-to-flute. In some instances there appeared to be an association between the larger changes in semiamplitude at the flute frequency and larger flute height differences.
2. The phases of the semiamplitudes tended to display an irregular cyclic behavior having a frequency of about 15 Hz. This corresponds to a period of about 12 flutes. There appeared to be some association between phase peaks and regions of larger flute height differences.
3. Despite the visual associations noted above, there appeared to be no strong statistical relationship between the semiamplitudes or phases of the measured signals and individual flute height differences.

As mentioned previously, the analysis of flute height differences indicated they display autoregression behavior, i.e., the flute height at time t is dependent on the previous flute height and a random component. The flute heights on the single-faced board are "set" at the pressure roll nip. While the variations in forming conditions in the labyrinth may affect the way the flutes are meshed at the pressure roll nip, the lack of a strong statistical association between top roll pressure, acceleration and web tension amplitude variations from flute-to-flute and high-lows suggests that conditions existing at the pressure roll nip should be

taken into account. In this way, it may be possible to explain the larger variations in flute height and also the autoregressive behavior.

LITERATURE CITED

1. Project 1108-22, Report Four, a progress report to FKBI, March 15, 1962.

2. Project 2696-1, Report One, a progress report to FKBI, Jan. 15, 1968.

3. Project 2696-7, Report One, a summary report to FKBI, Dec. 24, 1969.

4. Project 1108-22, Report Three, a progress report to FKBI, March 23, 1961.

5. Wilson, H. W., Fibre Containers 44, no. 4:69-72(April, 1959).

6. Peters, W. Pbd. Pkg. 46, no. 2:60-3(Feb., 1961).

7. Box, G. E. P., and Jenkins, G. M. Time series analysis. San Francisco, Calif., Holden-Day, 1970.

8. Nordman, L., and Toroi, M. Unpublished work.

9. How to improve corrugated board quality and operating efficiency. The Langston Co., A subsidiary of Harris-Invertype Corp.

10. Bliss, D. I. Periodic regression in biology and climatology. Bull. 615. New Haven, Conn., The Conn. Agricultural Exp. Station, Jan., 1958.

11. Blackman, R. B., and Tukey, J. W. The measurement of power spectra. N.Y., Dover Publications, Inc., 1958.

12. Bendat, J. S., and Piersol, A. G. Measurement and analysis of random data. N.Y., J. Wiley and Sons, 1966.

13. Granger, G. W. J. Spectral analysis of economic time series. Princeton, New Jersey, Princeton Univ. Press, 1964.

14. Foster, C. R., Pulp Paper 43, no. 4:56, 57(April, 1969).

15. Mitchell, L. D., and Lynch, G. A., Machine Design, May 1, 1969.

THE INSTITUTE OF PAPER CHEMISTRY

Michael J. Laughlin
Research Fellow

William J. Whitsitt
Research Associate

Robert C. McKee, Chairman
Container Section

APPENDIX I

MATHEMATICAL FILTERING

It is often desirable when analyzing a time series to alter the shape of the series' power spectrum. Some examples of such cases might be the following (13):

1. We wish to study only that portion of the data whose frequency content lies within the band w to w_2.
2. We wish to remove a particular frequency, w_o, from the data, so that other less dominant but significant frequencies can be studied.
3. We wish to remove high frequencies from the data so that longer term trends become apparent.

The requirements of each of the above cases could be met if it were possible to change the frequency content or power spectral shape of the time series. More specifically, the objectives of the above three cases would be met if the power spectral density vs. time curve in Fig. 35 (1a-3a) were multiplied by the curves shown in Fig. 35 (1b, 2b, and 3b, respectively). In Fig. 35, 1b, the value of the multiplying filter factor, $S^2(w)$, is zero for all frequencies except those between w_1 and w_2, for which it is unity. Thus, no matter what the power spectrum of the original time series looked like (Fig. 35, 1a), after multiplication by the function shown in Fig. 35, 1b, the result would be a power spectrum equalling zero for all frequencies except those between w_1 and w_2, for which the original spectrum shape would be preserved (Fig. 35, 1c). Thus, only that portion of the data with frequencies in the w_1 and w_2 band would be left in the time series.

The removal of a given frequency, say w_o, from a time series is accomplished by multiplying the original power spectrum (Fig. 35, 2a) by the function

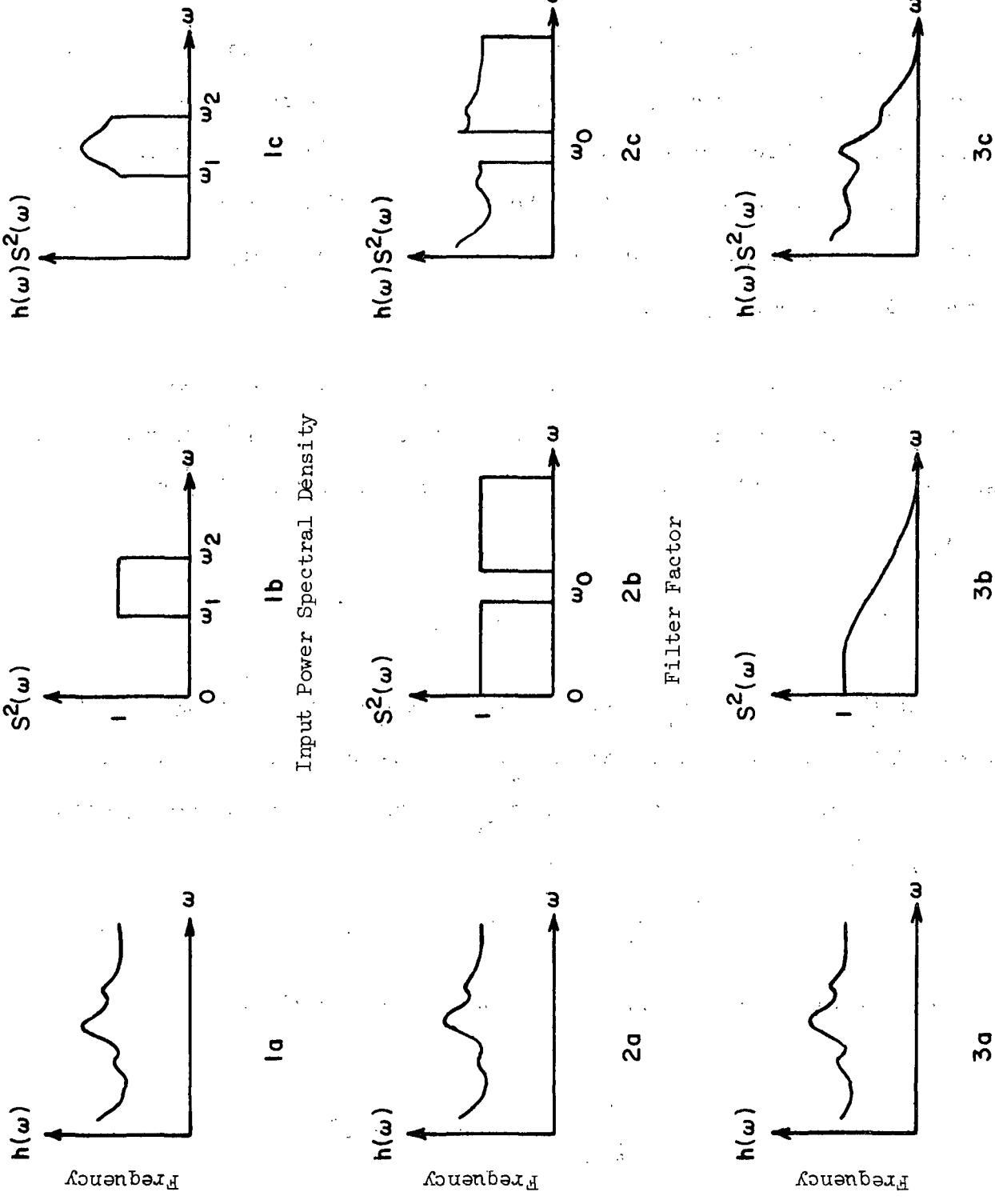

Figure 35. Illustration of the Effect of Various Types of Filtering on Power Spectrums (a = unfiltered spectra, b = filter spectra, c = spectrum after filtering)

Transforming Equation (16) by using multiple-angle trigonometric identities results in

$$y_t = A \cos (wt + \Theta) \sum_{j=-m}^{m} a_j \cos jw - A \sin (wt + \Theta) \sum_{j=-m}^{m} a_j \sin jw \quad (17)$$

The amplitude $[\underline{H}(\underline{w})]$ and phase $[\Gamma(\underline{w})]$ of the filtered series defined by Equation (17) is

$$H(w) = A \left\{ \left(\sum_{j=-m}^{m} a_j \cos jw \right)^2 + \left(\sum_{j=-m}^{m} a_j \sin jw \right)^2 \right\}^{1/2} \quad (18)$$

and

$$\Gamma(w) = \Theta - \tan^{-1} \frac{\Sigma a_j \sin jw}{\Sigma a_j \cos jw} \quad (19)$$

And since the amplitude and phase of the original time series, $\underline{x}_t$, are $\underline{A}$ and Θ, respectively, the square of the amplitude of the filter spectrum is given by Equation (20),

$$S^2(w) = \left(\sum_{j=-m}^{m} a_j \cos jw \right)^2 + \left(\sum_{j=-m}^{m} a_j \sin jw \right)^2 \quad (20)$$

and the phase change caused by the filter is given by Equation (21).

$$\phi(w) = -\tan^{-1} \frac{\Sigma a_j \sin jw}{\Sigma a_j \cos jw} \quad (21)$$

It is not always apparent how to select the filter constants, $\underline{a}_j$, to achieve a given filter power spectral curve. But, by using Equation (20), it is always possible to determine the exact filter spectrum shape as a result of selecting a particular set of filter constants, $\underline{a}_j$.

For example, consider the case of the simple process of differencing of a series of flute heights of single-faced corrugated board. That is, in order to eliminate the average flute height from the data to allow concentration on the

differences between flutes, a new time series, $\underline{y}_t$, is formed from the original series of flute heights, $\underline{x}_t$, as follows:

$$y_t = x_t - x_{t-1} \tag{22}$$

Relating Equation (22) to the generalized filter defined in Equation (14), we see that a similar transformation would be accomplished by choosing $\underline{m} = 1$, $\underline{a}_{-1} = -1$, $\underline{a}_o = 1$, $\underline{a}_{+1} = 0$. An expansion of Equation (14) for the case of $\underline{m} = 1$ gives

$$y_t = a_{-1} x_{t-1} + a_o x_t + a_1 x_{t+1}. \tag{23}$$

Substitution of the values for $\underline{a}_1$ chosen above results in a filter which operates on the data exactly as defined in Equation (22). To determine what effect such a transformation would have on the frequency content of the original series of flute heights, the power spectrum of the transforming filter is computed from Equation (20) and the chosen constants. The result of this computation is

$$S^2(w) = (1 - \cos w)^2 + (\sin w)^2 \tag{24}$$

which becomes

$$S^2(w) = 2(1 - \cos w) \tag{25}$$

A graph of Equation (25) is shown in Fig. 36, in which the ordinate represents the square of the filter power spectral density function, $\underline{S}^2(\underline{w})$, and the abscissa represents the frequency (cutoff frequency = π). This graph corresponds to Fig. 35, 1b, 2b, and 3b inasmuch as it is to be interpreted as that function which will be multiplying the power spectrum of the original time series as a result of the filtering operation [Equation (22)]. It may be seen from Fig. 36 that the filter factor, $\underline{S}^2(\underline{w})$, is zero at the zero frequency and increases continuously to 4.0 at the cutoff frequency. The effects on a time series of such a filter would be to remove the

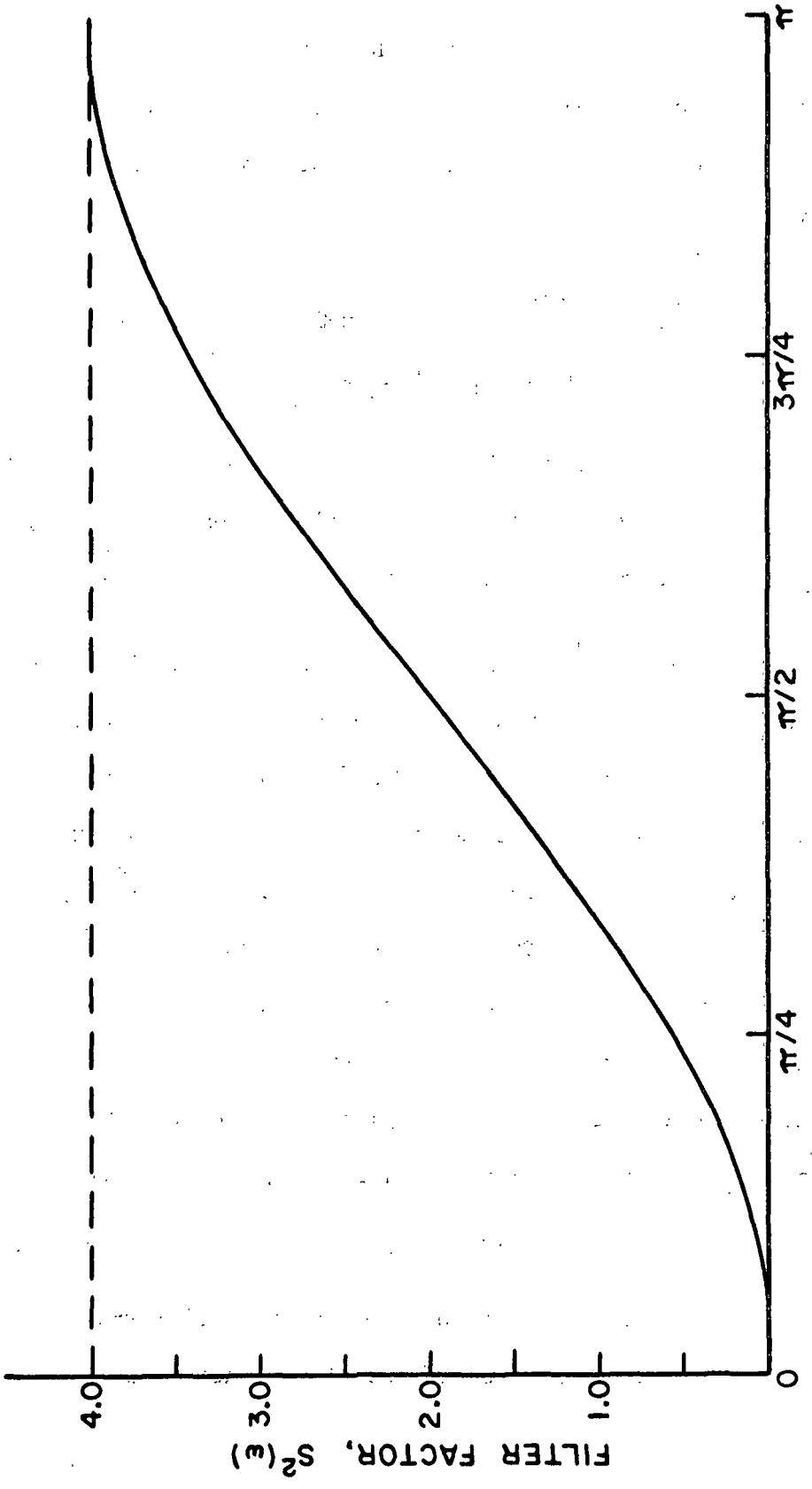

Figure 36. Shape of Filter Factor for Differencing Operation

average value (zero frequency), attenuate low frequencies, and amplify higher frequencies.

In the course of studying the pressure, tension, and acceleration signals from a corrugator, it was found to be desirable to attenuate a fundamental frequency and its three harmonics in the data. To accomplish this end, the following filter was utilized:

$$y_t = -0.0625\ (x_{t-24} + x_{t+24}) - 0.25\ (x_{t-16} + x_{t+16}) - 0.50\ (x_{t-8} + x_{t+8}) + 2.275\ xt. \qquad (26)$$

The filter factor for this filter, $\underline{S}^2(\underline{w})$, is shown in Fig. 37 as a function of frequency. It may be seen that the frequencies attenuated are $\underline{o}$, $\underline{F}$, $2\underline{F}$, $3\underline{F}$, and $4\underline{F}$, where $\underline{F}$ is the frequency of flute formation.

The filter defined in Equation (26) was applied to the data in order to reduce the power peaks of prominent frequencies and thereby produce data with more evenly distributed power. Such a "flat" power spectrum results in more accurate estimates of the power at each selected frequency. However, since the spectrum of the original data has been altered, the results of the spectral analysis reflect this charge and are, therefore, difficult to interpret. To allow for a straightforward interpretation, a process known as "recoloring" was performed. This process consists of multiplying the resultant power spectrum after analysis by the reciprocal of the filter factor used when modifying the spectrum of the original data. The filter factor is computed from Equation (20), using the constants from Equation (26):

$$S^2(w) = \{2.275 - 0.125\ [8 \cos 8w + 4 \cos 16w + \cos 24w]\}^2. \qquad (27)$$

To recolor the spectrum of the data to its original form, the power at each frequency is multiplied by the reciprocal of the filter factor defined in Equation (27).

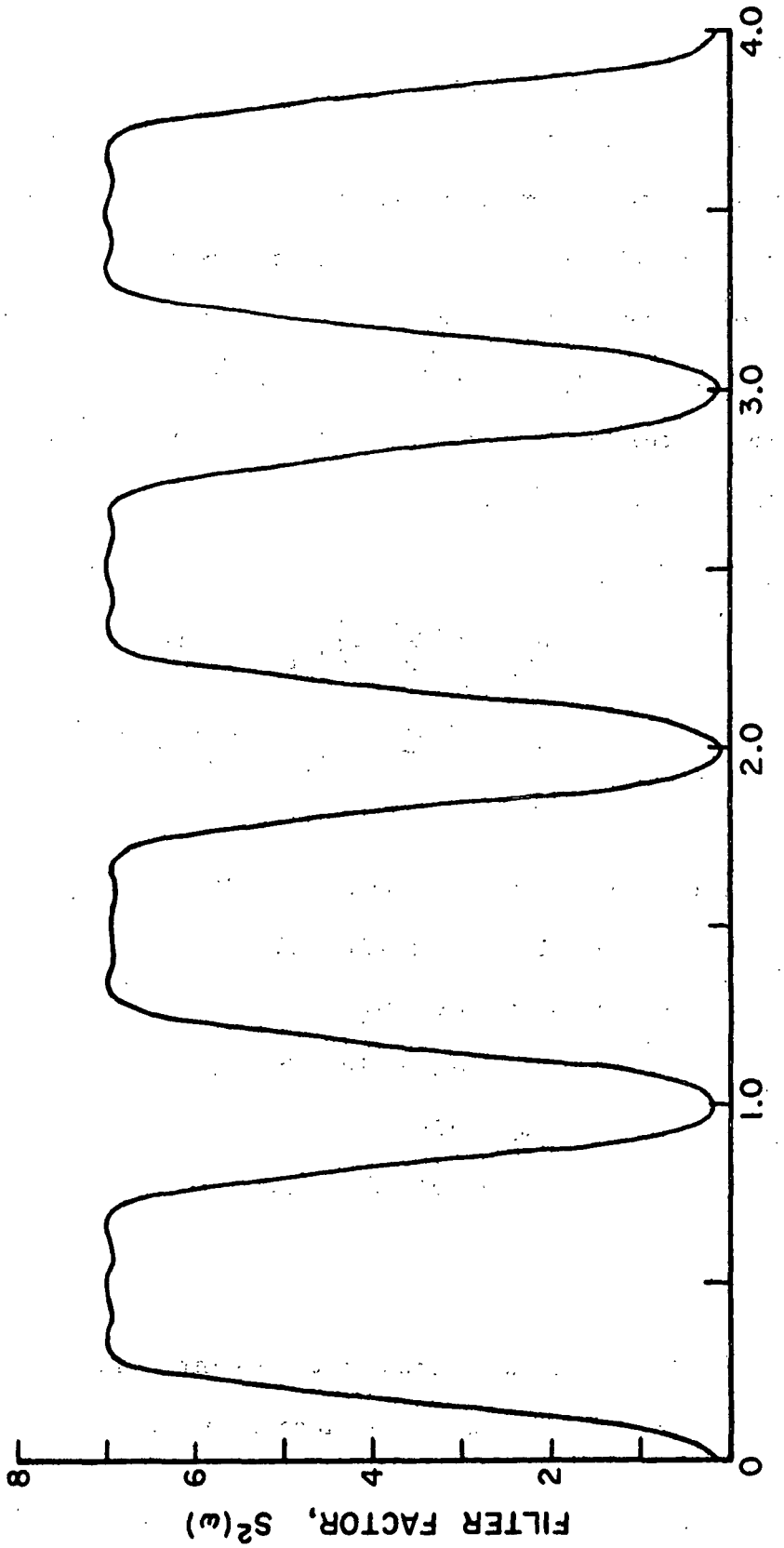

Figure 37. Shape of Filter Factor for Attenuating Flute Frequency Component and its Harmonics

APPENDIX II

CALCULATION OF FORCES

TRANSLATIONAL FORCES

To compute these forces, the assumption is made that the upper corrugating roll moves up and down as a rigid body, with both ends moving an equal amount so that there is no rotation of the roll in a plane parallel to its axis. The free body diagrams of forces acting on each end of the corrugating roll are shown in Fig. 38. The symbols F, p and $\ddot{y}$ refer to the force on the medium, piston pressure, and translational acceleration, respectively. The subscripts "op" and "dr" refer to the operating and drive sides, respectively. Combining forces and substituting known quantities, we have

$$F_{op} = \left(\frac{1033.7}{2}\right)\ddot{y}_{op} + \left(\frac{9\pi}{4}\right)p_{op} \qquad (28)$$

$$F_{dr} = \left(\frac{1033.7}{2}\right)\ddot{y}_{dr} + \left(\frac{9\pi}{4}\right)p_{dr} \qquad (29)$$

where

F_{op} = force on operating side medium, lb.

F_{dr} = force on drive side medium, lb.

$\ddot{y}_{op}$ = acceleration on operating side, g units

$\ddot{y}_{dr}$ = acceleration on drive side, g units

p_{op} = pressure on operating side, p.s.i.

p_{dr} = pressure on drive side, p.s.i.

ROCKING FORCES

The rocking forces are computed by assuming that the corrugating roll can rock or rotate from end to end in a plane parallel to its axis, as well as

translate as a rigid body along a line perpendicular to its axis. The free body diagram for such a case is shown in Fig. 39. It is further assumed that the corrugating medium acts as a linearly elastic foundation. After summing forces and solving the resulting two equations for the operating and drive side medium forces, we have:

$$f_{op} = (0.608)\,\ddot{y}_{op} - (0.385)\,\ddot{y}_{dr} + (4.17)\,p_{op} - (2.99)\,p_{dr} \qquad (30)$$

$$f_{dr} = -(0.385)\,\ddot{y}_{op} + (0.608)\,\ddot{y}_{dr} - (2.99)\,p_{op} + (4.17)\,p_{dr} \qquad (31)$$

where

f_{op} = force on operating side medium, lb./in.

f_{dr} = force on drive side medium, lb./in.

$\ddot{y}_{op}$ = operating side acceleration, g units

$\ddot{y}_{dr}$ = drive side acceleration, g units

p_{op} = operating side pressure, p.s.i.

p_{dr} = drive side pressure, p.s.i.

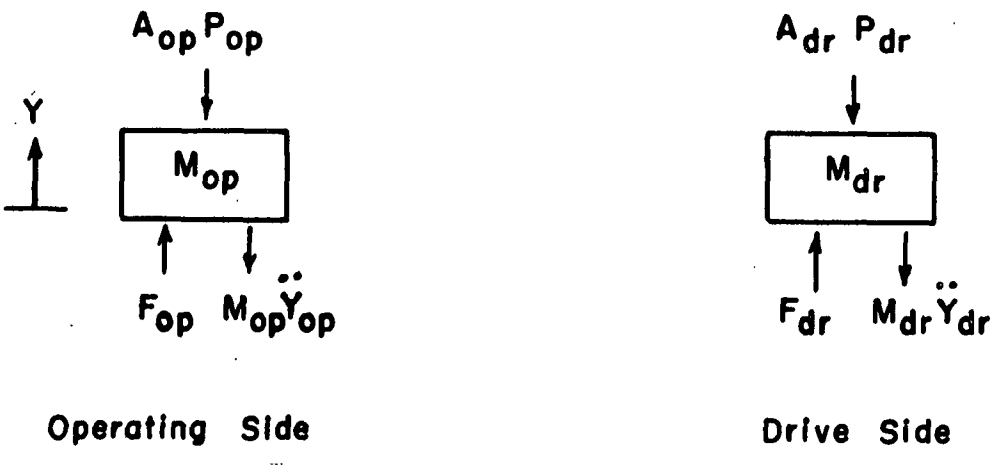

Figure 38. Free Body Diagrams for Translational Motion

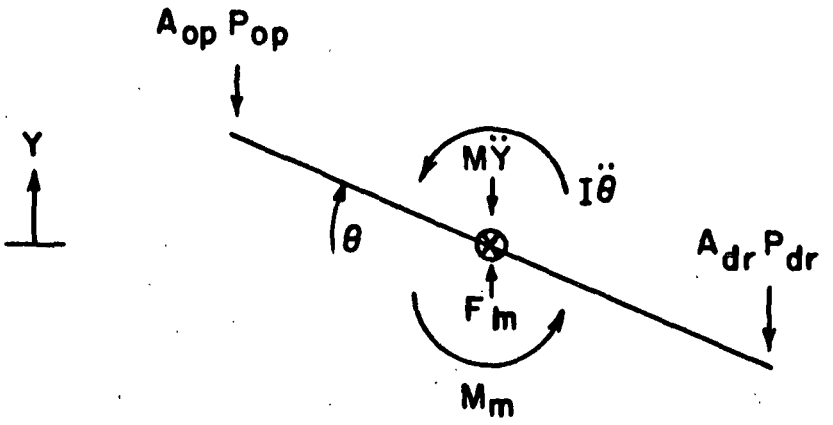

Figure 39. Free Body Diagram for Translational and Rotational Motion